

DOTTORATO DI RICERCA IN SCIENZE DELLA TERRA

CICLO XXXI

Portable Hyperspectral Sensor: A New Application in Cultural
Heritage Conservation

Dottorando


Dott. Cong Wang



(firma)

Tutore

Prof. Sandro Moretti



(firma)

Co-tutore

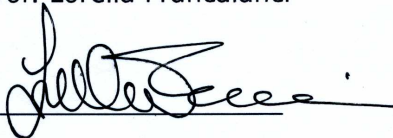
Dr. Mara Camaiti



(firma)

Coordinatore

Prof. Lorella Francalanci



(firma)

Anni 2015/2018 (di inizio e fine corso)

Chapter I Introduction.....	1
1.1 Characterization of materials	1
1.1.1 General characterization and non-invasive analysis	1
1.1.2 Painting characterization.....	4
1.1.2.1 Painting structure	4
1.1.2.2 Painting analysis procedure and major techniques	13
1.2 Reflectance spectroscopy.....	19
1.2.1 Basic theory of reflectance spectroscopy.....	19
1.2.2 General application in cultural heritage.....	25
1.3 Hyperspectral sensor ASD FieldSpec FR Pro	28
1.3.1 Background information of hyperspectral sensor.....	28
1.3.1.1 Structure	28
1.3.1.2 Hyperspectral vs. multispectral sensor	30
1.3.1.3 Curve understanding	31
1.3.1.4 ASD FieldSpec FR Pro	33
1.3.2 General application and its usage in cultural heritage	35
1.3.3 The influencing factors of reflectance spectra by FieldSpec FR Pro and database creation	38
1.3.4 Principle Component analysis (PCA) for data processing.....	40
Chapter II Aim of the thesis.....	41
Chapter III Experimental	45
3.1 Materials	45
3.1.1 Pure materials.....	46
3.1.1.1 Colorants	46
3.1.1.2 Binding media.....	57
3.1.2 Painting mock-ups	59
3.2 Instruments.....	65
3.2.1 Hyperspectral sensor.....	65
3.2.2 Data collection	67
3.2.2.1 Data collection Pigments	68
3.2.2.2 Data collection of binding media.....	69
3.2.3 Data processing.....	70
3.3 Other instruments used in the study.....	71

3.3.1 Optical microscopy	71
3.3.2 FT-IR spectroscopy.....	71
3.3.3 SEM-EDS	72
Chapter IV Results and discussion	73
4.1 Raw spectra and their 1 st derivatives transformation.....	73
4.2 Pure material characterization.....	75
4.2.1 Reference reflectance spectra database of colorants.....	76
4.2.1.1 Different methods of “Min” spectra collection.....	77
4.2.1.2 Comparative study between “Min” and “Max” spectra.....	81
4.2.2 Reference reflectance spectra database of organic materials.....	89
4.2.2.1 Comparison of organic materials on glass and Teflon supports	89
4.1.2.2 Identification of four different binders	90
4.2 Mixture identification	96
4.2.1 Characterization of binding media in mixtures.....	97
4.2.1.1 Egg yolk with pigments	97
4.2.1.2 Animal glue with pigments.....	99
4.2.1.3 Linseed oil with pigments.....	100
4.2.1.4 Gum Arabic with pigments.....	102
4.2.2 Binders and pigments from mixtures.....	103
4.2.2.1 Different amount of binders affect the spectra of mixture.....	103
4.2.2.2 Identification of four binders from mixtures with the same colorant	105
4.2.2.3 PCA analysis for binder identification in mixtures.....	110
Chapter V Case studies	123
5.1 Easel painting surface characterization.....	124
5.1.1 Basic information on an old painting by an unknown author.....	124
5.1.2 Identification of pigments and its binding medium	125
5.2 The characterization of the fresco in the church of Saint Stefano, Lamporecchio, Italy	129
5.2.1 history and pre-restoration works of the church	129
5.2.2 Current condition and preliminary scientific investigation of the fresco	130

5.2.3 Characterization work.....	131
5.2.3.1 Area S1 with grey (light blue) & blue colors on the ceiling..	132
5.2.3.2 Area S2 & varnishes on frescoes ..	140
5.2.3.3 Area S3 and green overpaints: ..	145
5.2.3.4 Area 4 and red/ violet colors:.....	151
Chapter VI Conclusion	156
Bibliography	164
Appendix.....	173
Acknowledgement	189

Chapter I

Introduction

1.1 Characterization of materials

1.1.1 General characterization and non-invasive analysis

In the field of cultural artifacts, there is a vast array of objects that are made of varied materials, including organic, inorganic, natural and synthetic components. Examples are stones, metals, ceramics, paintings, books, glass, textiles, woods, plastics and so on. Different techniques are also exploited to realize these objects from raw materials. As a matter of fact, almost all the raw materials are susceptible to degradation due to physical, chemical and/or biological causes, which lead to the formation of complex, undesired materials. Additionally, materials derived from conservation and restoration intervention can also be present.

To restore/repair an artwork, after a visual examination, conservation scientists select the areas of interest, and then they start the most essential step of conservation, materials characterization. As it is universally accepted, characterization of materials of an artifact always contains three fundamental aspects: firstly, identification of materials used for its structure; secondly, evaluation of the state of conservation of the

artwork and its degradation causes; lastly, proposal of suitable restoration materials and methodologies. Moreover, characterization is a valid help in provenance and authentication studies (knowledge of the past) [1], as well as in preventing possible deterioration causes such as wrong conservation/restoration operations, i.e. cleaning, consolidation or protection interventions [2-5] (knowledge of the future).

Thanks to fast development of technologies, many analytical techniques used both in labs and in-situ for material identification in the field of cultural heritage are now available. In general, they are divided into two categories depending on the type of analysis performed, i.e. non-invasive and invasive analysis. The term “invasive” refers to the analysis that is micro destructive to the detected targets, meaning that samples (micro particles or fragments) are needed to collect from an artwork for the analytical process. Invasive techniques are always very powerful and they are widely employed in the identification of both organic and inorganic materials. They include elemental analysis and molecular analysis. Techniques identify the inorganic species by detecting the presence of specific elements such as X-ray Florescence (XRF), Scanning electron microscopy-energy dispersive X-ray spectroscopy (SEM-EDS), X-ray photoelectron spectroscopy (XPS), particle-induced X-ray emission or proton-induced X-ray emission (PIXE), Auger electron spectroscopy (AES) and laser-induced breakdown spectroscopy (LIBS) etc. Other common analysis is based on molecule structure, X-ray diffraction (XRD) and (micro-)Raman spectroscopy are mainly applied for crystalline compounds and inorganic materials diagnosis. The

identification of organic species is achieved by other technologies like high-performance liquid chromatography (HPLC) and nuclear magnetic resonance (NMR) spectroscopy. Gas chromatography–mass spectrometry (GC-MS) is commonly used for the separation and identification of several classes of compounds, but it is also destructive towards sample. The most important methodology of analysis is Fourier-transform infrared spectroscopy (FT-IR) with its different accessories, thanks to its ability to detect both inorganic and organic substances without sample pre-treatment and with relatively high sensitivity.

Non-invasive techniques, on the contrary, are generally used for preliminary studies. In spite of the rapid advancement in scientific instruments/techniques, the non-invasive techniques are still not comparable with the invasive ones in terms of possible applications (or situations where they can be applied) and accuracy. Therefore, the main aim of the non-invasive instruments is to get a very general knowledge of the artwork and to identify the most suspected areas for an accurate sampling. Moreover, this kind of investigation is always addressed to the detection of surfaces, thus less information is acquired compared with invasive ones which often allow the investigation of cross sections (painting stratigraphy). Infrared reflectography, UV fluorescence, false color infrared reflectography etc. are used only for differentiating some inorganic and organic compounds. For inorganic materials identifications, portable XRF is a non-invasive instrument of analysis, but it can be used in limited cases by detecting some elements. Until now, the most frequently used

technique is the Fiber Optical Reflectance Spectroscopy (FORS). Since it was firstly used 30 years ago [6], it has now become a well-accepted technique for substances identification, in particular colorants (including inorganic pigments and organic dyes). On the contrary, the characterization of many organic materials on a painted surface in a non-invasive way is still a challenge.

In most cases, a well-accepted analytical sequence for surfaces characterization always proceeds as follows: first the non-invasive diagnosis is carried out, followed by the invasive techniques, when necessary. Nevertheless in some circumstances, e.g. for some masterpieces, sampling is not allowed. Therefore, non-invasive techniques are the only possibility to acquire information of an artwork, and gathering as much information as possible through non-invasive analysis is a target of conservation scientists. Thus, searching and improving a new non-invasive technique for materials characterization is always imperative in the field of fine arts.

1.1.2 Painting characterization

1.1.2.1 Painting structure

Undoubtedly, paintings conservation and restoration represents a large and critical sector in the field of cultural and historical objects. Under this category, various types of paintings are contained. In ancient times, paintings were carried out on easily

available supports like walls of caves. Later on, the evolution of depiction concepts required more appropriate supports, specifically designed to receive the paint layers, such as wood panels, canvases and walls. Now, the differentiation of species of painting is usually based on their support: canvas paintings are pictured on canvas (cotton, hemp, linen, silk); panel paintings are painted on different kinds of wood; mural paintings and frescoes are drawn on the wall; and illuminated manuscripts (a very special one) are painted and sometimes even gilded on the parchment. Early works were still panel paintings on wood, but around the end of the 15th century canvas became more popular as support, as it was cheaper, easier to transport, allowed larger works than wood, and did not require complicated preliminary layers. The basic structures of a painting on diverse supports are illustrated in Figure 1.1, but some paintings have more complicated structure due to intentional overpaintings or later conservation interventions. Preparation layer, painting layer and the varnish layer, these main layers of painting are discussed in the following parts.

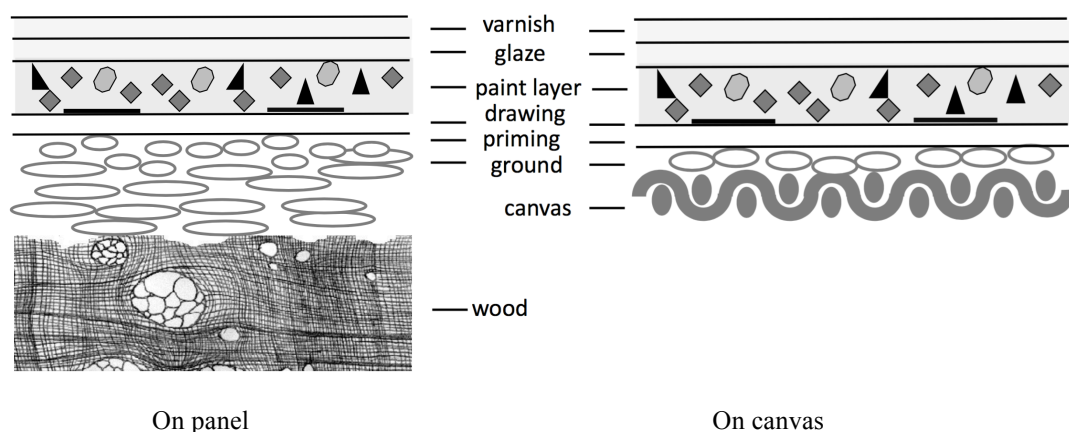


Figure 1.1 Painting structure on the two most popular supports

● ***Preparation layers***

Panel and canvas paintings often have a preparatory ground (or simply “ground”) that is a film or a layer lying between the support and the paint layers. Sometimes the painting structure may also contain a priming (also called “*imprimitura*”), which is a continuous layer between the ground and the paint layers, and may consist of a pigment in medium or of a medium alone. The layer of preparatory ground has several roles. Firstly, it allows the surface of the support to become flat and regular; secondly, it hampers the absorption of the liquid component of the binding media by the support, and allows the painting layer to remain on the surface; thirdly, it creates a layer chromatically influencing the final appearance of the upper paint layers, which reflects the style of the artist. The composition of the preparatory ground varies from region to region. In Italy, gypsum, called “gesso”, in the form of calcium sulfate dihydrate ($\text{CaSO}_4 \cdot 2\text{H}_2\text{O}$) and animal glue was widely used. But other forms of calcium sulfates, like Bassanite ($\text{CaSO}_4 \cdot 1/2\text{H}_2\text{O}$), which is also known as plaster of Paris, and anhydrous calcium sulfate (CaSO_4 , Anhydrite), were also applied as ground layer. Calcium carbonate (CaCO_3) with animal glue was the main material used for preparation in the central Europe. While in North Europe, people preferred to use the mixture of lead white (PbCO_3) with linseed oil on the support before drawing. The preparation layer was painted in thicker or thinner layer, but in some cases, artists were used to apply a canvas between the panel and the ground, which is called “*cencio di nonna*” (grandmother’s rag).

For mural paintings, painters always use slaked lime ($\text{Ca}(\text{OH})_2$) and sand as the ground layer on the stone support. Usually, a mixture of coarse sand and slaked lime is applied firstly, then the finer one with $\text{Ca}(\text{OH})_2$, and finally the finest one. The Italian names of these painting techniques are called “*arriccio*”, “*intonaco*”, and “*intonachino*”.

● *Under drawing*

Under drawing is the contour of paintings on the preparation layer painted with charcoal or other dark pigments. For panel and canvas paintings, painters used techniques like pouncing, tracing and so on, to draft the outline firstly on paper. It is proved that Vincent van Gogh’s *Basket with pansies on a stool* (1887) was drafted by a squaring technique [7]. For mural paintings and frescoes, artists also used similar strategies to prepare a draft before the final drawing, e.g. *Sinopia*, snapping cord, stencil, transfer through cartoon, etc.

● *Painting layers*

A painting layer is the main layer of the painting. A painting may have more than one layer due to overpaintings and restoration works. The one closest to the surface often determines the final appearance of a painting (if it is thick enough). The layers are composed of colorants and binding medium.

➤ Colorants

Colorants, i.e. natural or synthetic pigments and dyes, are inorganic or organic substances that are wavelength-selective absorbers and relatively stable in normal environmental conditions. Pigments are dry colorants, most of them are minerals, usually ground into a fine powder. The majority of pigments absorbs and reflects certain wavelength of visible light (350 -780 nm), the rest is colored by other principles. Organic colorants (mainly dyes), such as diazo or phthalocyanine compounds, contain in their molecules conjugated systems of double bonds, which are responsible for the color. Some inorganic pigments, such as vermilion (mercury sulfide) or cadmium yellow (cadmium sulfide), absorb light by transferring an electron from the negative ion (S^{2-}) to the positive one (Hg^{2+} or Cd^{2+}). The earliest known pigments were natural minerals, such as ochre, iron oxides, charcoal/ carbon black, and they have been used as colorants since prehistoric times. Mineral pigments, or pigments of biological origin were mostly used before the industrial revolution. The pigments based on minerals and clays often derive the name of the city or region where they were mined, like Siena earth. Pigments/dyes from unusual sources such as botanical materials, animal waste, insects, and mollusks were harvested and traded over long distances (gamboge, cochineal red, rose madder, indigo). Some natural colorants like blue and purple colors are produced in fewer amounts and expensive. To reduce the cost, synthetic pigments and dyes were produced to replace the natural ones after the Industrial and Scientific Revolution. Prussian blue was the first modern synthetic pigment, discovered by accident in 1704 [8], while lead white (“biacca”)

and Egyptian blue, the first synthetic pigments, were known since the ancient times. By the early 19th century, synthetic and metallic blue pigments had been added to the range of blues, including French ultramarine, a synthetic form of lapis lazuli, and the various forms of cobalt and cerulean blue. In the early 20th century, organic chemistry added Phthalo Blue, a synthetic, organometallic pigment with overwhelming tinting power. Synthetic pigments are always finer in particle size, stable in color (when mixing with other substances) and more resistant to environmental conditions.

Unlike pigments that are insoluble, the term “dye” is usually referred to colored and water soluble substances. Some dyes can be rendered insoluble with the addition of salt to produce a lacquer. A dye is generally applied on fabrics in an aqueous solution, and may require a mordant to improve the fastness of the dye on the fiber. The majority of natural dyes are derived from plant sources: roots, berries, bark, leaves and wood, fungi and lichens. Most dyes are synthetic, i.e. are man-made from petrochemicals. In the past, people dyed their textiles using common, locally available materials. Plant-based dyes such as woad, indigo, saffron, and madder were important trade goods in the economies of Asia and Europe.

➤ Binders

A binder is a material or substance which hold other materials together by adhesion and cohesion to form a whole. It is liquid or dough-like substance that harden by a

chemical or physical process and bind fibers, filler powder and other particles added into it. In art, a binder is used in painting, where it holds together pigments and sometimes filling material to form paints, pastels, and other materials. Binders are classified as organic and inorganic ones. In ancient times, on panel and canvas paintings, natural binders of both animal and vegetable origin were used. Binders of animal origin are egg yolk, egg white, animal glues, beeswaxes and so on. Vegetable binders include linseed oil, gum Arabic and starch. Egg yolk, as a kind of binding medium, was the primary panel-painting medium for nearly every painter in the European Medieval and Early renaissance periods. The paintings where egg yolk is used as binder are called “tempera painting” or “egg tempera painting”. Temperas are fast drying and permanent; it was a primary method of painting until 1500, and gradually replaced by drying oil. Oil painting has originated in Afghanistan between the 5th and 9th centuries, and migrated westward in the middle Ages. Commonly used drying oils include linseed oil, poppy seed oil, walnut oil, and sunflower oil. The choice of oil imparts some properties of painting, such as drying time, yellowing. Due to its excellent crosslinking/polymerization property, linseed oil was mostly applied, although its natural propensity for yellowing. The usage of animal glues as a binder, on the other hand, was not widespread. These proteinaucious glues are extracted from animals’ skins, bones and other tissues. Between 1500–1000 BC, animal glues were used as glue for wood furnishings and binder in mural paintings, but they were found even on the coffins of Egyptian Pharaohs. In addition to fats (oils) and proteinaceous

(animal glues) materials, polysaccharides are also used as binders, like gum Arabic, mainly used in watercolor paintings being soluble in cold water.

As for mural paintings, for drying paintings (“secco” in Italian), binders are almost the same used in easel paintings. On the contrary, for frescoes, the binder is an inorganic component (lime putty) which achieve the best binding effect after the natural carbonation process, as described in equation 1.1:



Calcium carbonate, surrounding the pigments grains, acts as binding medium. The pigments applied for frescoes should resist to an alkaline pH.

● *Varnishes*

The finishing varnish is a transparent, hard and protective film applied as the last treatment on the top of a painting, and is present in almost all the old master paintings. After being applied, a more and more hard film is formed during solvent evaporation. According to the literature, varnishes were applied on oil paints in the fifteenth century mainly to enhance the gloss of colors, giving a better aesthetic effect [1] because the refractive index of the varnishes is greater than that of air, and light can penetrate into the deeper pictorial layers resulting in a better color saturation. Moreover, these transparent coatings protect the pictorial layers from direct damage due to dust/dirt deposition, humidity, pollution and so on. Dating back to sixteenth century, the effect of varnishes was described by Armenini as follows: ‘There are then

the varnishes, whose effect is to enliven and draw out the colors and preserve their beauty for a very long time. Varnish also has the power to bring out all the minutes in a work making them very clear" [9].

Natural varnishes are usually as "spirit varnishes" or "essential oil varnishes", which are solutions of natural resins dissolved in a volatile solvent, typically oil of turpentine. Spirit varnishes were first mentioned in sixteenth century in Italy and widespread in both north and south Europe in the following century. The most popular natural resins used in spirit varnish are mastic or dammar. They are dissolved in turpentine and are still used for restoration of paintings. They show a gloss property, although the final effect is greatly influenced by the method of application.

In 1930s, synthetic polymers started to be used as varnish for paintings. The first synthetic resin was polyvinyl acetate (PVAc). About 20 years later, another class of synthetic polymers (poly-alkyl (metha)acrylates, e.g. Paraloid B67, Paraloid B72) was developed and used to varnish paintings. Together with poly-vinyl acetate and poly-alkyl (metha)acrylates, ketone resins (poly-cyclohexanone resins) found particular interest among scientist conservators because of their similarity, in terms of refraction index and good optical qualities, to natural resins [10]. Although synthetic polymers are considered to be more stable than natural resins, some of them have proved to be poorly resistant to ageing. Cross-linking reactions, due to photo-oxidation, are responsible for the insolubility of aged poly-alkyl

(metha)acrylates, with a possible jeopardizing removal during the cleaning treatments. Moreover, other weaknesses of most of synthetic polymers are their lower refractive index in respect to natural resins, and the high molecular weight. Both these conditions make the final varnish not good in terms of optical properties. As a consequence, they produce a different chromatic effect than that achieved using traditional varnishes. Even though, many conservators preferred, and still now prefer, to use natural resins instead of synthetic varnishes, some historical restoration work, as well as contemporary artworks, are varnished with synthetic resins. Therefore, in this study, both natural and synthetic resins were characterized and discussed.

1.1.2.2 Painting analysis procedure and major techniques

Characterization of painting components is of paramount importance before proceeding with any restoration intervention. Since a painting is constituted of more than one layer, with different inorganic and organic compounds mixed together, the identification of each component is much more complicated compared to other artworks (e.g. stone artifacts). Organic substances are widespread in all painting layers, and the ageing processes due to pollution, natural oxidation or photo-oxidation may alter strongly their original molecular structure and composition. Furthermore, possible past restoration interventions, which introduced new organic and polymeric materials, makes the identification more complicated [11-13]. The characterization needs to be carried out not only on the original layers and any intentional overpainting,

but also on the restoration layers to get information of the state of conservation and knowledge of the artwork.. One example of the importance of surface characterization is related to a cleaning process, where the efficacy of a cleaning methodology is evaluated by the presence or absence of undesirable compounds on the surface. In this case, painted surfaces are expected to be characterized before, during and after the cleaning procedures to reach minimum damage and maximum cleaning [14-16].

Like other artworks characterization, the optimization of the analytical sequence in function of previously defined and clear objectives is required. A general sequence of analysis of a painting starts from its documentation by photography and other *in situ* examinations. Common advanced techniques for scientific investigations of paintings are tomography (e.g. IR Reflectography, Radiography, Thermography, Optical Coherence Tomography, Nuclear magnetic Resonance) [17-20], multi-spectral imaging [21]. With the aid of these techniques, it is able to get knowledge of a painting, e.g. general structure, painting techniques used by the painter, possible under drawing or over paintings and so on. Further details can be acquired from more complex instruments as described in Chapter 1.1.1. Another technique, which cannot be underestimated, is the Fiber Optic Reflectance Spectroscopy (FORS). It was firstly used by Bacci M. [6,22,23] and has become the most frequently used non-invasive instrument for *in situ* materials identification in painting. Its most general application is the identification of pigments, especially on some particular items like illuminated manuscripts [24-25]. In any case, all the non-invasive techniques allow the

identification of chemical dis-homogeneity on the artworks to be documented, thus providing a better identification of the areas to be sampled. After sample(s) taken from the suspected regions on a painting, it (they) is (are) analyzed by micro-invasive instruments. Depending on the physical characteristic of the sample(s) (powder, fragments or components dissolved in specific solvents), the analysis is divided into bulk analysis, stratigraphic analysis and selective analysis with their corresponding methodologies. The mainly methodologies of analysis of powders and fragments from a painting are illustrated in Fig 1.2 and Fig 1.3.

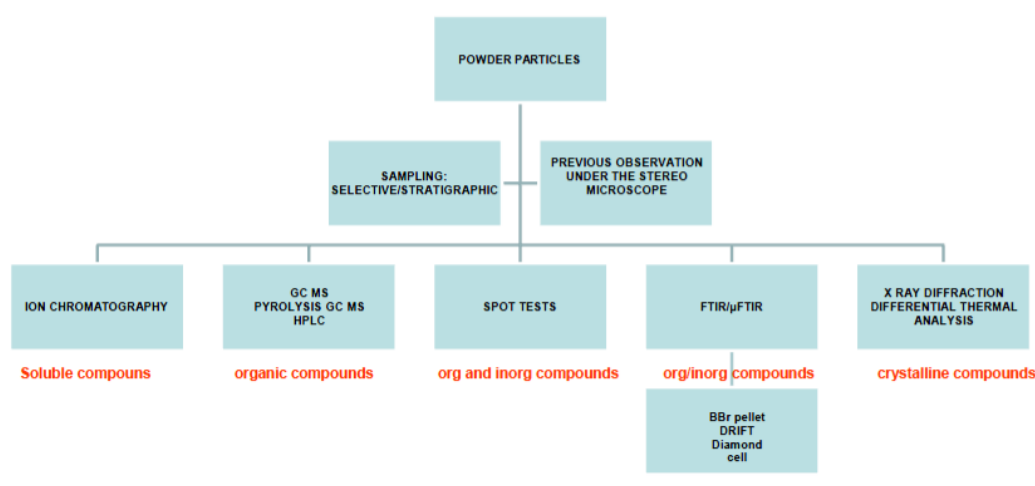


Fig 1.2 Analytical sequence for powder [14]

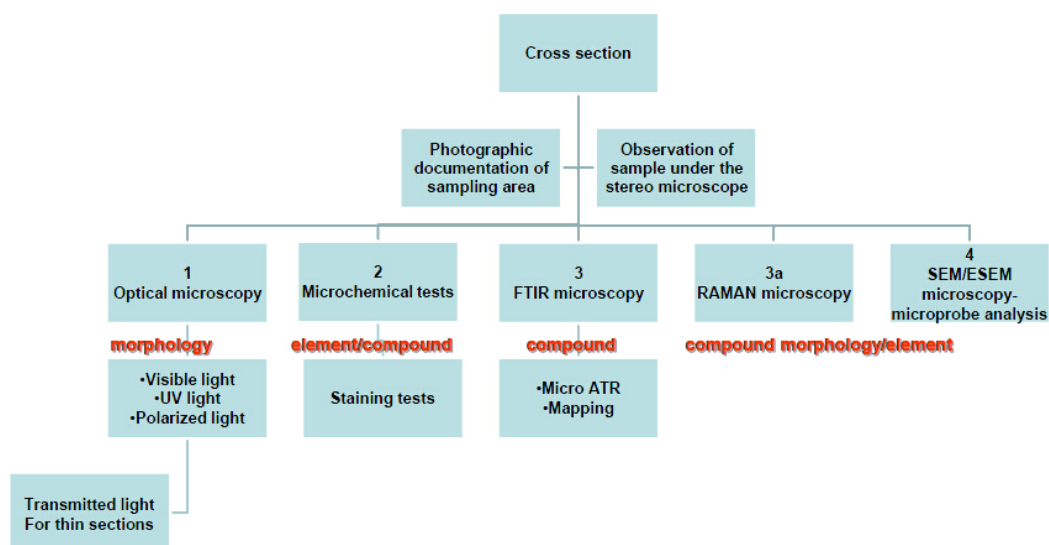


Fig 1.3 Analytical sequence for fragments embedded in resin and observed in cross-section [14]

During the sample analysis, the non-destructive techniques are first applied, then the micro-destructive and finally the destructive ones. For the analysis of inorganic materials, e.g. minerals used as pigments, instruments such as X-Ray Diffraction (XRD) and Differential Thermal Analysis (DTA) are useful for identifying these compounds, but they require relatively high amount of powder. This condition is not suitable and possible to satisfy when the samples must be taken from masterpieces of relevant historic and artistic importance [27]. SEM-EDS is able to distinguish pigments through the presence of some specific metal elements and through the observation and the analysis of the samples in cross section, it is possible to reconstruct the stratigraphy of the painting (i.e. different pictorial layers and ground).. For organic compounds, Gas chromatography–mass spectrometry (GC-MS) [28], is the most popular and efficient technique. It is based on the separation of different and

relatively small molecules present in some organic materials, such as egg, oils, natural resins, by their affinity to specific stationary phases which allows different retention on the substrate. From the retention times of each component and the signal intensity (peaks area), it is possible identify different compounds and their abundance (qualitative and quantitative analysis). GC-MS is a very accurate technique and it allows the identification of similar compounds (e.g. it is possible to identify linseed oil from walnut oil or poppy seed [29-31]). However, the main drawback of this technique is that the sample preparation is very time-consuming and the analysis is expensive. On the other hand, some equipment can analyze the samples without manipulation and identify both inorganic and organic materials, simultaneously. The most commonly used analytical methodologies are Fourier-Transform Infrared spectroscopy and Raman Spectroscopy [32]. Both these techniques provides spectra that represent the fingerprint of compounds and therefore it is possible their identification. With excellent spatial resolution and smaller amount of sample requirements, micro-Raman spectroscopy can recognize many species of materials. In the field of conservation and restoration of cultural items, it is mainly used in identifying pigments in paintings, and even their degradation products, providing insights into the working method of the artist and causes of degradation [33]. Moreover, it is also able to identify some organic materials, even if this possibility is less exploited than the characterization of pigments. Whereas, the Raman effect is intrinsically weak and some materials are inherently weak Raman scatters. On the other hand, some dark-colored or black pigments tend to absorb rather than scatter

radiation and laser irradiation may always pose the risk of altering the material analyzed. Also, Raman spectra are prone to disturbed baselines as a result of sample heating or fluorescence interference. FT-IR spectroscopy or micro-FT-IR spectroscopy can be fruitfully used to identify many types of pigments, dyes, organic and inorganic compounds [34] In particular, the identification of organic materials is better achieved than with Raman spectroscopy because the provided spectra are not disturbed by "scattering and fluorescence phenomena". Through the comparison of reference and unknown spectra, mainly in the fingerprint regions, it is possible assign each peak of the spectrum to specific pigments, binding media, varnishes and other compounds (e.g. degradation or restoration products), simultaneously. However, in some cases the spectra do not show clear and well-defined peaks and this makes difficult the identification of all compounds. The poor resolution of the spectra is due to several factors, such as the sample preparation, the contemporary presence of many compounds, the intensity of the absorption bands and the complex interacting vibrations within single molecules. As a result, a superimposition of bands is observed and compounds present in very low amount cannot be detected. Moreover, the identification of specific substances from one class of organic materials (e.g. dammar and mastic belonging to the class of natural resins) in a matrix is not possible.

The most equipment applied for paintings characterization is operate in lab conditions. However, since last decades a lot of portable techniques emerge to satisfy the

requirements of in-situ analysis. Although the resolution and accuracy of portable equipment cannot be comparable to laboratory instruments, they allow a preliminary and fast characterization.

1.2 Reflectance spectroscopy

Reflectance spectroscopy is the technique used to investigate the spectral feature of surface-reflected radiation with respect to its angularly dependent intensity and composition of the incident primary radiation [35].

1.2.1 Basic theory of reflectance spectroscopy

Light is an electromagnetic radiation within a certain portion of the electromagnetic spectrum. In the scientific definition, light refers to all electromagnetic waves. However, it has considered having wave-particle duality, because has properties of particles and waves volatility. As electromagnetic wave, light also has well defined energy. Once it irradiates on the surface, several circumstances may happen. Light may be reflected, diffracted, partially/totally absorbed, or transmitted by the irradiated surfaces depending on the energy of light and type of irradiated substrate. In most cases, all these four optical phenomena occur almost simultaneously, but ones of them will be dominated by many factors, such as the wavelength (λ) of light, material of irradiated surfaces, etc. The study of the interaction between matter and electromagnetic radiation is spectroscopy. Spectroscopic studies are developed by

quantum mechanics and include Max Planck's explanation of blackbody radiation, Albert Einstein's explanation of the photoelectric effect and Niels Bohr's explanation of atomic structure and spectra [36].

Based on the nature of interaction with matter, reflectance spectroscopy is a technique that measures the amount of (sun) light absorbed or reflected by the detected surfaces at specific wavelengths. More specifically, it investigates the spectral composition of surface-reflected radiation related to its angularly dependent intensity and composition of the incident primary radiation. When discussing reflectance, there are two essential limit cases: regular (specular) reflection from a smooth surface, and diffuse reflection from an ideal matte surface. Since the microscopic surfaces of the particles that constitute the layer behave like elementary mirrors and are directed in space with an angular distribution, the surface reflection can have a different direction than the specular one, as shown in Figure 1.5. The fact is that no surface is ideally matte, and the reflected radiation would not be isotropically distributed. All possible variations found in real practice are between these two extremes as described in G. KortUm.

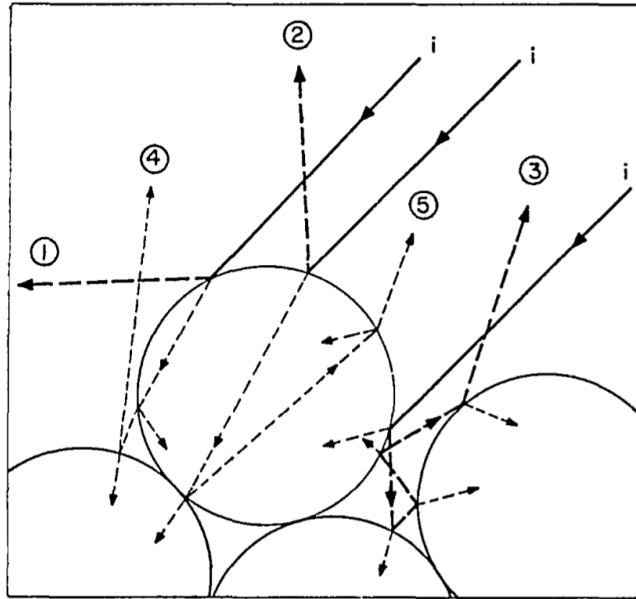


Figure 1.4 Interaction between electromagnetic radiation and the top layer of particles comprising a mat surface. [37]

Figure 1.4 gives a general view of the light behavior when it irradiates the matte surfaces. The sum of the part of the radiation which has not entered the sample is called surface reflectance R_s , which is represented by lines 1-3 in the figure. While the sum of the part of the radiation which has entered the sample and is then reflected after being partially refracted and transmitted by the particles, is defined as the volume reflectance R_v (lines 4-5 in Figure 1.5). Therefore, R_v contains the main spectral information. R_s and R_v are affected by many factors. Besides the intensity of the incident light and the smoothness of the surface, the absorption coefficient of a medium and the thickness of the transmitting medium also play a fundamental role. As a result, the reflectance spectra are greatly affected by these factors [38].

According to Kubelka–Munk (KM) phenomenological theory for diffuse reflectance from opaque surfaces, the scattering and absorption coefficients (s and k , respectively) also need to be taken into consideration. If the incident radiation is diffused and any regular reflection is excluded, the so-called KM function (F) can be obtained (Eq. 1.2), where R_∞ is the reflectance when the layer's depth can be said to be infinite; that is, the reflectance does not change under any further increment in depth [39].

$$F(R_\infty) = \frac{(1-R_\infty)^2}{2R_\infty} = \frac{\alpha}{s} \quad (\text{Eq. 1.2})$$

However, R_V is influenced by several parameters such as wavelength, chemical and physical structure of materials (e.g. particle dimensions, surface roughness and packing density, scattering and absorption coefficients, refractive index). For example, in a crystal, whose dimensions are large compared with the wavelength, but small compared with the cross-section of the beam of radiation, it is possible to distinguish between rays striking the crystal and those passing by it. The formers are partly reflected and partly refracted, in many cases repeatedly, so as to give a definite angular distribution of the corresponding radiation flux. In the latter case an incomplete wave front is formed, and because of the Huygens principle, interference of the elementary waves leads to diffraction phenomena, which give a quite different angular distribution of the corresponding radiation intensity depending on the form and dimensions of the crystal, though not on the nature of the crystal and its surface. Finally, the total reflectance R_T is the balancing of R_S and R_V , resulting in different band shapes depending on the dominance of the R_S or R_V factor [38]. If the peak is

very strong and materials constituted by large particles compared to the wavelength, R_S dominates; while, for weaker bands and small particles, R_V has a dominant role resulting in a minimum for R_T .

Through reflectance spectroscopy it is possible to analyze the electromagnetic radiation absorbed, emitted or scattered by atoms and molecules as they undergo transitions between energy levels. Energy levels, refers to the discrete states in molecules and atoms in quantum theory. The difference between the two energy levels is associated with frequency (ν) of the magnetic radiation and Planck constant (h) like the equation shown in Eq. 1.3. The energy level in a molecule is described as the sum of the atomic and molecular motions due to translational, rotational, vibrational, and electronic energies. Reflectance spectroscopy is the combination of atomic and molecular motions due to the interaction of the radiant energy and the material.

$$\Delta E = h\nu \quad (\text{Eq. 1.3})$$

The UV-VIS region spans an energy range sufficiently wide to encounter effects due to several different electronic processes. Molecules containing π -electrons or non-bonding electrons (n-electrons) can absorb energy in the form of ultraviolet or visible light to excite these electrons to higher anti-bonding molecular orbitals. The more easily excited the electrons (i.e. lower energy gap between the HOMO and the LUMO), the longer the wavelength of light they can absorb. There are four possible types of transitions ($\pi-\pi^*$, $n-\pi^*$, $\sigma-\sigma^*$, and $n-\sigma^*$), which can be ordered as follows:

$\sigma\text{-}\sigma^* > n\text{-}\sigma^* > \pi\text{-}\pi^* > n\text{-}\pi^*$. Analytes, such as transition metal ions, highly conjugated organic compounds, and biological macromolecules, can be determined in this electromagnetic region.

Near-infrared reflectance spectra, however, apart from few electronic transitions, mainly result from the periodic motions (or vibrational modes) of atomic nuclei within their respective molecules [41]. Periodic motions refer to, nuclei move together or apart along a straight-line vector. Relative to their centers of gravity in a molecule, nuclei in corresponding molecules rotate, vibrate, wag, and bend, where can be observed through their spectra in near-infrared region. Translational energy has no effect on molecular spectra, whereas the other motions affect the spectral characteristics, such as rotational energy, which is proportional to the angular velocity of rotation for each molecule. Only the vibrational excitations or absorptions are seen in the infrared spectrum when a change in the dipole moment of a molecule occurs. The single factor most important to affect the dipole moment is the symmetry of the molecule. Depending upon the bond type, there are multiple types of molecular vibrations of near-infrared energy and each vibration has a unique frequency where absorption occurs [34]. Typical applications of NIR spectroscopy include the analysis of food products, pharmaceuticals, combustion products, and a major branch of astronomical spectroscopy. As a result, these reflectance spectra can be used to detect, identify and quantify information about the atoms and molecules.

1.2.2 General application in cultural heritage

In the field of cultural heritage, reflectance spectroscopy in the visible region was applied to the study of paintings for the first time during the decade from 1930 to 1940. This methodology was subsequently developed at the Conservation Laboratories of the National Gallery, London [42]. Despite of its early application, reflectance spectroscopy had become a less commonly used analytical method due to its relatively low resolutions and complexity of spectra themselves. Its popularity was mainly in the geological field, especially when used in remote sensing. G. R. Hunt studied the earliest applications in 1966 [43]. The absorption of visible light in the minerals used as pigments is mainly due to four main mechanisms of electronic transition in UV-VIS range [44]: 1) charge transfer between ions and ligands; 2) transition among d–d orbitals due to the ligand field; 3) transition from valence to conduction band attached to specific elements in semiconductors; 4) delocalized molecular orbitals. The reflectance spectra of many fundamental geological minerals were illustrated in the work of G.R. Hunt; [45]; moreover, the shift of the absorption peaks caused by some important atoms, which frequently emerged in the minerals, were also considered. Later, Clark and Hunt improved the technique by increasing the spectral resolution [46]. They created a database of minerals in earth on USGS [47], which is well accepted by other researchers who studied in the reflectance spectroscopy field.

Thanks to the work did by G. R. Hunt, the application in the works of art conservation has been re-emphasized. Starting from the beginning of the 1980, portable spectrophotometers equipped with optical fibers that operate in the visible and near infrared regions have been extensively used and improved. M. Bacci et al. used this technique to understand the color inalterability of pigments and monitor the color changed during aging, as well as to identify pigment mixtures on the frescoes in the Brancacci Chapel [48,49]. In the following 30 years, with the advent of fiber-based instruments, applications of UV-VIS-NIR reflectance spectrophotometry to cultural heritage have grown rapidly since fiber optic reflectance (FORS) firstly mentioned in 1992 [50]. Now, it was quickly becoming one of the most widely used analytical tools for the non-invasive analysis of cultural relics [51]. The analytical range provided by the instruments locates between 290-1000 nm, and only recently, M. Aceto et al. extended the analytical range up to 1700 nm. During the last 30 years, not only the wavelength, but also the number of analytes detected by reflectance spectroscopy has been expanded: from identification of mainly inorganic materials i.e. pigments [52-54] to some organic ones [55,56], as well as different kinds of objects (from ancient paintings to contemporary art collections) [56,57]. More recently, J. K. Delaney and his groups worked on the identification of alkyd resins and linseed oil by reflectance spectroscopy and X-Ray fluorescence imaging spectroscopy [58]. But the characterization and identification of a wide range of organic materials is still very limited. A. Cosentino discussed the effect caused by different binders (egg yolk, linseed oil and calcium carbonate in frescoes) for the detection and identification of

historical pigments. However, the reflectance equipment used, mainly the technical photography, did not include the near infrared and short wave infrared regions [59]. Very recently, Daveri A. etc gave a perspective view in the characterization of painting materials by using hyperspectral imaging in the MWIR (2700-5500 nm), with only one example of zinc white mixed with different binders [60]. Since the essence of pigments is a mineral, Clark and Hunt's work still played an essential role even in the field of cultural heritage. The most used database of reflectance spectroscopy in this field is that of USGS [61] and IFAC [62].

Considering that the reflectance spectroscopy is a totally non-invasive technique to artworks, and can analyze organic and inorganic compounds simultaneously, recent researches are still far from being completely exhaustive. First, the much less discussed region of reflectance spectra is located between 1000-2500 nm, which is the region where important information due to vibration process of chemical bonds is found. Secondly, the analysis of organic compounds should be much more extended, as well as the study on the possible interactions between organic and inorganic materials. Last but not least, some reflectance spectra reported in the literature are only addressed to some special cases, and therefore valid for the situations similar to that discussed in the corresponding works. For instance, Aceto M. and coworkers illustrate the standard spectra of the most frequently used colorants on illuminated manuscripts [24-26]. A. Cosentino created a database of the reflectance historical pigments in powder and mixed with different binders within the spectral region 200-900 nm [63]. However,

they cannot treat as standards the pure compounds because the spectra were collected after mixing pigments with egg yolk and application on parchment and paper. Besides, spectra in full range found in USGS database are in general for mineral study, some characteristic peaks may be affected by impurities or symbolic minerals, which may cause interference when they are used for pure material identification. Moreover, there are several factors may influence the final spectra when the spectra are acquired using fiber optics. Because of the complex diversity of research materials, a database for this discipline is urgently demanded.

1.3 Hyperspectral sensor ASD FieldSpec FR Pro

1.3.1 Background information of hyperspectral sensor

1.3.1.1 Structure

Hyperspectral sensors are designed to collect tens to hundreds of narrow spectral bands of a surface (such as images of a scene) nearly simultaneously. From the spectral power distribution, the radiometric, photometric, and colorimetric quantities of light can be determined in order to measure, characterize, and calibrate light sources for various applications. A spectroradiometer, which uses hyperspectral sensor(s), is a special kind of spectrometer where detectors, other than photographic film, are mounted to measure how materials reflect or transmit light, i.e. giving information of the distribution of radiation in a particular wavelength region.

It consists of four main units: an input optic, a monochromator, a photo detector and a system of control and logging. A general schematic structure of a spectroradiometer is shown in Figure 1.5. Input optics allows gathering irradiation from a specific field of view and then delivering it to the monochromator. The kind of material lenses, diffusers, or filters can determine the waveband of radiation which will reach the monochromator. For example, in the case of measuring short wavelength UV, inside of glass, quartz lenses, optical fibres etc. are needed for radiation. A monochromator has a diffraction grating or a prism, which is able to isolate a narrow band of wavelengths, which is the paramount important part for spectra analysis. Diffraction gratings are preferable due to their versatility, low attenuation, extensive wavelength range, lower cost, and more constant dispersion. While, the photo detector is to measure the intensity at each designated wavelength, which is sensitive to the radiation in the desired visible spectral region and can receive diffuse and total reflection. The basic detector technologies are divided into three groups: photoemissive detectors (e.g. photomultiplier tubes), semiconductor devices (e.g. silicon either as a single detector or an array), and thermal detectors (e.g. thermopile). The type of detector used for this measurement will be determined by the wavelength range, dynamic range and sensitivity required of the measurements. Silicon photodiode, for instance, is used for 200-1300 nm; InGaAS is more specific for near infrared region (800-1800 nm). Photomultiplier tubes are the most sensitive detectors in the UV and visible by several orders of magnitude, but they require a specialized

power supply and are not as rugged as the semiconductor devices. They are also temperature sensitive so for accurate measurements in a changing environment they should be temperature stabilized. The last unit, the control and logging system is often performed by a personal computer. It acquires diffuse reflectance to describe color in CIE terms and also the total reflectance to analyze the intensity of the light beam.

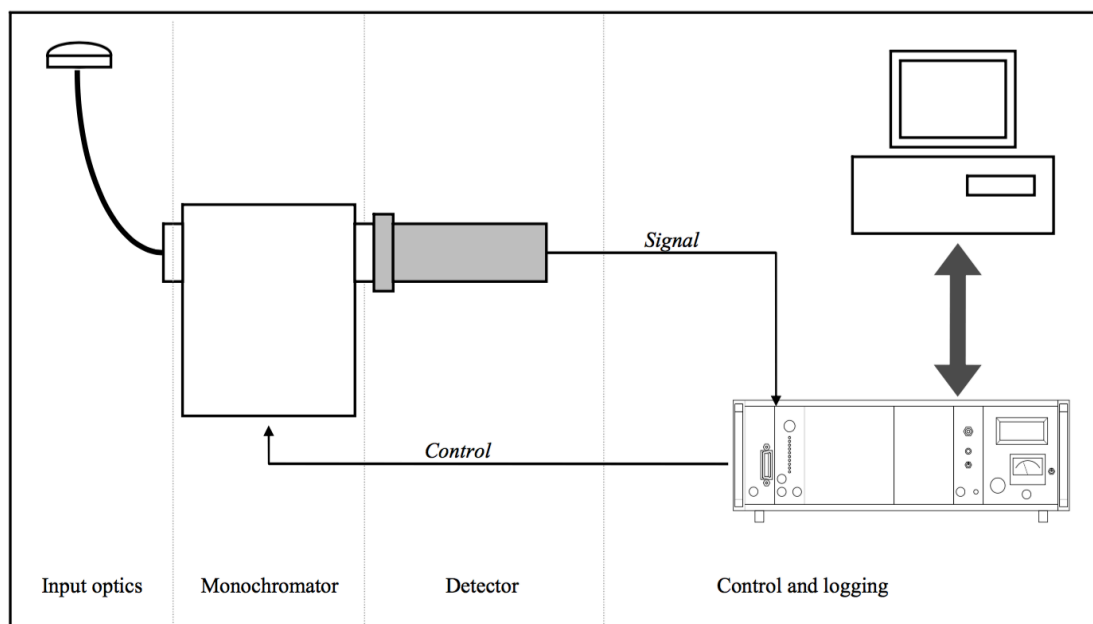


Figure 1.5 The basic structure of a spectroradiometer [64]

1.3.1.2 Hyperspectral vs. multispectral sensor

Known as Imaging Spectrometers, hyperspectral sensors are a systems technology whereby images of a scene are collected in tens to hundreds of narrow spectral bands nearly simultaneously [65]. They represent the next step in the spectral dimension of the evolution of multispectral imaging radiometers currently represented by satellite sensors such as the Landsat Thematic Mapper, which collects data in seven simultaneous bands. The data collected are often termed an “image cube” where the

two spatial dimensions are joined by the third spectral dimension. Compared with multispectral sensors, hyperspectral sensors acquire images in many continuous spectral bands with a narrow bandwidth (width of an individual spectral channel in the spectrometer), which permits acquisition of laboratory-like spectra also from remote sensors. These sensors are able to acquire continuous spectral bands which are constrained to a relative narrow bandwidth [66], as it is shown in Figure 1.6.

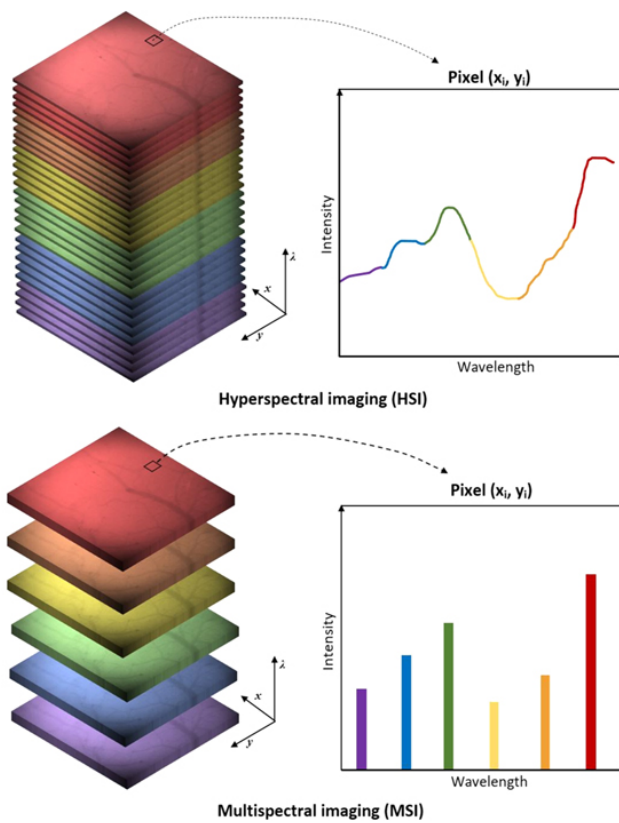


Figure 1.6 Comparison of hyperspectral and multi-spectral imaging and their spectra [66]

1.3.1.3 Curve understanding

A spectrum is obtained in a particular region when the amount of power reflected/transmitted by a material is plotted in a curve as a function of wavelength.

The shape of the curve provides fingerprint characteristics of its chemical and physical nature [67]. In the visible region of a spectrum, the color of a material is indicated at the top of the spectroscopic curves in the monograph from the basic three dimensions of the color-hue, saturation and lightness. Hue can be visualized approximately from the reflectance maximum. If a sample looks green, an absorption peak in 495-570 nm can be found. And yellows reflect green, yellow, orange, and red, which visually mix additively to make yellow. The examples are shown in the Figure 1.7. Saturation may be indicated from the contrast between the reflectance minimum and maximum. More the contrast is, a higher saturation of the color has and lightness from the amount (intensity) of reflectance is [67].

The negative curves, i.e. absorption maxima/shoulders, give information of electronic and combination bands of atoms and molecules, like what is already discussed in Chapter 1.2.1. The light absorption in the infrared region, rather than electronic excitation of the substance in the visible region, mainly corresponds to different kinds of vibrational excitation. These excitations are characteristic of different groups in a molecule that can in this way be identified.

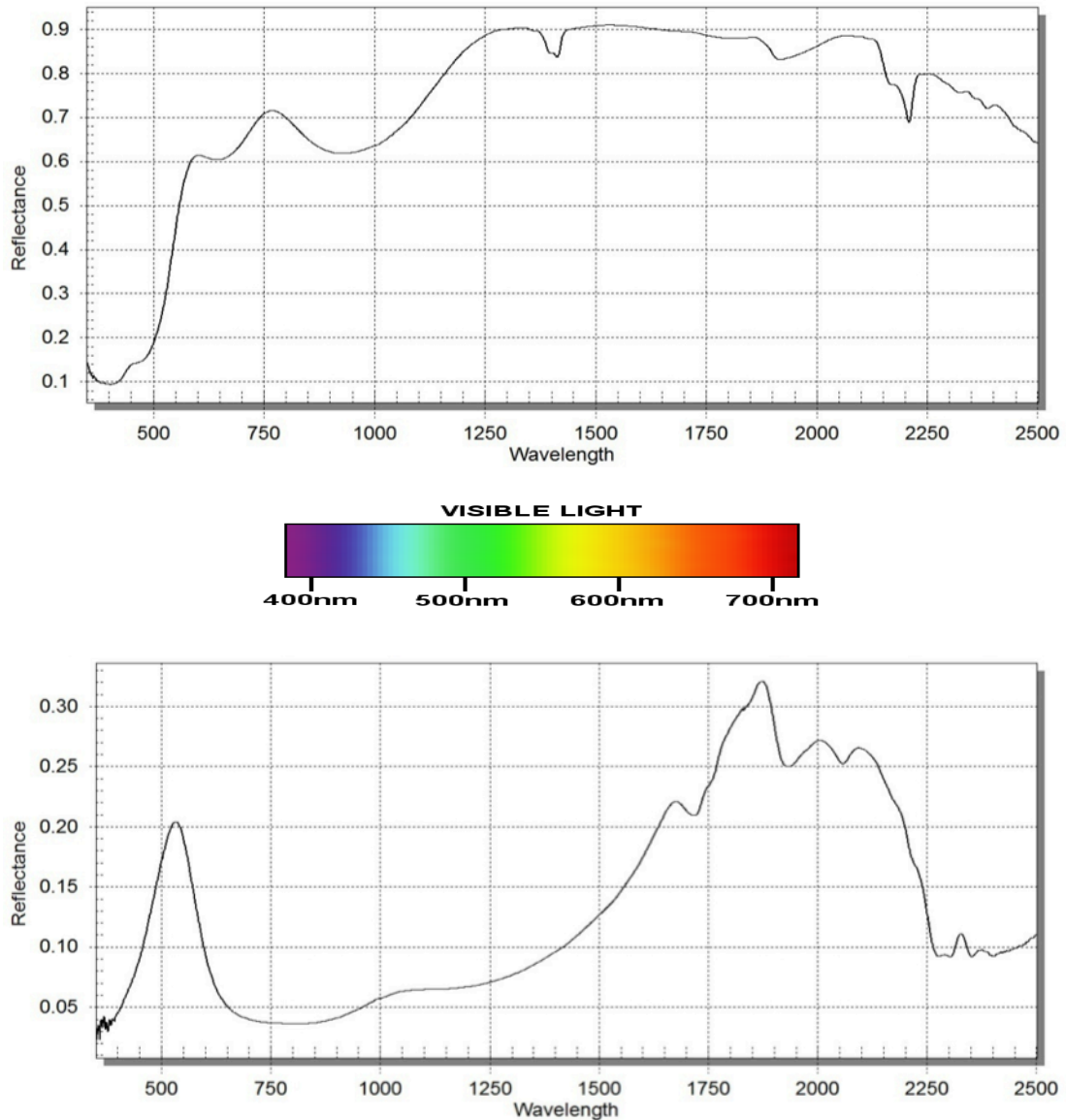


Figure 1.7 Curve understanding of spectra in full UV-Vis Near Infrared region.

1.3.1.4 ASD FieldSpec FR Pro

Among hyperspectral sensors, Analytical System Devices FieldSpec FR (full range) Pro 3 (ASD FieldSpec FR Pro/FieldSpec in brief) was selected. It is a portable sensor and measures the optical energy that is reflected by, absorbed into, or transmitted through a sample within the range of 350-2500 nm. Optical energy refers to a wavelength range that is greater than the visible wavelengths, and is often called

electromagnetic radiation or optical radiation. In its most basic configuration, the instrument views and detects the form of radiant energy defined as radiance. With accessories, various set-ups, and built-in processing of the radiance signal, the instrument can measure: spectral reflectance, spectral transmittance, spectral absorbance, spectral radiance and spectral irradiance [68]. The grating separates light collected by fiber cable and reflects the wavelength components for independent measurement by the detector. The first spectrometer, covering from 350 to 1000 nm, is based on a 512 elements photodiode array. Because the wavelength coverage of this spectroradiometer is more than one octave, a multi-element order-sorting filter is mounted on top of the detector array. This filter prevents second order (and higher) diffracted light from reaching the detector [69]. The second and third spectrometers, covering from 1000 to 1800 nm and from 1800 to 2500 nm respectively, cover a wavelength range that is less than one octave. The detector in each spectrometer has a long pass filter, with wavelength cut-off of 980 nm and 1750 nm respectively. Additionally, FieldSpec FR Pro 3 has a contact probe as an artificial light with fixed illumination 45°, which avoids the direct reflection and permits to collect total and diffuse reflection. What more important is that there is a halogen lamp inside the probe. Thus, it is able to use both ambient solar irradiation (when turn off the lamp) and artificial irradiation.

As which discussed above, the instrument acquires continuous reflectance spectra in the range of 350-2500 nm, which covers visible (VIS), near infrared (NIR) and short wave infrared (SWIR) regions. This character allows people to identify both inorganic and organic materials. The shape of spectra curves in visible range provides useful information to differentiate colours of materials; while, the spectra absorptions in the VNIR regions is a function of different electronic and vibration processes of molecules. Pigments and dyes can be identified by their own specific spectra. Besides, hydroxyl, which is often a part of the crystal structure of a mineral and closely related with organic materials, is often infrared active. H₂O and CO₃²⁻ can also be identified in 900 to 2500 nm range because of the overtones and combinations bands [70]. Equipped with a high resolution and fast capturing speed, a good spectrum can be collected in as short as 0.2 s. In addition, a spectrum can be obtained with either constant artificial light (by using a Contact Probe) or natural light, meanwhile, it is easy to carry by its specific backpack, which allow analysis done even *in situ*.

1.3.2 General application and its usage in cultural heritage

Hyperspectral sensors are the instruments which used to provide inflight radiometric calibration of optical sensors, their ability permits acquisition of laboratory-like spectra also from remote sensors [70]. Their application is relatively recent. Its applications are widely used in the field of geology, i.e., remote sensing, including almost all areas of Earth science [71]: land, water and atmospheric topics. Regard to

the land application, it includes vegetation studies [72] (species identification, plant stress, productivity, leaf water content, canopy chemistry), soil science (type mapping and erosion status [73]), geology (mineral identification and mapping [74]) and hydrology (snow grain size, liquid/solid water differentiation). Lake, river and ocean applications include biochemical studies [75] (photo-plankton mapping, activity), water quality (particulate and sediment mapping) and bathymetry. Atmospheric applications include parameter measurement [71] (water vapor, ozone, and aerosols) and cloud characteristics (optical thickness, cirrus detection, particle size).

For the works of art, more frequent application of hyperspectral sensor is in the reflectance hyperspectral imaging, also called reflectance imaging spectroscopy (RIS) since 2000, which introduced in the 1980s by Goetz and co-workers [74]. It is a sophisticated technique that enables the capture of hundreds of images in contiguous narrow band, and now has become more widespread in the field of conservation science [76]. New compact and sophisticated spectrometers and spectroradiometers allow researchers to address the natural heterogeneities, and to develop the so-called “field spectroscopy”, which greatly improves its potential applications. The earliest application of the hyperspectral sensor was used as a non-invasive technique for *in situ* characterization of stone surface alterations (Vettori et al. 2008, Camaiti et al. 2011) [77-79]. To better understand the alterations of gypsum affecting the marble, Fieldspec data collection was done on the façade of the Santa Maria Novella church. Then it was used to monitor and identify the organic materials applied on historical

stone surfaces as protective agents (Alparone et al. 2011, Camaiti et al. 2013) [80]. For paintings, the application is not so common. Thanks to the high sensitivity of the color of reflectance instruments, the main application of reflectance analysis in artworks are concentrated in pigment identification. Maynez-Rojas M.A. (2017) used the same equipment to acquire spectra of natural red and purple dyes, which proved its use for the differentiation ability on textiles [81]. P. Riccardi and etc. used ASD FieldSpec FR 4 to identify the green pigments (malachite and verdigris) on the illuminated manuscripts, but the identification fingerprints still locate at the wavelength before 1700 nm [82]. For organic material study, I studied the detection of varnishes on painting surfaces after a Er:YAG laser cleaning for master degree [14]. Delaney. and his groups applied the instrument to identify egg yolk and animal glue from gypsum ground [83], also for the identification of linseed oil and alkyd in the painting [58]. Although some characteristic peaks in some regions between 1000-2500 nm of these binders were compared to their FT-NIR spectra, a general comparison of these binders are less-discussed, moreover, the interaction caused by the mixture of pigments and the lack of mock-ups as standard were not mentioned.

All the above discussed on the theoretical knowledge and the previous work indicates that, this hyperspectral sensor, ASD FieldSpec FR pro is capable to identify both inorganic and organic materials in painting surfaces. Although it gives us less information than FT-IR and Raman analysis, the process is totally non-invasive and

rapid. Compared with the most similar technique FORS, it has extended spectral range giving more information, which allows the development of reflectance spectroscopy in the characterization of paintings. Thus, a systematic study of the characterization by this instrument should be explored. And the results should be confirmed by other techniques. Only in that way, FieldSpec could be used as a powerful tool for characterizing the heterogeneous surface in a non-destructive and non-invasive way.

1.3.3 The influencing factors of reflectance spectra by FieldSpec FR Pro and database creation

To get the best reflectance/absorption spectra, it is a necessity to find a correct methodology for collecting a spectrum. As described in Chapter 1.2.1, there are many factors that can affect the quality of spectra. There are three main factors which influence the irradiation received by detectors. The first one is the amount of electromagnetic radiation reached to the surface, which influences the intensity of spectrum peaks. This factor determines mainly by the light source, the distance between light source and surface. It is true that total and specular reflection is not effective on the spectra, while diffuse reflection becomes more essential, more specifically, surface reflection R_S and volume reflection R_V (more considered). Consequently, the optic geometry of the spectroradiometer can also make a difference because the incident angle can eliminate specular reflection. Second factor is the

properties of the substance itself. Apart from absorption coefficient and scattering coefficient, the parameters such as particle sizes, size contributions also influence the final spectrum. Regardless of the optical properties, the last factor that may affect the quality of a reflectance spectrum is the roughness of the surface. For solid substance in powder form, the amount of substances or the particle concentration on the surface is more essential.

In our case, a contact probe has been used to collect reflectance spectra. It provides a fixed optical geometry (45°), which avoids specular reflection. The inside lamp of the contact probe provides a constant artificial light, which get the radiation light at the same wavelength and intensity at every time. At the same time, the way that direct contact on materials makes the distance between the detected surface and light source constant. The Contact probe is very easy to hold and reduce the systematic errors caused by manual operations. The major of tested substances are commercial products (mainly colorants) with more or less homogeneous particle sizes and size distributions. Thus, in our research, the main factor affecting the reflectance spectra on pure pigments is the roughness of the surface mostly based on the amount of pigment powder. For organic and organic mixtures, the influence of surface roughness on the signal intensity of the spectra is not discussed because of this factor is impossible to control on the surface after the organic and organic mixture are applied and dried. After the comparisons, a database of reflectance spectra of historical materials with most characteristic features was created.

1.3.4 Principle Component analysis (PCA) for data processing

First introduced by K. Pearson and then developed by H. Hotlin, principal component analysis (PCA) is a statistical procedure that uses an orthogonal transformation to convert a set of observations of possibly correlated variables into a set of values of linearly uncorrelated variables called principal components. In practical topics, in order to comprehensively analyze a problem, many variables (or factors) related to it are often proposed, because each variable reflects certain information of the subject to varying degrees, in our case the values of each wavelength. The size of the information is usually measured by the sum of squared deviations or variances. The PCA reduces the dimensionality of a multivariate data set by projecting the large data space into a smaller space. This is a useful feature when dealing with a large number of variables, as with the detectors used in the current reflectance spectroscopic technique, which are able to read a huge number of reflectance/absorption value and corresponding wavelengths. The principal component analysis has been used in remote sensing for different purposes, as well as multispectral imagery. In this work, we intend to take advantage of this analytical method to identify some common organic binders used in paintings, when mixed with specific pigments.

Chapter II

Aim of the thesis

Non-invasive characterization always plays an essential role in the conservation of painting surfaces, since more information may be obtained with less sampling for invasive analysis. Reflectance spectroscopy is a well-established technique for acquiring compositional information of materials for paintings. However, due to the limit of the resolution of reflection instruments, it is not widely used as when it was first introduced in 1930. It was re-emphasized until fiber optic reflectance was proposed and used in this field. The majority of researchers applied different kinds of spectrometers and spectrophotometers for pigments study; the main analytical regions of investigation they use are in the range of 250 to 1100 nm, and mainly inorganic materials are detected. Moreover, the general database of reflectance spectra they used is the mineral spectra from USGS library. It has several disadvantages, when using it to characterize painting materials: 1) its relative old spectra are acquired with relative low resolution; 2) possible interferences caused by some associated minerals; 3) the lack of some specific colorants (such as artificial pigments and dyes). As regard the organic materials, only recently a few researchers mentioned some comparison between organic binders, but they compared pure materials and their studies were mainly focused on illuminated manuscripts. Moreover, the possible shifts caused by

the mixing of pigments and binders are not mentioned yet, which is of paramount importance for the identification of paintings components.

Hyperspectral sensor, ASD Field Spec FR Pro, is a spectroradiometer designed to acquire reflectance spectra which covers the full range, i.e. 350 to 2500 nm, giving the possibility to improve the diagnosis in this particular field of application. Within this range, a reflectance spectrum can give both elemental and molecular information of a material: the features of spectra in visible and near infrared range are due to several mechanisms of electronic transition; while the short wave infrared range is characterized by the presence of vibrational transitions, mainly overtones and combination bands. Therefore, the spectra collected in this range make possible the identification of inorganic and organic materials, and even mixtures of them, which is particularly important for heterogeneous artworks, e.g. painted surfaces. As a non-invasive technique, it not only owns a high resolution but also fast capturing speed. A good spectrum is acquired within 0.2 s. Last but not least, this spectroradiometer is portable which allows in-situ diagnosis. All these advantages make this instrument a powerful tool for scientific investigations on masterpieces of whatever dimension.

The main aim of this thesis is the validation of an hyperspectral sensor as a spectroscopic analysis instrument for the identification of both inorganic and organic materials when mixed together as in a painted surface. The so called “matrix effect”

responsible for spectral feature changes will be evaluated in order to use the acquired spectra as reference for imaging spectroscopy, which is not included in this work because it requires a hyper camera to collaborate with. The detailed aims of my research are as follows.

First and foremost, a database of painting materials is created with best reference spectrum of each pure substance. Pure materials include the inorganic and organic pigments widely used both in the past and in restoration interventions, as well as four different natural binders (i.e. egg yolk, animal glue, linseed oil and gum Arabic). Since colorants are in powder, the factors that may influence their spectrum quality will be discussed. Besides, the spectra collected by different methods will be compared. For organic materials, in our case binding media specifically, their identification work will be highlighted by the recognition of their characteristic features in reflectance spectra.

The surface of painting mock-ups (different colorants mixed with binders) will be then analyzed by FieldSpec FR Pro. Based on their specific and characteristic spectral region/regions, the distinction of each binder from its mixture with colorants will be carried out. The possible band shifts of each binder caused by the mixing of varied pigments will be interpreted, as well as effects caused by the amount of organic substances. Then, the identification of different binders mixed with the same pigment

will be elaborated, through their raw and 1st derivative spectra as well as the Principle Component Analysis (PCA).

Finally, the newly established research protocol above mentioned will be verified by employing it on two case studies. The first case is the characterization of colorants and binder in a XIX century canvas painting by an unknown author. The other one is the identification work of colorants and varnishes on a XVIII century fresco located in the Church of Saint Stefano in Lamporecchio – Florence).

Chapter III

Experimental

In this chapter, the materials and methods employed in the thesis were illustrated. The first section is dedicated to the description of the materials, sample preparations and the methodology used to acquire the reference data of both organic and inorganic materials. The second section describes the adopted experimental methodology and instrumental during the study. In the last part, the method of data processing is discussed.

3.1 Materials

To verify the ability of the hyperspectral sensor in identifying application the components of painted surfaces, pure materials were analyzed firstly. The pure materials include the principal components of a canvas painting, i.e., canvas, pigments, binder and varnishes. And then laboratory model of canvas painting (i.e. painting mock-ups) were prepared on canvas which was already prepared with ground layer. Materials were mixed together to paint on the canvas in the way as for ancient easel painting. During preparation, each layer of paintings was characterized by the hyperspectral sensor.

3.1.1 Pure materials

3.1.1.1 Colorants

Colorants analyzed by the hyperspectral sensor are the most commonly materials used historically by artists. All the synthetic colorants, listed in the Table 3.1, were purchased from Zecchi, Florence. Some natural minerals come from specific regions, such as natural cinnabar which comes from Amiata Mountain, and lapis lazuli, still as rock fragment, from Afganistan.

Table 3.1 Pigments used in the experiment.

Category	Colorants	Main Chemical composition	Used for making painting mock-ups or not
	Armenian bole	$\text{Fe}_2\text{O}_3 + \text{Al}_2(\text{SiO}_4)_3 + \text{Kaolinite}$	Yes
	English red	$\text{Fe}_2\text{O}_3 + \text{CaSO}_4$ (more)	Yes
	Ercolano red	$\text{Fe}_2\text{O}_3 + \text{CaSO}_4$ (less)	No
Red	Natural Cinnabar (Monte Amiata)	HgS	Yes
	Synthetic cinnabar	HgS	No
	Cadmium red	CdS	Yes

	Yellow ochre	$\text{FeO(OH)} \cdot n\text{H}_2\text{O}$	Yes
Yellow	Naples yellow (light)	$\text{Pb(SbO}_3)_2/\text{Pb}_3(\text{SbO}_4)_2$	Yes
	Naples yellow (dark)	$\text{Pb(SbO}_3)_2/\text{Pb}_3(\text{SbO}_4)_2$	No
Orange	Lead oxide	Pb_3O_4	Yes
	Malachite	$\text{Cu}_3\text{CO}_3(\text{OH})_2$	Yes
Green	Verdigris	$\text{Cu(OH)}_2 \cdot (\text{CH}_3\text{COO})_2 \cdot 5\text{H}_2\text{O}$	Yes
	Green earth	$\text{K}[(\text{Al}, \text{Fe}^{\text{III}}), (\text{Fe}^{\text{II}}, \text{Mg})(\text{AlSi}_3, \text{Si}_4)\text{O}_{10}(\text{OH})_2]$	Yes
	Azurite	$\text{Cu}_3(\text{CO}_3)_2(\text{OH})_2$	Yes
Blue	Egyptian blue	$\text{CaOCuO(SiO}_2)_4$	Yes

	Lapis lazuli	$(\text{Na,Ca})_8(\text{AlSiO}_4)_6(\text{S,SO}_4,\text{Cl})_{1-2}$	Yes
	Smalt	$[\text{Co,Ni}]\text{As}_{3-2}$	Yes
	Prussian blue	$\text{Fe}_4[\text{Fe}(\text{CN})_6]_3 \cdot x\text{H}_2\text{O}$	No
	Ultramarine blue	$3\text{Na}_2\text{O} \cdot 3\text{Al}_2\text{O}_3 \cdot 6\text{SiO}_2 \cdot \text{Na}_2\text{S}$	Yes
	Indigo	$\text{C}_{16}\text{H}_{10}\text{N}_2\text{O}_2$	Yes
	Lead white	Pb_3O_4	Yes
	St. John white	$\text{Ca}(\text{OH})_2$	Yes
White	Titanium white	TiO_2	Yes
	Zinc white	ZnO	Yes

Red pigments

Red ochre (Armenian bole, English red/Ercolano red)

Red ochre, or iron (III) oxides, is widely used as durable and inexpensive pigment in paintings. Armenian bole is a kind of soft, sticky and reddish clay, which contains variable percentage of red ochre. It can be used as it is, or acts as the “ground layer” for gilding and/or giving an obscure effect to the painting layers. The bole used in the experiment also contains kaolinite and potassium magnesium silicate. English red and Ercolano red are two different kinds of natural red ochre. Their main constitution is iron oxide, with some accessory minerals like quartz and also small amount of gypsum.

Cinnabar (HgS)

Cinnabar is a type of red mercury ore that was mixed with an equal amount of burning sulphur to create an expensive red paint that was highly popular with the Romans, where it was used for cosmetic and decorative purposes. Cinnabar was painted on the Pompeian baths of Titus, as well as on statues of the gods. Starting with the Song Dynasty, cinnabar was used to color Chinese carved lacquerware. Today, a safer resin-based polymer is used instead of the toxic cinnabar pigment.

Cadmium red (CdS)

The cadmium red is a red pigment with good permanence and tinting power. It has better resistance to the light irradiation compared to cinnabar, and the red color

remains the same when mixed with other colorants. It is always used when blending with silver white. When mixed with Naples yellow, the mixture gets a constant reddish color.

Carmin (Cochineal) (C₂₂H₂₀O₁₃)

The dye is extracted from the body of a small insect called *Coccus cacti*. The dye was introduced into Europe from Mexico, where it had been used long before the coming of the Spaniards. The red carmine is relatively stable and can be mixed with different kinds of binders (especially with different kinds of glue).

Yellow pigments

Yellow ochre [FeO(OH)·nH₂O]

Yellow ochre is a natural mineral that mainly consists of silica, clay and iron oxides. This color is found in the earth in the mountains, where there are certain seams resembling sulphur and where the seams are, there is found synopia, and terre-verte, and other kinds of color [50].

Naples yellow [Pb(SbO₃)₂/Pb₃(SbO₄)₂]

It is one of the oldest synthetic pigments, dating from around 1620. Naples yellow was used extensively by the old Masters and well into the 20th century. The genuine pigment is toxic, and its use today is becoming increasingly rare. Most paints labeled "Naples yellow" are instead made with a mix of modern, less toxic pigments.

Green pigments

Malachite $[CuCO_3 \cdot Cu(OH)_2]$

Malachite, which is a mineral basic copper carbonate, is moderately permanent pigment of varying color. It is perhaps the oldest known green pigment which is sensitive to acids and alkali, as well as heat. Occurs in Egyptian tomb paintings and in European paintings, it seems to have been of importance mainly in the 15th and 16th centuries.

Verdigris $[Cu(OH)_2 \cdot (CH_3COO)_2 \cdot 5H_2O]$

Copper (II) acetate gives the materials a vivid green color which makes Verdigris in this form as a pigment. It was first produced as the patina on the corroded bronze surface. Thanks to its property of lightfastness, it was widely used in the oil paintings since 15 century. It is a fickle pigment that requires special preparation of the painting. Even though Leonard da Vinci recommended its use, it was used only in a short period.

Green earth $[K(Al, Fe^{III}), (Fe^{II}, Mg)(AlSi_3, Si_4)O_{10}(OH)_2]$

Green earth, also known as terre verte and Verona green, is an inorganic pigment derived from the minerals celadonite and glauconite. It was firstly used in Roman period and was also found in the mural paintings at Pompei and Duro-europos. The color is also used as the bole and undercoating' materials for some fresh colors.

Blue pigments

Azurite [2CuCO₃· Cu(OH)₂]

Azurite is also called “Lapis Armenius”. It is a widely used blue pigment which is very easy to be confused with Lapislazuli. It was used in ancient times and also in 15th to 18th century. Because it is cheaper than Lapislazuli and the similar color, it is always used as a mixture with Lapislazuli by painters. The chemical composition is unstable, and it is very easy to change into malachite.

Egyptian blue [CaCuSi₄O₁₀ or CaOCuO(SiO₂)₄]

Egyptian blue is one of the most ancient colorants, which is considered as the first synthetic pigment. It was known to the Romans by the name *caeruleum*. It was used in Egypt for thousands of years, continuing in use until the end of the Greco-Roman period (332 BC–395 AD). Its characteristic blue color, resulting from one of its main components-copper-ranges from a light to a dark hue, depending on differential processing and composition. Due to the production process of the Egyptian blue, it does not have a definitive composition. And it always contains unreacted quartz and may also contain CaO and CuO.

LapisLazzuli (Untramarine blue) [3Na₂O· 3Al₂O₃· 6SiO₂· Na₂S]

Lapislazuli is natural and can be found in rocks together with deposit, mica, amphibole and calcite. This pigment was used from Egyptian, Greeks and Romans and

remained in use until the Renaissance period. To get a better color, the original mineral has to be grinded into very fine particles. It is one of most expensive and precious pigments in the ancient world.

Smalt $\{[Co,Ni]As_{3-2}\}$

The mineral smaltite ($[Co,Ni]As_{3-2}$) is the principal source of the cobalt used in the preparation of smalt in Europe, since the time of the Middle Ages. In the 17th and 18th centuries as associated cobalt mineral serythrite ($[Co,Ni]_3[AsO_4]_2 \cdot 8H_2O$) and cobaltite($CoAsS$) were probably also employed. The cobalt ore was roasted. The cobalt oxide(CoO) thereby obtained was melted together with quartz and potash or added to molten glass.

Prussian blue $\{Fe_4[Fe(CN)_6]_3 \cdot xH_2O\}$

Prussian blue is the first modern pigment, which is made from different reagents and its slightly different color stems from different impurities. It is significant since it was the first stable and relatively lightfast blue pigment to be widely used following the synthesis of Egyptian blue.

Indigo $[C_{16}H_{10}N_2O_2]$

The dye is derived from the plant *Indigofera tinctoria* and related species. It was originated from Eastern Asia and its first used dating back to 4000 BC. The color of indigo is blue-violet and it is often used in oil painting.

White pigments

Lead White [PbCO₃]

Lead white can be also called Silver white, which is more bright than other white colors. Even though lead white is poisonous, it was still one of the oldest color used in the antiquity until 19th century. Some artist (like Van Dyck) immerse the pigment into water and leave it for a long period. The color of lead white becomes more beautiful. It can also speed up the drying process of siccativ oil. White can be used as pure color or mixture with yellow to control the variable tonality of painting for a long period.

Saint John white (Bianco di San Giovanni) [Ca(OH)₂]

Bianco di San Giovanni is lime white pigment first described in literature by Cennino Cennini [84]. It is a pigment of inorganic, natural mineral origin from limestone deposits. It is dried lime which is reduced to powder and then immersed in the water for eight days that is changed each day. It is then made into small cakes that are left to dry in the sun. It is then grounded finely. Bianco di San Giovanni primarily consists of calcium hydroxide, also known as slaked lime, in a chemical compound with calcium carbonate. Bianco di San Giovanni is composed of slaked lime, and because it is dried in the sun, it absorbs CO₂ from the atmosphere and partially converts to calcium carbonate, or lime. Bianco di San Giovanni is considered the white pigment for fresco painting, and it is used also in tempera and grounds while it is not advised in oil and encaustic painting techniques.

Titanium white (TiO₂)

Generally Titanium white is sourced from ilmenite, rutile and anatase. It is the most widely used white pigment because of its brightness and very high refractive index, in which it is surpassed only by a few other materials. TiO_2 is also an effective opacifier in powder form, where it is employed as a pigment to provide whiteness and opacity to paintings.

Zinc white (ZnO)

The pigment was firstly used in oil painting in 1781 in Paris, which partially replaced lead white not only due to its non-toxicity but also the stability of the color when mixing with other colorants. The pigment naturally occurs in mineral zincite, but it is mostly artificially produced. Painters such as Böcklin, Van Gogh, Manet, Munch etc. used it in their works.

For characterization study, powder of pigments was accumulated on a substrate which is both transparent in appearance and to the radiation. Spectra were taken by depositing different amounts of colorants for collecting reference spectra. It will be discussed in the following part. Due to the fact that colorants are commercial products, the compositions of them were further confirmed by FT-IR spectroscopy (with the diamond cell, 64 scans and 2 cm^{-1} as resolution).

3.1.1.2 Binding media

Binders are also called binding media. In this study, four different organic materials i.e., Egg yolk, linseed oil, animal glue and gum Arabic, were selected and analyzed.

Egg yolk

Egg yolk is a binder which always used on panel and mural painting, and during restoration it was used as binder and/ or fixative. Once it is dry, it forms a film with good mechanical properties (cohesion, adhesion, flexibility). Fats give the right plasticity to the film. Besides, it does not yellow with age (the *egg lipids* are *not drying agents*).

Animal glue

Animal glue, in our case rabbit skin glue, has low molecular weight (40,000-10,000). It is mainly made of collagen, which is a fibrous protein with linear polypeptide chains arranged parallel to each other. It is considered stable compounds, but the presence of humidity strongly reduces their stability. It is insoluble in cold water, but soluble at 40-50°C. It undergoes partial hydrolysis and products with lower molecular weight are formed. Animal glues are extracted from animal tissue such as tendons, skin (skin glue) and bone (bone glue) and various parts of fish (fish glue). Thanks to their good adhesive power, animal glues have also been used as adhesives for wood

and tissue, binding of pigments, and in the preparation of pictorial support, e.g., gypsum with glue.

Linseed oil

Linseed oil is a type of drying oil. It is film-forming agent in protective or decorative coatings, was known since the antiquity. The property of forming films (hardening of oils) by the "drying oils" is due to the presence of unsaturation (C=C bonds) (e.g. linoleic acid, linolenic acid). The hardening is due to the polymerization (radical chain polymerization); on the contrary, the oxidation reaction (degradation) causes the formation of small molecules. There are many factors influencing the hardening of oils, such as light, presence of different metal ions in pigments, the thickness of painting film, degree of oil pre-curing and so on.

Gum Arabic

Gum Arabic, also called acacia gum, is the most famous vegetable gum. It is produced by the acacia trees to close wounds, or to stop the destruction of plant tissues, or to defend themselves against infection by microorganisms. Gum Arabic is made of sugars and uronic acids. They have complex structures, containing different sugars arranged in more or less long chains. They are soluble in water or form dispersions. It is also able to form a film after drying.

Egg yolk was firstly prepared on a Petri dish and analyzed until it was totally dried. Animal glue was first put into water in the room temperature 24hs for swelling and then heated to less than 50°C. Then it is applied on a Teflon substrate. Linseed oil which was purchased in 2003 was already prepared in 2010. While, gum Arabic was dissolved in the cold water and then applied onto the Teflon substrate to dry and form a film.

3.1.2 Painting mock-ups

The purchased canvas was divided into small squares with 10*10 cm² dimension. The stratigraphic composition of the laboratory models by simulating the canvas painting is schematized in Figure 2.1. Twenty-one pigments with different chemical compositions and various colors were selected, as marked in Table 3.2, 3.3, 3.4 and 3.5. Four binders were mixed with pigments and then evenly painted by brushes on the surface of the substrate. During the mixing, some water was added into the mixture like described by Cennino Cennini [84].

Table 3.2 Preparation of mock-ups with egg yolk as binding medium.

Color	Colorants	Weight of colorant (g)	Weight of egg yolk (g)
	Bolo	0.386	0.112
	Cinnabar (MA)	0.459	0.157
Red	Cadmium red	0.450	0.143

	Red lake	0.258	0.147
	Red ochre	0.464	0.197
	Green Earth	0.447	0.131
Green	Malachite	7.223	6.71
	Verdigris	0.642	0.259
	Azurite	6.101	6.098
	Smalt	1.163	2.038
	Egypt blue	1.19	1.716
Blue	Lapis Lazuli	3.095	3.983
	Indigo	0.334	0.156
	Ultramarine blue	0.499	0.212
Yellow	Naples yellow (Dark)	3.016	3.008
	Yellow ochre	2.823	5.201
	Lead white	3.589	3.600
White	Saint John's white	2.673	0.248
	Titanium white	0.321	0.094
	Zinc white	0.393	0/118
Orange	Lead oxide		

Table 3.3 Preparation of mock-ups with linseed oil as binding medium.

Color	Colorants	Weight of colorant	Weight of linseed oil
--------------	------------------	---------------------------	------------------------------

	Bolo	1.845	2.232
	Cinnabar (MA)	0.672	0.586
Red	Cadmium red	0.728	0.46
	Red lake	0.401	0.539
	Red ochre	1.092	0.621
	Green Earth	0.977	0.663
Green	Malachite	1.462	0.773
	Verdigris	1.477	1.505
	Azurite	1.340	0.558
	Smalt	0.585	0.597
	Egypt blue	0.902	0.577
Blue	Lapis Lazuli	0.309	0.282
	Indigo	0.577	0.823
	Ultramarine blue	0.354	0.373
Yellow	Naples yellow (Dark)	0.880	0.338
	Yellow ochre	0.384	0.402
	Lead white	0.848	0.315
White	Saint John's white	0.602	0.323
	Titanium white	0.551	0.344
	Zinc white	0.709	0.568

Orange	Lead oxide	0.775	0.317
--------	------------	-------	-------

Table 3.4 Preparation of mock-ups with animal glue as binding medium.

Color	Colorants	Weight of colorant	Weight of animal glue solvent
	Bolo	0.699	0.478
	Cinnabar (MA)	0.416	0.251
Red	Cadmium red	0.441	0.288
	Red lake	0.257	0.192
	Red ochre	0.492	0.392
	Green Earth	0.64	0.372
Green	Malachite	1.341	0.778
	Verdigris	1.876	1.58
	Azurite	1.796	2.765
	Smalt	1.051	1.409
	Egypt blue	1.791	1.131
Blue	Lapis Lazuli	0.272	0.246
	Indigo	0.313	0.173
	Ultramarine blue	0.499	0.299
Yellow	Naples yellow (Dark)	0.716	0.271
	Yellow ochre	0.332	0.318

	Lead white	1.395	0.553
White	Saint John's white	0.783	0.462
	Titanium white	0.324	0.233
	Zinc white	0.399	0.307
Orange	Lead oxide	0.732	0.330

Table 3.5 Preparation of mock-ups with arabic gum as binding medium.

Color	Colorants	Weight of colorant	Weight of gum Arabic
	Bolo	0.516	0.754
	Cinnabar (MA)	0.379	0.230
Red	Cadmium red	0.313	0.208
	Red lake	0.210	0.295
	Red ochre	0.456	0.250
	Green Earth	0.588	0.303
Green	Malachite	1.621	1.516
	Verdigris	2.132	1.839
	Azurite	1.971	1.436
	Smalt	1.28	0.943
	Egypt blue	0.895	0.725
Blue	Lapis Lazuli	0.301	0.307

	Indigo	0.236	0.188
	Ultramarine blue	0.895	0.725
Yellow	Naples yellow (Dark)	0.743	0.313
	Yellow ochre	0.290	0.655
	Lead white	0.622	0.307
White	Saint John's white	0.563	0.321
	Titanium white	0.302	0.279
	Zinc white	0.350	0.268
Orange	Lead oxide	0.589	0.249



Figure 3.1 A digital image of some prepared painting mock-ups.

3.2 Instruments

3.2.1 Hyperspectral sensor

ASD-FieldSpec FR Pro 3, a portable high-resolution spectroradiometer that is able to measure radiant energy, has been employed for the study. The FieldSpec spectroradiometer is a compact, field portable and precision instrument designed to acquire visible and near-infrared (VNIR: 350–1000 nm) and short-wave infrared (SWIR: 1000–2500 nm) punctual reflectance spectra in a rapid data collection time (0.2 s per spectrum). The sampling unit constitutes three separated spectrometers i.e., VNIR (350–1000 nm), SWIR1 (1000–1830 nm) and SWIR2 (1830–2500 nm). The sampling interval is 1.4 nm and 2 nm for the VNIR and SWIR spectral regions respectively. The VNIR spectrometer has a standard spectral resolution (full-width half maximum of a single emission line) of 3 nm at around 700 nm; while in the SWIR region the spectral resolution is 10 nm at 1400/2100 nm. The specifications of the instrument are summarized in Table 3.6.

Table 3.6 ASD-FieldSpec FR Pro spectroradiometer specifications.

Parameters	VNIR	SWIR
Spectral range	350-1000 nm	1000-2500 nm
Spectral resolution	3 nm	10 nm
Spectral intervals	1.4 nm	2 nm
Detector	One 512 element Silicon	Two separate, TE cooled,

	photodiode array	graded index InGaAs photodiodes
Scanning time	100 ms	
FOV	1.2 cm * 1.0 cm	
Weight	12 lbs (5.2 kg)	

The data collections were under the artificial condition with a contact reflectance probe (A122317, ASD Inc.) that provides an internal light source. Spectra were acquired by ASD-FieldSpec FR Pro without involving the typically used ambient solar illumination considering the possible effects caused by time and weather. The internal light, at fixed illumination angle (12°) and shot, provides a uniform and constant illumination for the surface being investigated. The contact probe directly contacted with detected materials, with the spot analysis area about 1.5 cm². The illumination light (5000 lux) was incident on the surface only during data collection so as to minimize light exposure.

The data acquisition time was 5s per spectrum (0.2 for single, 25 averages). Then all the collected spectra were processed by the software ViewSpec Pro. Spectra were firstly subjected to “splice correction” to eliminate the discontinuous caused by the changing of the detector. An original spectrum of a substance is the statistic of 10 spectra from the same data collecting position without further normalization. The first derivatives of the reflectance spectra are calculated using a derivative gap of 5. Zero

crossing points in the first derivative spectra correspond with maxima/minima of absorption features in the reflectance spectra. The derivative spectra can aid in visualizing the presence of spatially overlapped components.

3.2.2 Data collection

Considering several factors that can affect the quality of reflectance spectra, the first factor to control is the illumination reached to detected subjects. Thus, the artificial light inside the contact probe of FieldSpec was used during spectra collection. Besides, to ensure constant irradiation, the probe directly contacted with the surface of target substances, e.g., powder of pigments and painting surfaces. It is true that non-contact mode is generally preferred for real artworks investigation, and it is proved that it also works well to operate it with the constant distance. However, in our case, this contact method allowed us to obtain spectra with the same irradiation which serve as reference spectra. Before spectra acquisition, white reference of the instrument is a necessity. White Teflon plate and other Teflon pieces were used because they have no absorptions in 350-2500 nm. Unlike mixed materials, the reflectance spectra of pure substances were not easily collected. Special attention should be paid on preparation of pigments, binders and varnishes. Compared with mixtures or mock-ups, relative smooth colored surfaces created by deposition of pure material were more complicated to achieve. As a consequence, the corresponding spectra were critical to use as references-in the later identification work.

3.2.2.1 Data collection Pigments

Similar to the discussion in Chapter 1, the main factor that affects spectrum quality of the matt surface is the amount of a material. In our case, it becomes paramount importance in the discussion of pure material identification, especially colorants. To acquire the reference spectra with the most evident peak features for characterization, spectra with different amounts of one single substance were obtained and compared. Considering the most extreme conditions, the maximum and minimum of the tested amounts need be compared. The maximum amount refers to the amount that a substance (colorant powder) is thick enough to avoid light penetration to support. Pigment powder was accumulated about 2-3 mm height. The spectra collected by this way was called Max spectrum (Max S in brief) of a substance. While, the minimum amount indicates the minimum amount detected by the instrument, and the spectra collected in this way were called Min spectra (Min S in brief).

For the sake of acquiring the best spectrum and simultaneously avoiding the contamination of the Teflon plate, we explored spectra collection on different optically transparent supports, i.e. glass support (petridish/glass slides) and the cling film. Cling film was selected because it was so thin that colorant powder can stick on it due to electrostatic effect. In order to eliminate the effect caused by the support, White reference needs to be taken on the support by which is covered. Max S were simply collected on glass support (upon the white Teflon). However, for the

collection of spectra in the Min S condition, the deposition of a very thin layer of substance on the support was not easy. Therefore, several methods were used:

1. simply brushing the pigments to deposer on the glass support;
2. using pigments dispersed in water or other solvents (e.g., acetone, chloroform, ethanol, ethyl acetate) with boiling points between 50-100 °C as a mobile agent to depose powders onto glass slide by a brush;
3. putting the pigment powder on the cling film by the electrostatic power. More specifically, firstly, a thin layer of the cling film was placed on glass slides; secondly, air bubbles between the cling film and the glass slides were removed by gently brushing; thirdly, spectra were collected on the film where glass slide (the white Teflon plate as White Reference as always) is located; finally, a small amount of materials (less than 1mg) on the cling film was brushed and stuck on.

Min S collected by these methods were compared at first, and then the best ones were selected for the comparison with Max S. Finally, larger or smaller amount for having the reference reflectance spectrum of a material was decided.

3.2.2.2 Data collection of binding media

The spectra collection of binding media and varnishes were carried out on the materials on another Teflon holder (to avoid the contamination of Teflon plate).

Animal glue and gum Arabic were dissolved in the water; varnishes were dissolved in ketone, and then were tested after totally drying like in Figure 3.2. Egg yolk was

firstly dried, and then it was put on a glass and Teflon support as a thin layer. The effects which may be caused by different supports were compared. Linseed oil, however, was the one which was already prepared in 2010 and dried (for 4 years).



Figure 3.2 Animal glue was dried on a Teflon hold to form a film for spectra collection.

- Mixture data collection

The spectrum of the mixture substances, i.e., painting surfaces, was collected placing the probe directly with the surfaces, after they were dry.

3.2.3 Data processing

Although the characterization of binders can be carried out with both their raw and first derivative spectra, a more straightforward dataset is still necessary to be obtained. Considering that each reflectance spectrum described by 2151 points (350-2500nm) depending on the features, principle component analysis (PCA) should be helpful in

order to classify four kinds of binders from this large database. However, what has to be taken into consideration are two points: first, a reflectance spectrum always has broader bands rather than a spectrum of NMR, FT-IR spectroscopy; second, the identification of binding media from pigments mixtures is one of the main purposes of the thesis rather than its color. Therefore, the PCA will be done on an appropriate selection of the points is mandatory.

3.3 Other instruments used in the study

3.3.1 Optical microscopy

The specimen morphology was documented by taking the microphotographs of original specimen and specimen. In this experiment, Leiz MZ 125 Stereomicroscope equipped a digital camera (Canon 500D) capturing system.

3.3.2 FT-IR spectroscopy

To verify and confirm the results obtained by ASD-FieldSpec FR Pro, Fourier Transformation Infrared Spectroscopy (FT-IR) was exploited. Infrared spectra were recorded by a FT-IR Spectrometer Perkin Elmer Spectrometer (Spectrum 1000) P and spectra were processed by the software Spectrum v.3.0202. Using the diamond anvil cell as sample support to collect spectra, all spectra were recorded in the mid-IR range (4000 cm^{-1} to 400 cm^{-1}), with 2 cm^{-1} as resolution and 64 scans.

3.3.3 SEM-EDS

The samples collected from the frescos were characterized at MEMA (University of Florence) using a Zeiss EVO MA 15 SEM equipped with an RSD detector and Oxford INCA 250 X-EDS. Polished cross sections of all samples were firstly prepared using an epoxy resin (EPO 150 with its hardening agent) and polished with abrasive paper with grain size from 800 to 2500 meshes. The cross sections were carbon sputtered before SEM analysis. Images in backscattered electrons (BSE) were acquired, and chemical analysis and elemental mapping were done operating the instrument at 15 KeV, pressure of 1 Torr and current of 2.4 μ A.

Chapter IV

Results and discussion

In this chapter, a database of painting materials will be created with best reference spectrum of each pure substance. Pure materials include the inorganic and organic pigments widely used both in the past and in restoration interventions, as well as four different natural binders (i.e. egg yolk, animal glue, linseed oil and gum Arabic). Since colorants are in powder, the factors that may influence their spectrum quality will be discussed. Besides, the spectra collected by different methods will be compared. For organic materials, their identification work will be highlighted by the recognition of their characteristic features in reflectance spectra. Based on their specific and characteristic spectral region/regions, the distinction of each binder from its mixture with colorants will be carried out. The possible band shifts of each binder caused by the mixing of varied pigments will be interpreted, as well as effects caused by the amount of organic substances. Then, the identification of different binders mixed with the same pigment will be elaborated, through their raw and 1st derivative spectra as well as the Principle Component Analysis (PCA).

4.1 Raw spectra and their 1st derivatives transformation

As described in Chapter 3.2.1, after spectra optimization, the average spectrum of 10

spectra collected from the same point of one material was used. Here the spectra are reported as their original and 1st derivative spectra. The use of derivative spectra is a common method in the analysis of hyperspectral data. The derivative spectrum is obtained by applying the derivative function to the original spectrum. The 1st derivative is a function of a real variable measures the sensitivity to change of the function value (reflectance) with respect to a change in its argument (wavelength). After one spectrum was dealt with ‘1st derivative’ option in the software, one peak in the original spectrum changes into two peaks in both positive and negative direction which are located at the symmetrical position of the original peak, as shown in Fig 4.1. As a consequence, both negative and positive peaks can be recognized as the characteristics peaks of a substance. The approximation used for the 1st derivative is (Eq 4.1):

$$F(\lambda) = [F(\lambda + \Delta\lambda) - F(\lambda - \Delta\lambda)] / 2. \quad (\text{Eq 4.1})$$

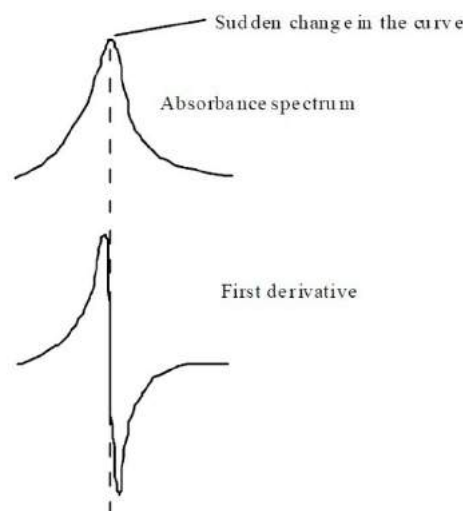


Fig. 4.1 the 1st derivative spectrum [85]

The use of derivative spectra has several advantages: firstly, it may swing greater

amplitude than the original one and meanwhile the peaks of overlapping bands become more distinguishable (separated out); secondly, derivative spectra yield good signal-to-noise ratios only if the difference of noise levels at the end points of the interval is small enough to yield a noise equivalent $\Delta F/d\lambda$ calculation much smaller than the absorbance; more importantly, the small change of the peaks in the original spectra can be well illustrated in their derivative spectra, which makes the identification of materials more easily.

4.2 Pure material characterization

The characterization of pure materials is discussed in the first place, as they act as standard spectra for further identification work. Two sections will be dedicated to the study of pure materials, i.e. colorants and binding media. They are divided in separated parts because: 1) from physical point of view, they are in different form and the factors which influence the reflectance spectra are different; 2) from chemical point of view, their spectra give elemental or molecular information about their components which result in different behaviors in the spectral region. As mentioned in Chapter 1.2.1, there are several factors influencing reflectance spectra of powder materials, and the main factor is the amount of substances. Different methods for acquiring reference spectra of pure materials were explored in the experimental part. In this chapter, spectra of powder substances collected by different methods will be compared and discussed. After comparative study, the database will be finally created

accordingly. For organic binders, the identification work will be fulfilled by the recognition of the characteristic features in both original and derivative spectra. The characteristic peaks and regions will be highlighted because they will be used as “fingerprints” in the later identification work for mixed materials.

4.2.1 Reference reflectance spectra database of colorants

The analyzed objects in this section are colorants mainly in powder form. As introduced in Chapter 1.3.3, reflectance spectra collected on matte surfaces are determined by the electromagnetic wave irradiated and reflected on the surfaces. Employing this hyperspectral sensor, i.e. ASD-Field spec FR Pro, we are able to control the illumination and optic geometry. Moreover, by directly contact with the substances, the light and dimension of analyzed area are easy to control, there is no deviation caused by operators. Thus, the volume of incident electromagnetic irradiation is constant. As regard to colorants, their optical characters determined by absorption and scattering coefficients are constant, thus causing fewer problems to standard spectrum. In the field of cultural heritage, colorants used by artists are generally commercial products that are in similar particle size and relatively homogeneous in dimension distribution. Therefore, for determining the reflectance spectrum of a pigment in a defined area (within the size of contact probe), the amount of pigment powder, or the particle concentration, affects the roughness of mat surfaces. In our work, spectra of one colorant with different amounts were registered

and compared. To acquire the reference spectra with the most evident peak features in the full range, we selected spectra obtained with “maximum” and “minimum” amount of substances to discuss.

4.2.1.1 Different methods of “Min” spectra collection

As describe in Chapter 3.2.2, three methodologies were developed for collecting spectra in “minimum” amount of pigments. Its corresponding spectrum is called as Min S in later discussion. Figure 4.2 shows the Min spectra (raw and 1st derivative spectra) of one commercial red ochre, English red, prepared in these three ways: green line is when the pigment is deposited on glass by simply blushing; blue is when it is deposited on cling film; while, the red spectrum is when it is deposited on glass with a dispersing reagent. The dispersing agent refers to an agent which can be used as a mobile solvent for dispersing powder upon a glass support by brushing. Among poisonous liquids, like water and other solvents (e.g. acetone, chloroform, ethanol, ethyl acetate), those with boiling points between 50-100°C were suitable for this cases. In fact, colorant powder can cover the glass slide much evenly by this way, which decrease the effect caused by the roughness of the surface, thus allows for a more accurate data collection. The dispersing reagent used in this case was chloroform, because it provided the best results.

As it can be seen, iron oxide as chromophore of this pigment is easy to identify from

all these methods. The S-shape (Figure 4.1a) in the spectrum region from 600 to 900 nm indicates the presence of hematite, $\alpha\text{-Fe}_2\text{O}_3$. Absorption band due to ligand field transition, centered around 850–900 nm, is usually present [86]. In the 1st derivative spectra as Figure 4.1b, the maximum peaks all lies in the 575–590 nm range from semiconductors, and then followed with a characteristic positive slope in the region above 600 nm which generates a less pronounced inflection point around 700 nm.

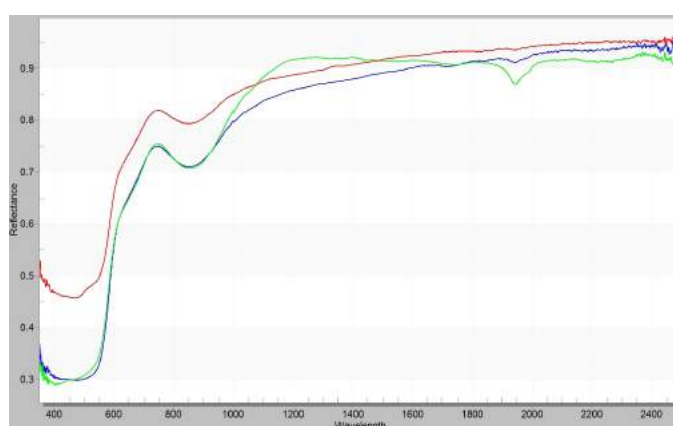


Figure 4.2a MinS of English red on different supports in full spectral range. Green = collected on glass; blue = collected on cling film; red = collected on glass with Chloroform.

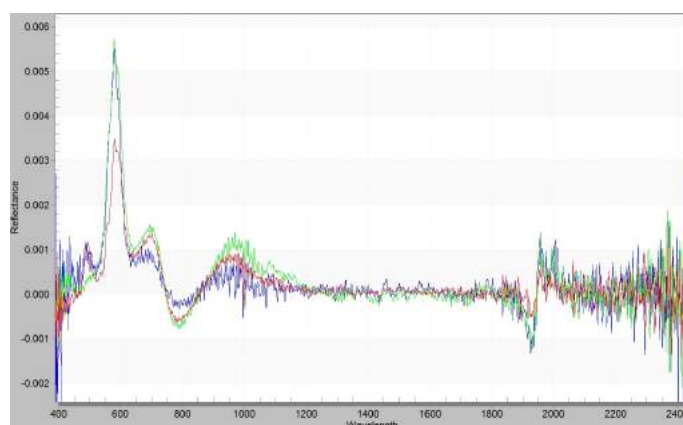


Figure 4.2b 1st derivative “Min” spectra of English red on different supports in full spectral range. Green = collected on glass; blue = collected on cling film; red = collected on glass with Chloroform.

The differences of their raw spectra mainly locate in the region between 1900- 2020 nm. It can be seen that although the amount is the same when collected on glass

(green) or on a cling film (blue), the spectrum collected on the cling film is less clear than when it collected on the glass, especially in the shortwave infrared region. The presence of a small amount of gypsum as additive colorant in English red can be much more easily identified from the characteristic peaks located in 1450-1540 nm, 1600-1800 nm and 1945-1950 nm spectral ranges [87]. A similar situation happened in their 1st derivative ones. As a consequence, the “Min” spectrum of English red is better to acquired by simple brushing a small amount of the colorant on the glass support).

In fact, as regard to the second method, it is not convenient to apply. Sometimes, the fast evaporation of some solvents may leave colorants stick on the brush. More concern is that, regardless of dye, some additive components of commercial pigments may be dissolved or react with the dispersing solvent, resulting in unpredictable loss of information in their corresponding spectra. Gypsum ($\text{CaSO}_4 \cdot 2\text{H}_2\text{O}$), for example, can no more be identified by the combination bands of O-H bond in the NIR-SWIR region when using H_2O as the dispersing agent. It is true that it is almost impossible to find a reagent that fulfills all the requirements suitable for dispersing all the colorants: first, with low boiling point but easy to apply; second, no reacting with any component of general pigments; last but not least, no harmful for human beings and environment.

Through the third method, i.e. by using dispersing agents and depositing pigment

powder on cling film by electromagnetic effect, it is able to acquire a much smaller amount. However, its drawbacks are also evident. One problem is that gas bubble between the glass and cling film is impossible to remove, showing a “wave” shape in the NIR-SWIR regions like one example in Figure 4.3 Another is that the support material used: cling film (plastic wrap) is a polymer--polyvinyl chloride (PVC) which has absorption bands in near infrared region. Even though white reference including the cling film before collecting any information, it may still influence the final spectra due to the difference in thickness, especially in their 1st derivative ones that are sensitive to the change of spectrum curve. These two disadvantages will have a bigger impact on the colorants which have absorption peaks in the region of 1000-2400 nm, and finally causing the loss and confusion of information.

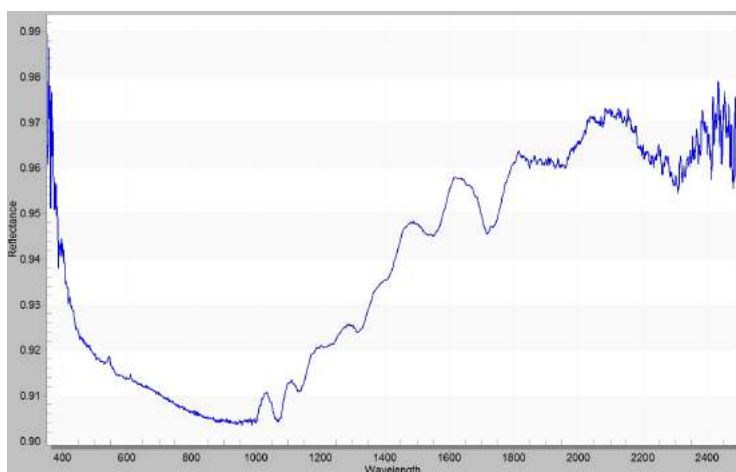


Figure 4.3 The “waves” observed in a spectrum when collected on the cling film

Thus, considering the spectral quality and the feasibility of sampling methods, the method of collecting the “Min” spectra of colorants should be simply brushing

powder on a glass support. The white reference will be taken on the surface of the corresponding glass and the Teflon plate each time.

4.2.1.2 Comparative study between “Min” and “Max” spectra

Once the “Min” and “Max” spectra of one substance were collected, comparative studies were carried out to determine which is more indicative for identification. The comparisons will be discussed on some colorants.

➤ *Natural and synthetic cinnabar*

As previously mentioned, the spectra of cinnabar in both natural and synthetic form were collected. Their “Min” spectra, “Max” spectra were illustrated in Figure 4.4a, 4.4b. As a semiconductor, the most characteristic feature of cinnabar can be found in these four raw spectra (Figure 4.4), due to the absorption of UV-Vis radiation at ca. 500 nm. And they have no absorptions in the NIR-SWIR. However, when the reference spectra were collected of bigger amount, “Max” spectra of synthetic and natural cinnabar are the same (Figure 4.4b). The difference of these two ones can be seen in the visible range of 450-550 nm, only when they are collected in a small amount, as “Min” spectra (Figure 4.2a). In their 1st derivative “Min” spectra, it is evident that that the positions of their inflection points are not in the same position (Figure 4.5). However, the relative uncertainty of the position of the inflection point is not influenced by the amount. It just proves that this is a bathochromic or a hypochromic shift of the spectral edge caused by the presence of impurities in the

semiconductor possibly which can influencing the energy gap, by decreasing or increasing its value [24].

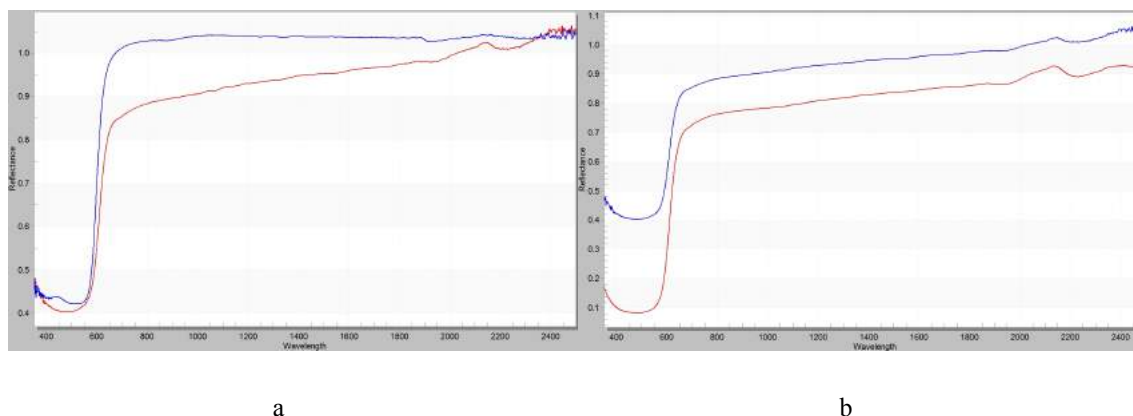


Figure 4.4 The raw spectra of natural and synthetic cinnabar collected on glass of different amount in full spectral range. a = Min spectrum; b = Max spectrum. Black = natural cinnabar from Mountain Amiata; red = synthetic cinnabar;

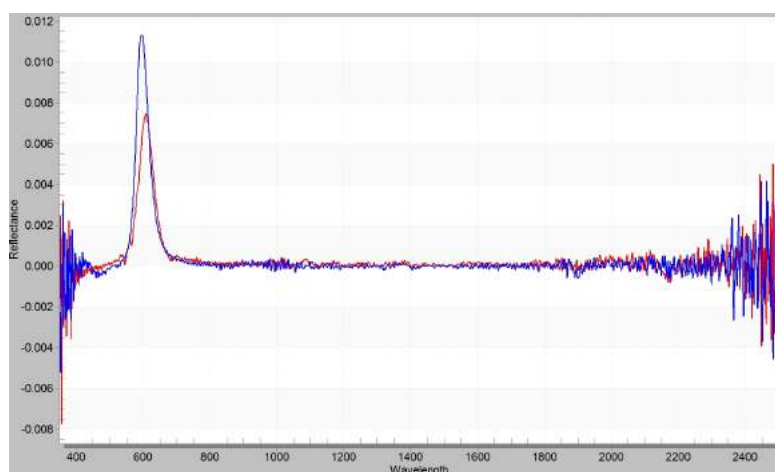


Figure 4.5 The 1st derivative Min spectra of natural and synthetic cinnabar in full spectral range. Blue = natural cinnabar from Mountain Amiata; red = synthetic cinnabar;

➤ *Three kinds of red ochre*

Most of the commercial colorants include some additives to give the final color with different hue and saturation to meet the needs of painters. Red ochre is one typical

example. As mentioned in chapter 3, spectra by FieldSpec were collected on three different kinds of red ochers, i.e. Armenian bole, Ercolano red and English red. These three iron oxide based commercial products are in red color due to the presence of hematite, but their chromatic intensities differ slightly due to their different accessory ingredients. Figure 4.6 illustrates the reflectance spectra of these three colors tested indifferent amount.

In the Vis-NIR region of Min and Max spectra, they all have a shoulder between 400–610 nm with distinct slopes and starting positions. But their main composition differences are better observed in the NIR-SWIR region of Max one (Figure 4.7b). As it can be seen that, Ercolano red and English red have absorption peaks of gypsum ($\text{CaSO}_4 \cdot 2\text{H}_2\text{O}$). But Ercolano red has a higher amount than English red due to its stronger peak intensity. The spectrum of Armenian bole however was quite different from the others, in terms of both peak position and peak intensity. The absorption peaks at ca.1400, 2165 and 2210 nm and the shoulder centered at ca. 1900 nm indicates the presence of kaolinite (hydrous aluminum silicates) [88], which corresponds to its composition mentioned in literature. The identification can be done in both two spectra, as obtained in bigger or smaller amount. However, a better observation will be obtained from their Max spectra from higher amount in SWIR region.

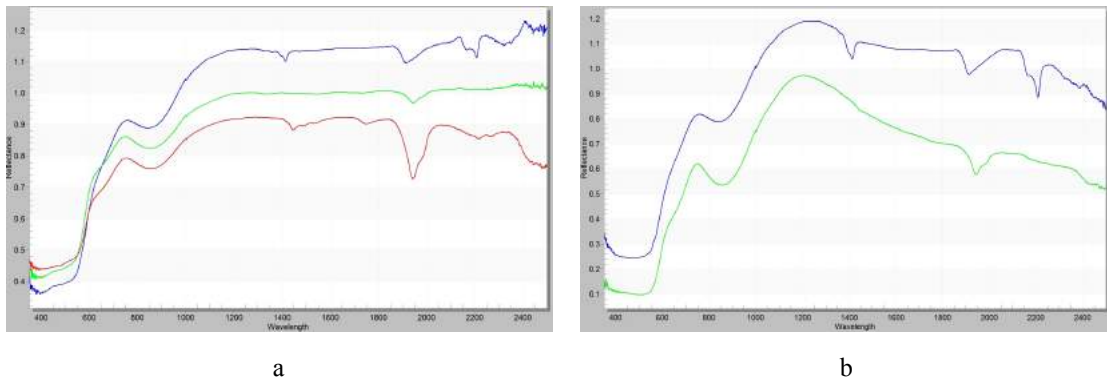


Figure 4.6 raw spectra of three red ochers both collected on glass of different amount in full spectral range. a = Min spectrum; b = Max spectrum. Blue = Armenian bole; green = English red; red = Ercolano red.

These differences in chemical composition were also proved by the FT-IR spectroscopy (Figure 4.7). The major component (Fe_2O_3) of these three colorants is well shown by the strong peak at 466 cm^{-1} in all the three spectra, while the strong peaks at 3616 cm^{-1} , 1041 cm^{-1} , 910 cm^{-1} , 797 cm^{-1} attributed to the characteristic absorption bands of kaolinite and quartz differ Armenian Bole clearly from the other two.

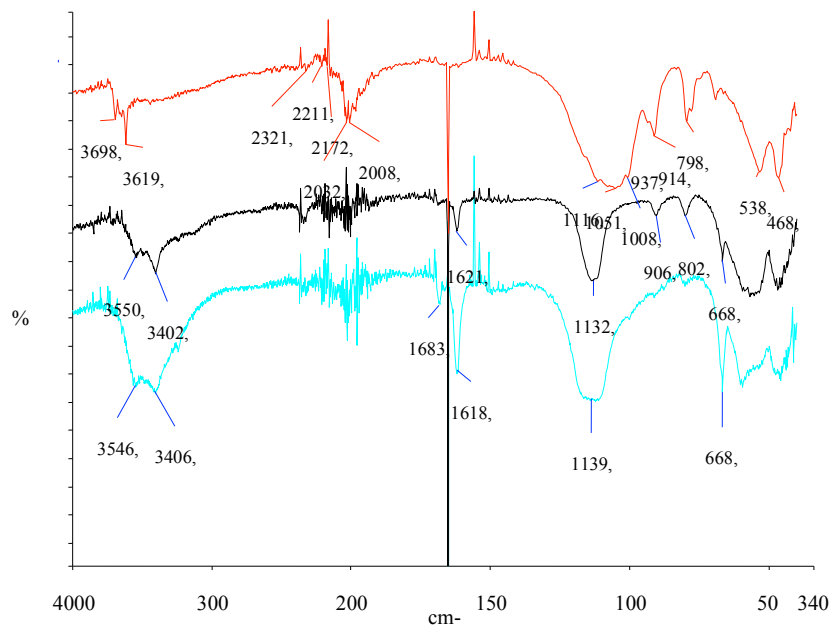


Figure 4.7 FT-IR spectra of three red ochers. Red = Armenian bole; black = English red; blue = Ercolano red.

➤ *Azurite*

Figure 4.9a and 4.9b show two spectra of azurite collected on the glass support of different amount. The Min spectrum of azurite (Figure 4.8a) shows a maximum absorption peak about 638 nm together with a wide shoulder between 750 and 1000 nm. These two important characteristics were also seen in the spectra of the painting “*Christ in Majesty with Twelve Apostle*” (Author: Pacino di Bonaguida) [26]. On the contrast, these features are not visible in its Max spectrum. Moreover, the position of inflection point in MinS (ca. 485 nm) and MaxS (ca. 475 nm) vary, and the position in MinS is more accurate in respect to the results of other researchers [89]. But both the positions are right, because one important factor causing a shift of the inflection point could be concentration of pigments on the detected surface [90]. However, all peaks, no matter strong, medium or weak, attributing to the presence of overtones and combination bands of hydroxyl and carbonate groups of azurite, can be easily identified in the 1100-2500 nm range of Max spectrum instead of its Min one.

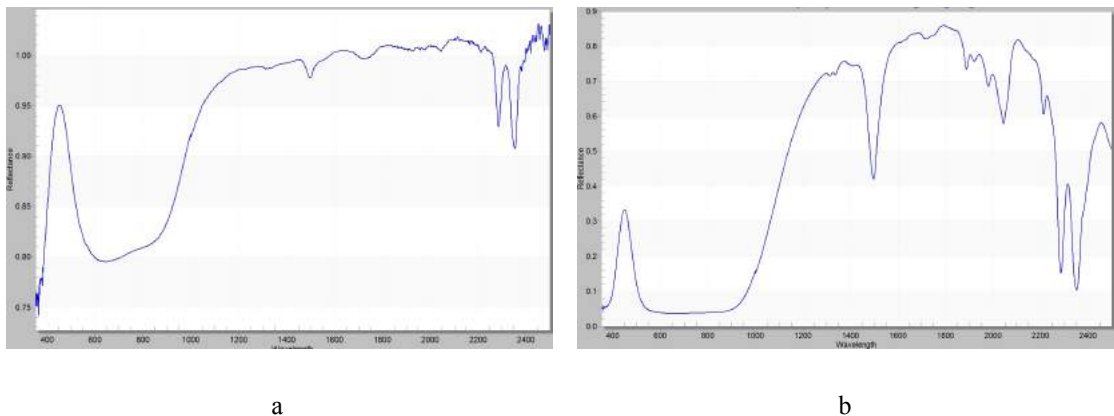


Figure 4.8 Raw spectra of same pigment, azurite both collected on glass of different amount in full spectral range. a = Min spectrum; b = Max spectrum.

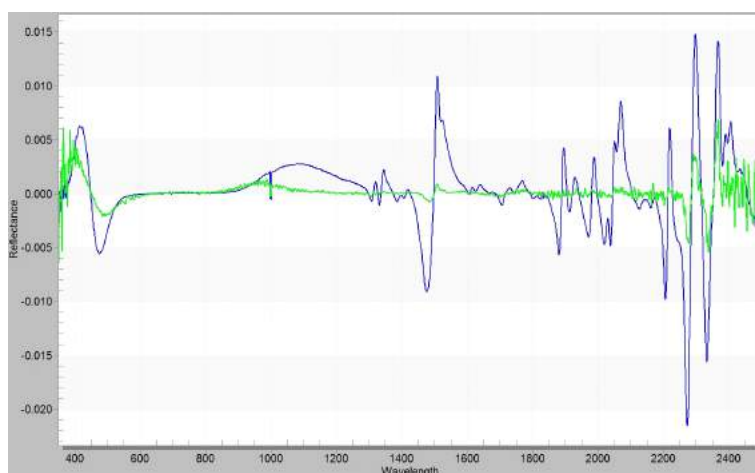


Figure 4.9 1st derivative spectra of azurite both collected on glass of different amount in full spectral range. a = Min spectrum; b = Max spectrum.

➤ *Prussian blue*

Figure 4.10a and b illustrate the Min and Max spectra of another blue pigment, Prussian blue, iron cyanide, which is the classic example of a mixed-valence iron(II)-iron(III) inorganic complex. In its “Min” spectrum, it reveals a rising reflectance edge at ca. 400 nm in the blue portion of the visible range with a maximum reflectance at ca. 450 nm related to its intense blue color. Moreover, there is a intense absorption band centered at ca. 700 nm, which due to the intervalent charge transfer of an electron from iron (II) to iron (III) ion [91]. However, this characteristic feature cannot be found in their “Max” spectra is hidden, which replaced by a big shoulder (1100-1800 nm). It is proved that Prussian blue sometimes reflects a yellowish and reddish color. The reason of the absence of this absorption in Max spectrum may be due to the abundance of pigment powder that limit the scattering of light and finally resulting in less absorption. On the other hand, the

characteristic features in shortwave infrared range of Prussian blue are much more evident and with more accurate position in "Max" spectrum rather than the "Min" one. The peaks related with vibration modes of C-N, and O-H bonds are well defined, i.e., the combination of C-N at 2145 and 2185 nm, the combination of C-N stretching at 2404 and 2379 nm, as well as at 1923 nm due to O-H the bound water (xH_2O).

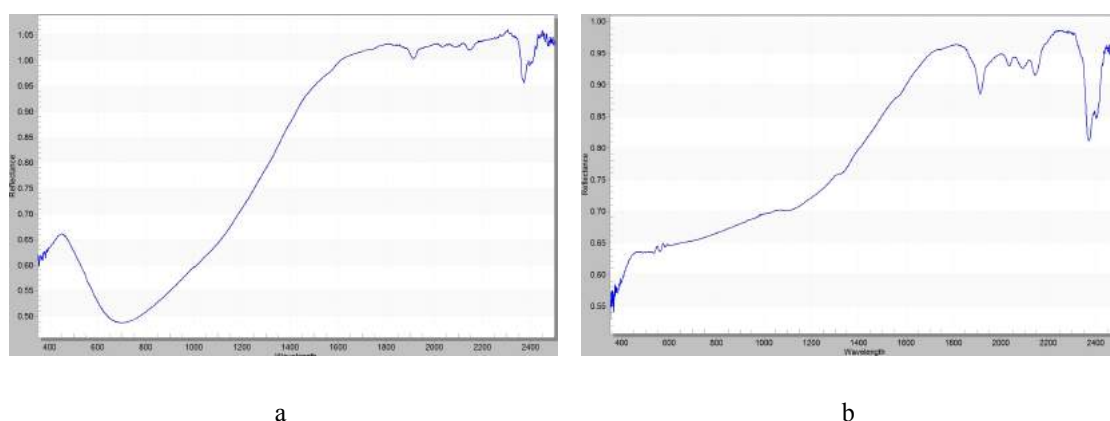


Figure 4.10 raw spectra of Prussian blue both collected on glass with different amount in full spectral range. a = Min spectrum; b = Max spectrum.

All the above comparative studies of Max and Min spectra show that reflectance spectroscopy is more influenced by the amount of detected substances compared to other analytical spectroscopic techniques. Max spectra, collected with a larger amount of materials showing stronger peak intensity in the full region, have spectra features in the NIR-SWIR range (1000-2500 nm) more clear and readable. This is of paramount importance in the identification of colorants which have characteristic features in this region, especially the commercial products which generally contain additives. However, the large amount of substances also induces too much absorption

in the VIS-NIR range (350-1100 nm), resulting in the loss of some significant spectral features (i.e. peaks, shoulders) due to electronic processes. Min spectra, with much weaker peak intensity in the spectra, have the exactly opposite results. Through Min spectrum of a substance, a better understanding will be obtained at lower wavelength. But the identification is harder where has very low absorption, and the peak positions become hard to detect. More importantly, their corresponding 1st derivative spectra have lots of noise which is not suitable for identification.

In summary, the selection of Max and Min spectrum depends on whether a colorant has absorption peaks in near infrared and short wave infrared regions. For example, a colorant like cinnabar, which only has characteristic features in shorter wavelength, Min spectrum is selected as the standard spectrum. While, for a colorant, especially organic dyes, VIS-NIR (350-1000 nm) of Min spectrum and NIR-SWIR (1000-2500 nm) of Max spectrum should both be exploited to better understand the substance in terms of color and chemical composition. For commercial products which may contain different additive components, Max spectrum is also suggested in order to maximize the presence of undesirable substances (impurities). The 1st derivative spectrum of colorants will be obtained by transforming their corresponding standard spectrum (either Min or Max spectrum).

Finally, a database of original spectra of colorants listed in Chapter 3 has been created with Min spectra and/or Max spectra (collected on a glass support). Raw reflectance

spectra and the corresponding 1st derivative reflectance spectra of all colorants collected by FieldSpec are shown in Appendix.

4.2.2 Reference reflectance spectra database of organic materials

4.2.2.1 Comparison of organic materials on glass and Teflon supports

The collection of reflectance spectra of pure organic materials is not as complicated as the inorganic ones. However, different results may be obtained when different supports for the deposition are employed. In the past, other researchers took the spectra on a glass support [55]. As describe in Chapter 3.2.2, in this work egg yolk was prepared on glass and Teflon support for spectra comparison as shown in Figure 4.11. It is evident that spectrum collected on Teflon shows more details of the characteristic features of egg yolk. The region more evident is located in short wave infrared region. The reason is that silicon oxide has some absorption peaks in the 1100-2500 nm region (Figure 4.12). In fact, there are two sharp peaks for glass located at 1400 and 2200 nm respectively. The first one is assigned to the Si-O (2 ν) stretching. As a result, Teflon needs to be the support for organic materials' data Collection (reference spectra).

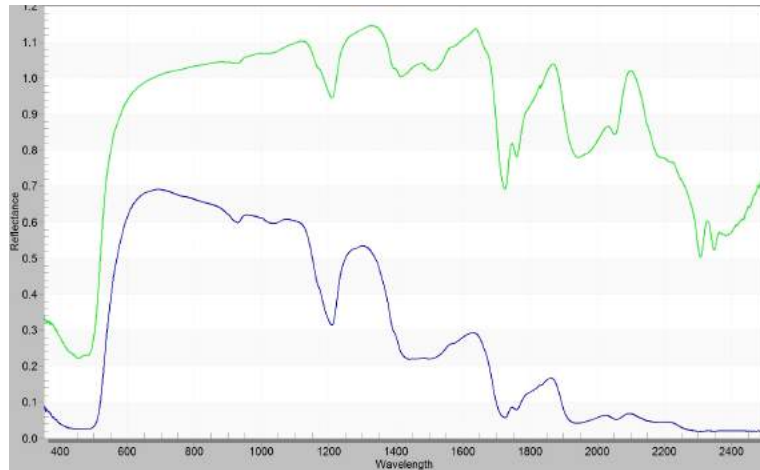


Figure 4.11 Reflectance spectra of egg yolk on different supports in full spectral range. Green = when it is deposited on teflon; blue = when it is deposited on the glass.

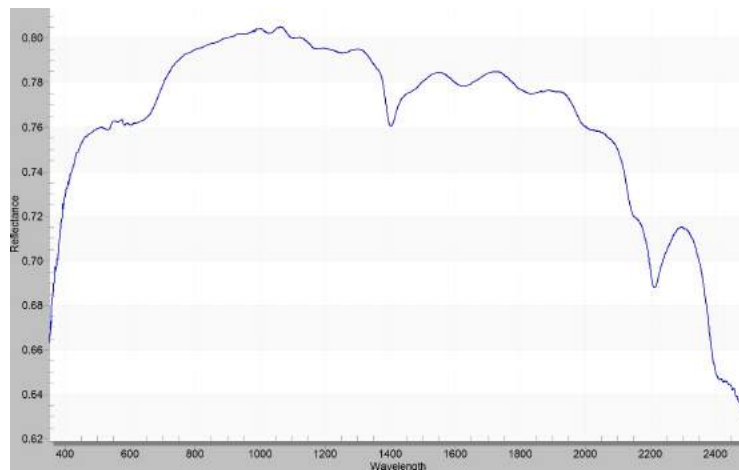


Figure 4.12 Reflectance spectra of glass in full spectral range.

4.1.2.2 Identification of four different binders

The raw reflectance spectra of egg yolk, animal glue, linseed oil and gum Arabic, as collected in the full range (350-2500 nm), are shown in Fig. 4.13 while the wavelengths of the most characteristic peaks of each binder are listed in Table 4.1. As color is not diagnostic for their identification, the differences detected in the visible range are not discussed here, but their main dissimilarities are searched and found in

the region between 1100 and 2400 nm.

Table 4.1 Experimental wavelengths (nm) of four binding media. Each peak can be assigned to overtones and combinations bands of specific chemical bonds [41,92].

Binding media	Experimental Wavelength (nm)
Egg yolk	1211, 1441, 1507, 1727, 1762, 1942, 2058, 2177, 2309, 2347
Animal glue	878, 1182, 1447, 1506, 1690, 1730, 1946, 2049, 2177, 2286, 2347
Linseed oil	1206, 1434, 1727, 1754, 1932, 2132, 2304, 2347
Gum Arabic	1450, 2100, 2280, 2322, 2330, 2335

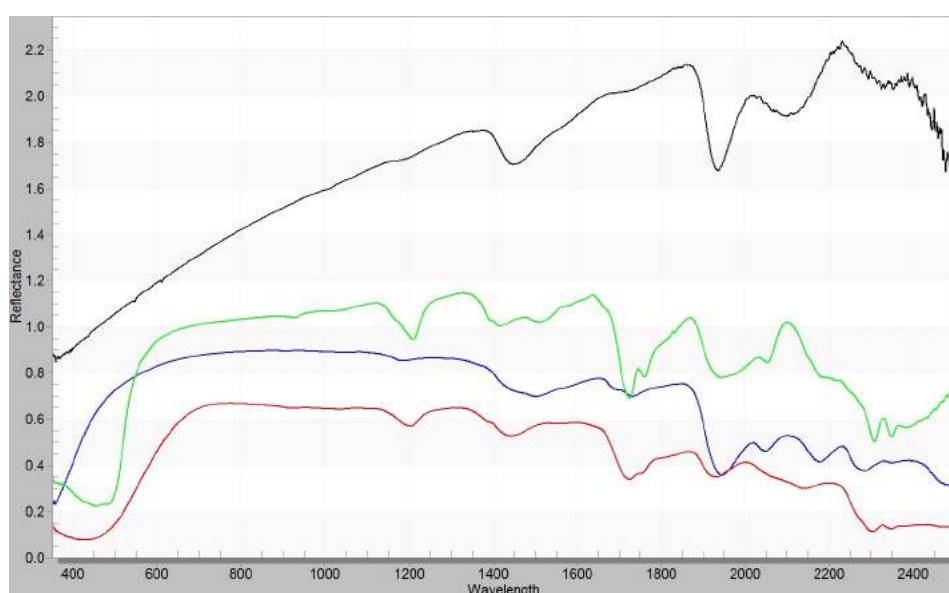


Figure 4.13 Reflectance spectra of four binding media in full spectral range. Green = egg yolk; blue = animal glue; red = linseed oil; black = gum Arabic.

The most evident variances among the four studied binders are marked in Figure 4.14, when the investigated region is zoomed. Gum Arabic has the characteristic features of polysaccharides, i.e. carbohydrates, which mainly have C-H, O-H and C-O bonds. Animal glue, in this study rabbit glue, is mainly composed by collagens; while, linseed oil is made by fatty compounds. Egg yolk, however, contains mainly albumins

with low quantities of fats; its raw spectrum contains features of both lipidic and proteinaceous components. It is noticed that gum Arabic has the less structures spectrum compared with the other three. The main differences among these four binders are well visible in three regions (1150-1250 nm, 1650-1800 nm and 2300-2400 nm) (shadow areas in Figure 4.14), where the reflectance peaks are assigned to overtones and combination bands of C-H bonds for oil, egg yolk and animal glue. Polysaccharides have no evident peak features in these regions. Due to the presence of lipid contents in egg yolk and linseed oil, the spectral features of these two binders are more comparable than that of animal glue. However, although the wavelength of the reflectance peaks in egg yolk and linseed oil are sometimes very similar in these regions, their absorption intensity varies greatly, i.e. the same peaks in egg yolk are sharper and stronger than in linseed oil. For example, the first overtone of CH₂ stretching mode is observed at around 1730 nm for both these two binders, whereas the peak intensity is stronger for egg yolk than for linseed oil. On the other hand, the differences in the wavelength (and peak intensity) of the overtones and combination bands of C-H bonds between animal glue and the other two binders are more evident. For example, the second overtone of methylene stretching locates at about 1210 nm for egg yolk, while for animal glue it is shifted, being at around 1182 nm. Another more distinguished peak to identify animal glue is the absorption peak at 1690 nm. It is assigned to C-O-NH₂ specifically due to peptide N-H and C=O groups at right angles to the line of the peptide backbone referred to as the β -sheet structure [41], which can only be found in proteins.

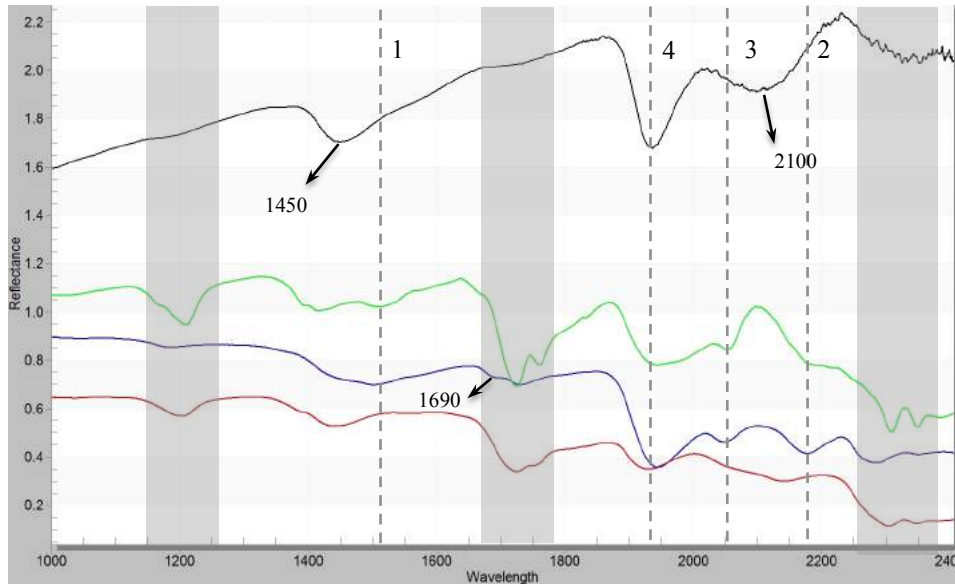


Figure 4.14 Reflectance spectra of four binding media in 1200-2400 nm region marked with the most evident variances. Green = egg yolk; blue = animal glue; red = linseed oil; black = gum Arabic.

Other additional features that characterize gum Arabic are located at 1450 nm and 2100 nm as shoulders. The shoulder at 1450 nm has been previously assigned as stretching modes of O-H (2ν) and \cdot O-H bonds (which can also be found in linseed oil). While, at 2100 nm, where the signal is assigned to two chemical band simultaneously, i.e. C=O and C-O stretching, and to the combination band of O-H bending and C-O stretching of the polysaccharide. The broad shape of the peak may be due to the overlapping of all these bands. Other variances marked with dashed lines are also essential for distinguishing these binders. At around 1507 nm (dashed line 1), the first overtone band of N-H stretching mode is identified in both egg yolk and animal glue as a shoulder, which cannot be found in linseed oil. Similar circumstance occurs at 2177 nm (dashed line 2) where the first overtone band of carbonyl stretching mode (Amide I + Amide II) is observed. Linseed oil, however, has a combination band of

C-O stretching and C-H stretching peak at about 2132 nm in the closer region as a shoulder. Another important characteristic signal of those two proteinauceous materials, found at about 2050 nm (dashed line 3), is the combination band of N-H stretching and bending. All the peaks attributed to proteins are stronger in animal glue than in egg yolk; this is in accordance to the fact that glue is totally composed of proteins, while egg yolk also contains oils. The last dashed line (dashed line 4) locates at around 1950 nm, where the four binders show a very strong peak but their positions and intensity vary. In fact, the second overtone of the C=O stretching of esters in oils occurs at 1932 nm as a shoulder; whereas, the combination band of O-H stretching and bending in proteins are seen at about 1950 nm as a medium strong peak, but in polysaccharides, it is found a sharp peak at shorter wavelength 1945 nm.

Although the original reflectance spectra of pigment/binding medium mixtures can give us useful information for their identification, a more accurate differentiation can be achieved from their derivative spectra. Figure 4.15 shows the 1st derivative spectra of the three pure binders. In these spectra the differences among the binders are increased and it is possible to take in consideration not only the wavelengths of maximum/minimum, but also the ratio of their intensity. Therefore, the discrimination of these organic materials is much improved.

The most evident differentiations to identify egg yolk, linseed oil and animal glue are located in two regions: from 1140 to 1260 nm, and from 1660 to 1800 nm (Figure

4.16a and 4.16b).

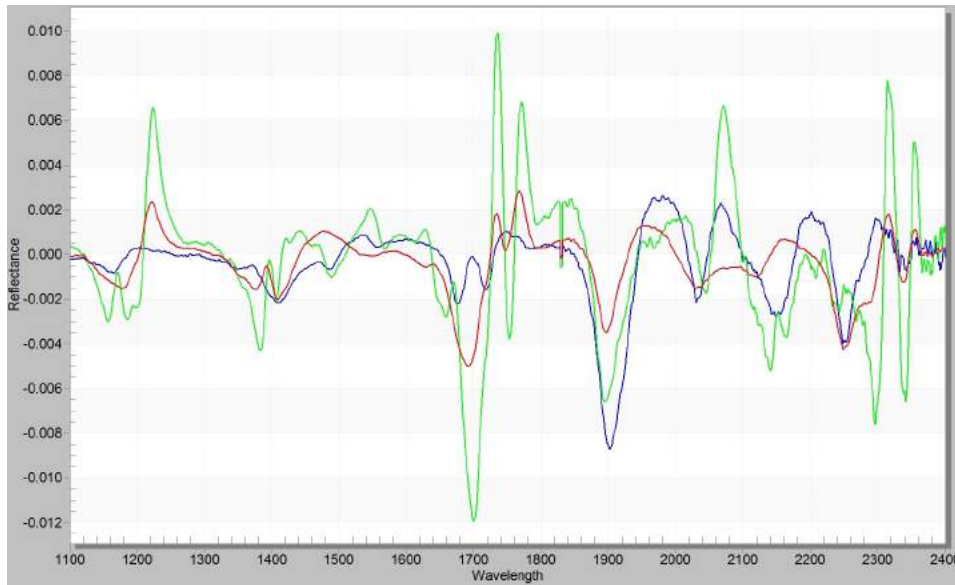


Figure 4.15 1st derivative spectra of three binding media in full spectral range. Green = egg; blue = animal glue; red = linseed oil.

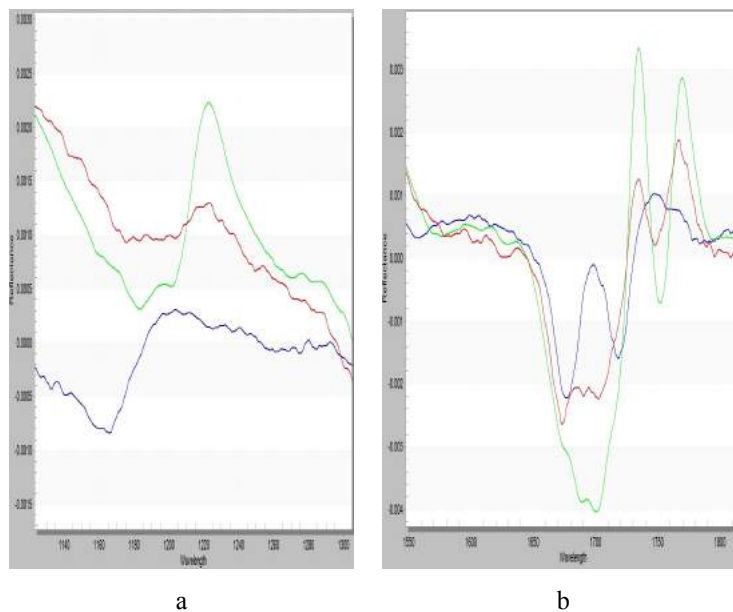


Figure 4.16a and 4.16b 1st derivative of reflectance spectra of the three binders in the spectral ranges 1150-1250 and 1670-1700 nm. Blue = animal glue; Green = egg yolk; Red = linseed oil.

In the first region, animal glue has a negative medium peak around 1172 nm, while egg yolk has three ones, two negative at 1190 and 1205 nm, and one strong and positive at 1222 nm. In the case of linseed oil, a similar peak at 1220 nm as in egg

yolk is observed, but its intensity is much lower. The observation of the peak positions in the spectral range 1670-1725 nm give evidence that egg yolk has a strong negative peak at about 1700 nm, while animal glue has a negative peak at 1670 nm, a positive one at 1700 nm and another negative at 1725 nm (Figure 4.16b). Linseed oil has three negative peaks, where the one at the shortest wavelength (about 1670 nm) is the strongest. It is also well evident that the ratio of the reflectance at 1730 and 1775 nm differs for each binder. These two characteristic spectral ranges can also be used to discriminate the components in pigment/binder mixtures.

4.2 Mixture identification

As discussed above for pure binding media, the wavelength of the peaks or the spectral feature in well-defined spectral ranges can be considered diagnostic elements for the identification of these binders even when they are mixed with pigments (i.e. in painted layers). However, shifts in wavelength in respect to pure materials are expected when a matrix with pigments is realized. Possible shifts of peaks and changes in signal intensities will be discussed in the following. In this part, a pigment with no absorption features between 1200-2400 nm was selected to mix with a binder to see the possible changes in the spectrum; and then, the spectra of the same pigments with different binders are illustrated for differentiation. Finally, data were simplified with suspected regions for principle component analysis.

4.2.1 Characterization of binding media in mixtures

4.2.1.1 Egg yolk with pigments

Figure 4.17 shows the reflectance spectra of pure egg yolk and its mixture with synthetic cinnabar in the range 1200-2400 nm. Since cinnabar has no absorption feature in the NIR-SWIR region, the spectrum of the painted surface is expected to be similar to that of pure egg yolk. Actually, egg yolk is well identified from its distinctive features, but three changes in respect to the pure egg spectrum are observed. One is the disappearing of the shoulder at 1507 nm. The second is the shift of the broad peak at about 1943 nm to 1922 nm, due to the combination of the O-H stretching and bending mode, along with the broadening of the peak itself. The last change occurs at about 2050 nm, where the combination band of N-H stretching and bending shifts to 20 nm longer.

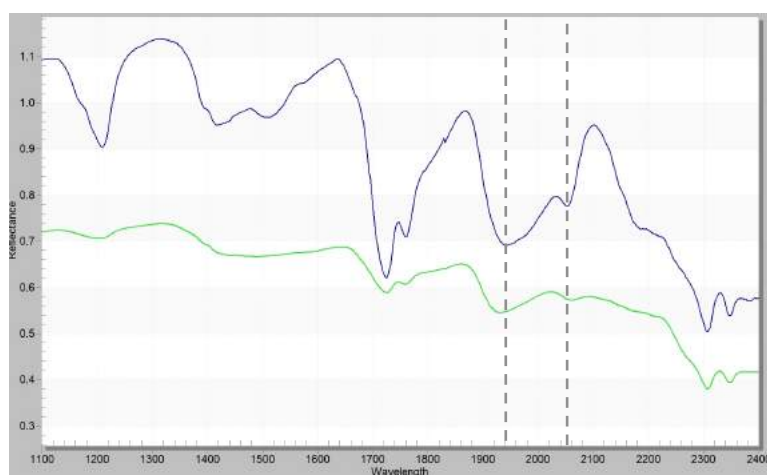


Figure 4.17 Reflectance spectra of egg yolk mixed with cinnabar (green) in 1100-2400 nm region. Egg yolk (blue) is also reported for comparison.

A similar behavior is also found when egg yolk is mixed with other pigments,

regardless of the type and color of pigments, and regardless of whether the pigment has absorption peaks in these regions or not. An example is shown in Figure 4.18a and Figure 4.18b, when two kinds of blue pigments, i.e. azurite and lapislazuli, were mixed with egg yolk, and azurite has some absorption peaks in the detected spectral range.

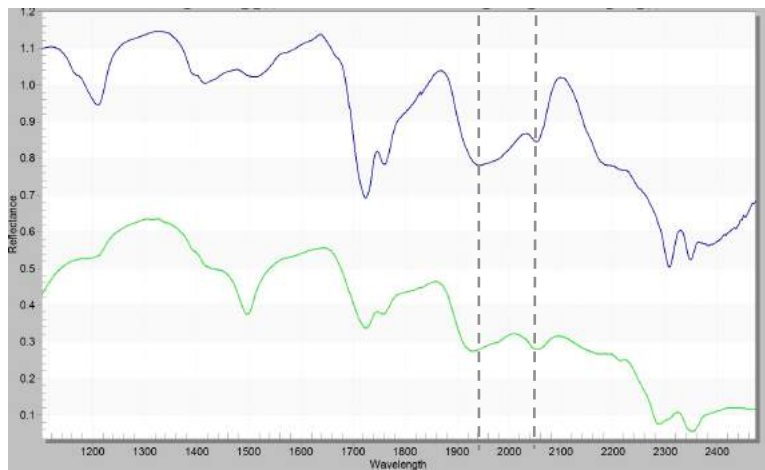


Figure 4.18a Reflectance spectra of egg yolk with azurite (green) in 1100-2400 nm region. Egg yolk (blue) is also reported for comparison.

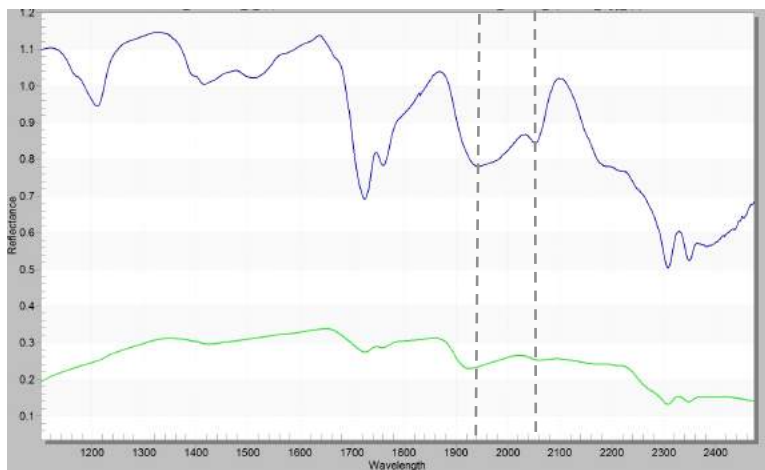


Figure 4.18b Reflectance spectra of egg yolk with lapislazuli (green) in 1100-2400 nm region. Egg yolk (blue) is also reported for comparison.

4.2.1.2 Animal glue with pigments

Naples yellow (dark) has no absorption features in NIR-SWIR regions. As cinnabar, when this yellow antimonite is mixed with binders, the spectra can provide information about the possible effects caused by mixing organic and inorganic compounds. Figure 4.19 illustrates the reflectance spectrum of the mixture of animal glue with Naples yellow (green color), and the blue one is the raw spectrum of animal glue. It can be found that the characteristic features of animal glue attribute to the overtone and combination bands of C-H bonds are the most evident ones, i.e. ca. 1180 nm for second overtone of C-H, 1685 nm and 1725 nm for the overtone band of aromatic and methylene (C-H) groups respectively. However, the second overtone band of N-H stretching at 1507 nm cannot be observed, as well as that at 2174 nm which is assigned to the combination of C-O-NH₂ of amide I and amide II modes. The reason that caused the disappearance of these proteinaceous features might be the presence of Pb in the pigment. It can interact with the amidic group, causing a shift of the signal or a decreasing of its intensity. Moreover, the shift of the broad peak at about 1943 nm to 1922 nm that is found in the mixture of egg yolk, occurs also in the mixture of animal glue, as well as the broadening of the peak itself.

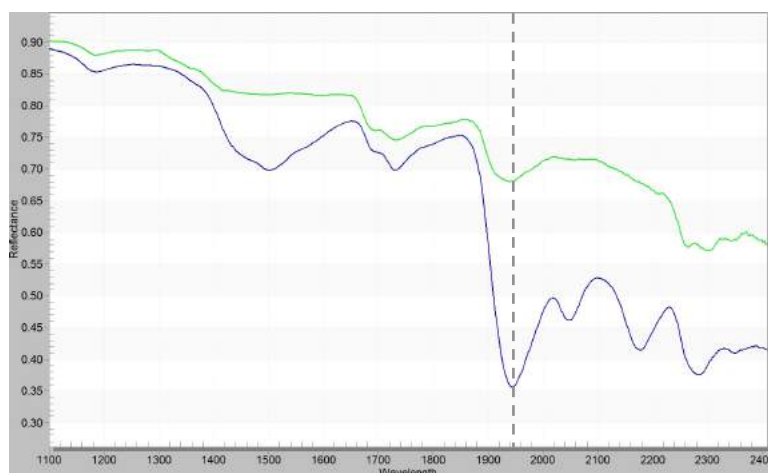


Figure 4.19 Reflectance spectra of animal glue mixed with Naples yellow (green) in 1100-2400 nm region. Animal glue (blue) is also reported for comparison.

4.2.1.3 Linseed oil with pigments

In the case of the mixture of linseed oil with white pigments, titanium white, which has characteristic features only in the visible region, is selected as the pigment for spectra comparison (Figure 4.20). Unlike other two binders, all the features of linseed oil are well evident in the mixture with TiO_2 . The broad peak at ca. 1929 nm in the pure linseed oil is shifted only 5-10 nm (ca. 1920 nm) to lower wavelength in the mixture with TiO_2 . This result is confirmed by the spectra of linseed oil with other two white pigments, i.e. lead white and Saint John white, as shown in Figure 4.21 and Figure 4.22 respectively, although these two pigments have absorption features due to the overtone and combination bands of C-O and O-H bonds.

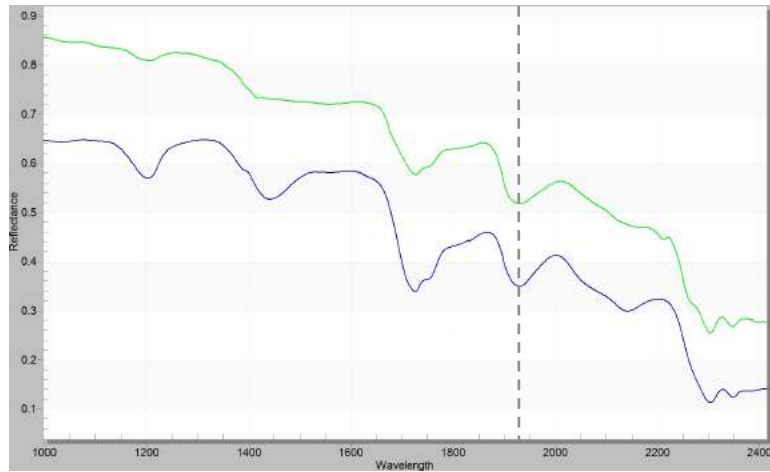


Figure 4.20 Reflectance spectra of linseed oil mixed with titanium white (green) in 1100-2400 nm region. Linseed oil (blue) is also reported for comparison.

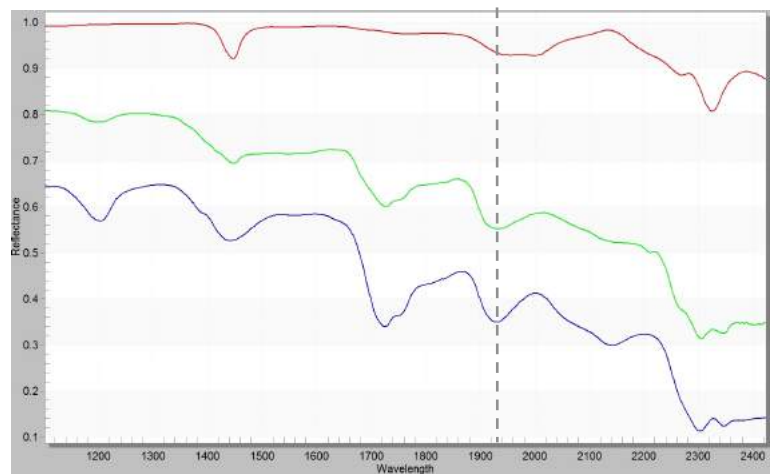


Figure 4.21 Reflectance spectra of linseed oil mixed with lead white (green) in 1100-2400 nm region. Linseed oil (blue) and lead white (red) are also reported for comparison.

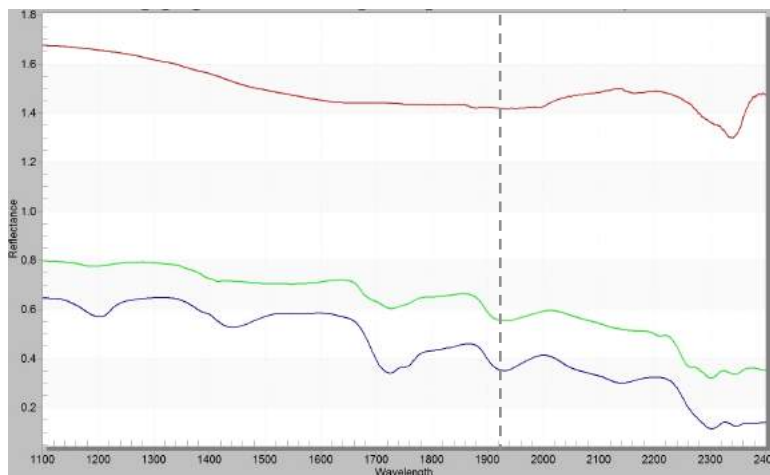


Figure 4.22 Reflectance spectra of linseed oil mixed with Saint John white (green) in 1100-2400 nm region. Linseed oil (blue) and Saint John white (red) are also reported for comparison.

4.2.1.4 Gum Arabic with pigments

Figure 4.23 and Figure 4.24 illustrate the reflectance spectra of two blue mixtures with gum Arabic—indigo and synthetic ultramarine blue, regardless their different chemical essences the range 1100-2400 nm. Synthetic ultramarine blue has much less absorption feature in the NIR-SWIR region than indigo. Gum Arabic is not as evident as other binders from other mixtures, which may due to two reasons when compared with other three binders: first, gum Arabic has broader bands; second, less amount used makes a weaker peak intensity. However, it still can be found some common behaviors in these spectra of paints. 1) The shift of the peak at about 1938 nm to 1918 nm, due to the combination of the O-H stretching and bending mode, along with the broadening of the peak itself. 2) The overtones and combination bands of C-H bonds at the wavelength of 1720 nm and 2280 nm in the mixtures become more evident.

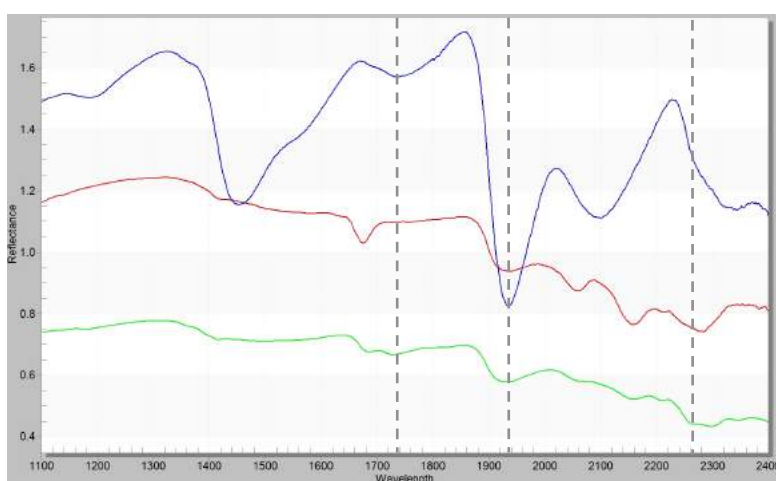


Figure 4.23 Reflectance spectra of linseed oil mixed with indigo (green) in 1100-2400 nm region.

Linseed oil (blue) and indigo (red) are also reported for comparison.

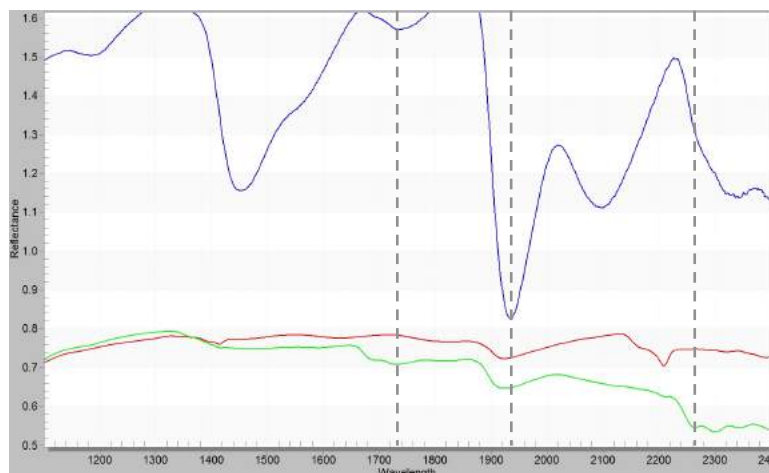


Figure 4.24 Reflectance spectra of linseed oil mixed with synthetic ultramarine (green) in 1100-2400 nm region. Linseed oil (blue) and synthetic ultramarine (red) are also reported for comparison.

4.2.2 Binders and pigments from mixtures

4.2.2.1 Different amount of binders affect the spectra of mixture

It is known that the amounts of materials used by artists to paint vary from one to another. As the effects caused by the amount of inorganic materials to the reflectance spectra has already discuss above (in Chapter 4.1.1.2), now it is also necessary to discuss how the amount of organic materials influences the spectrum of mixtures. In Figure 4.25, the raw reflectance spectra of azurite mixed with different amount of egg yolk, along with its 1st derivative transformation is reported. As expected, the spectra where bigger amount of egg yolk is used owns stronger peak intensity compared to those collected with smaller amount, especially in the regions where the overtone and combination bands of C-H bonds. As it can be seen in Figure 4.25a, even with bigger amount of organic substances, the absorption maxima at ca. 1507 nm, which is

assigned to the first overtone band of N-H stretching mode for egg yolk, can still not be found. Moreover, the shift caused by the mixing of an inorganic material at the wavelength of ca. 1943 nm remains the same regardless of the amount of the egg yolk. Figure 4.25b illustrates the 1st derivative when bigger and smaller amounts of egg yolk are used. The positive and negative peaks remain the same in these two spectra. The only difference between these two spectra is the intensity of the peak. Except the ratio of positive and negative peaks between 2275-2290 nm that is changed, the peak ratios of positive and negative peaks of the main characteristic absorptions remain constant, which indicates that the 1st derivative reflectance spectrum can be used for materials' identification.

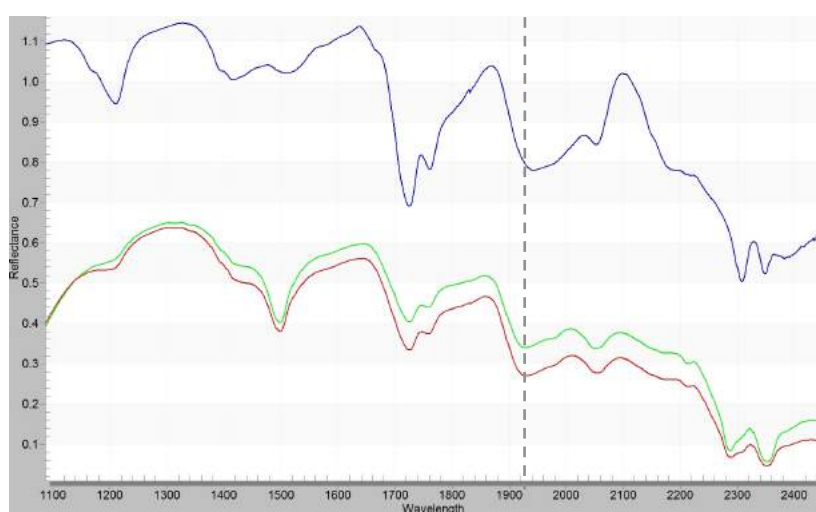


Figure 4.25a Reflectance spectra of azurite mixed with different amounts of egg yolk in 1200-2400 nm region. Green = azurite mixed with less egg yolk, Red = azurite mixed with more egg yolk. Egg yolk (blue) is also reported for comparison.

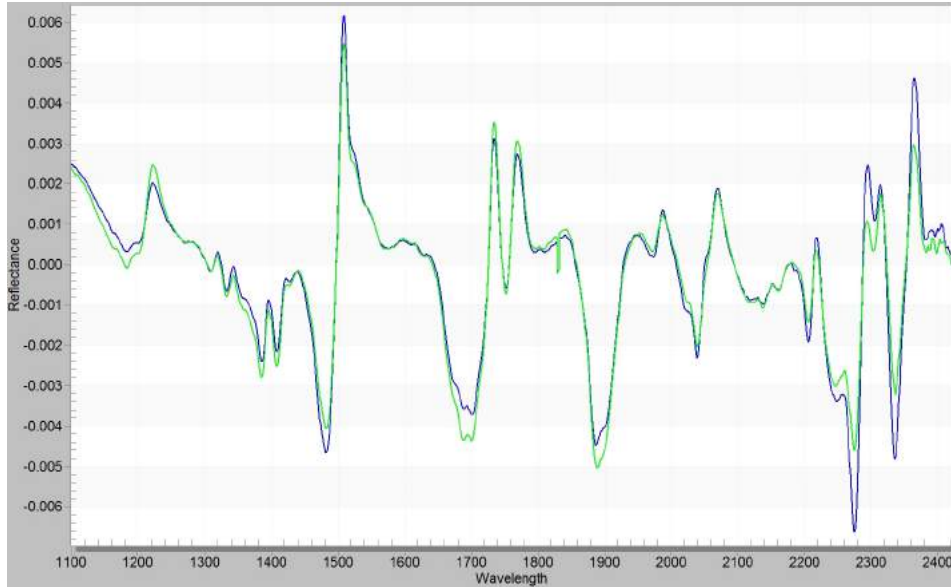


Figure 4.25b 1st derivative reflectance spectra of azurite mixed with different amounts of egg yolk in 1200-2400 nm region. Green = azurite mixed with less egg yolk, Red = azurite mixed with more egg yolk.

4.2.2.2 Identification of four binders from mixtures with the same colorant

Since colorants include inorganic and organic materials, the study for their identification when mixed with organic binders has been conveniently done separately.

➤ *Inorganic pigments*

When these binders, i.e. egg yolk, animal glue, linseed oil and gum Arabic, are mixed with the same pigment, their reflectance spectra often show features comparable to those of pure binders, and their identification is possible. Figure 4.25 illustrates the reflectance spectra in the region 1200-2400 nm of yellow ochre in the three different

mixtures: egg yolk, linseed oil and gum Arabic.

Similarly, the medium-weak peaks of animal glue and egg yolk these two proteinaceous materials around 1500 nm disappear in the spectra of the mixtures giving a similar spectral feature for all the four binding media. It is notable that the broad peak between 1930 and 1945 nm of these binders (i.e. 1942, 1946 and 1932 nm for egg yolk, animal glue and linseed oil, respectively) shifts for all binders to a shorter wavelength about 5-20 nm. Although linseed oil shifts shorter compared with others, it still has the combination band of O-H stretching and bending at the shortest wavelength 1920 nm. Another difference in mixtures between these spectra happens at around 2050 nm. Just like pure materials, yellow ochre with egg yolk has the same band at longer wavelength about 2070 nm rather than 2045 nm when mixed with animal glue. Whereas, the shoulder for linseed oil at around 2135 nm cannot be observed.

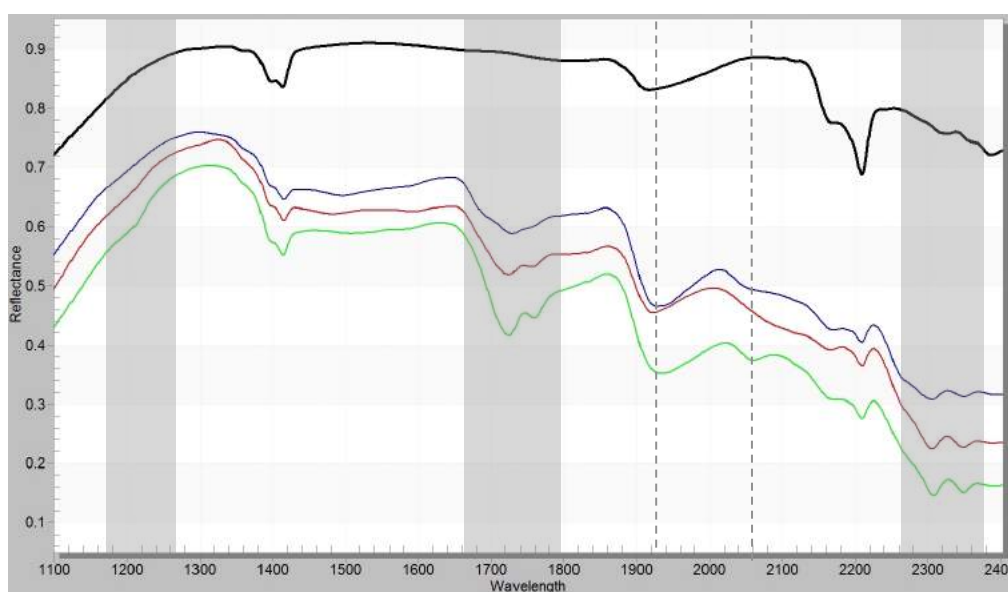


Figure 4.26 Reflectance spectra of three binding media mixed with yellow ochre. Black = pure yellow

ochre; blue = yellow ochre mixed with animal glue; red = yellow ochre mixed with linseed oil; green = yellow ochre mixed with egg yolk.

In fact, when pigments and binders have overlapping peaks, the identification of binders through the original reflectance spectra at some specific positions will be very hard. One example is the case of pigments containing O-H group or/and H₂O molecules (e.g. azurite, malachite, yellow ochre, etc.). The peaks at about 1440 nm and 1945 nm, assigned to O-H overtone and combination bands, are no more diagnostic. Thus, the 1st derivative transformation which illustrates the change of raw spectra's curve can be helpful in the characterization work. Figure 4.27 and Figure 4.28 show two examples of the application of the 1st derivative spectra to mixtures. Considering that egg yolk, linseed oil and animal glue show the most similar raw spectra of mixtures compared to gum Arabic, thus the comparison of the 1st derivative spectra of these three binders is emphasized. In the examples, yellow ochre (Figure 4.26) and azurite (Figure 4.27) were mixed with the three binders. As expected, the two regions (dashed rectangular in the figures) highlighted in the pure material identification are diagnostic for the different binders.

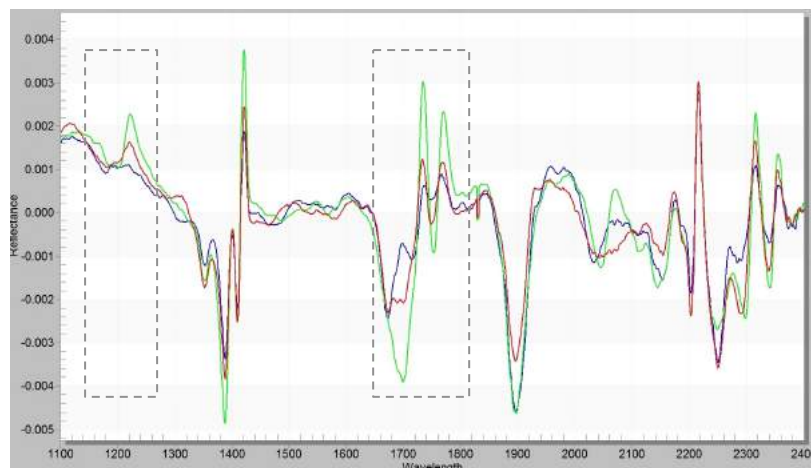


Figure 4.27 1st derivative of reflectance spectra of yellow ochre separately mixed with binding media. Blue = yellow ochre with animal glue; Green = yellow ochre with egg yolk; Red = yellow ochre with linseed oil.

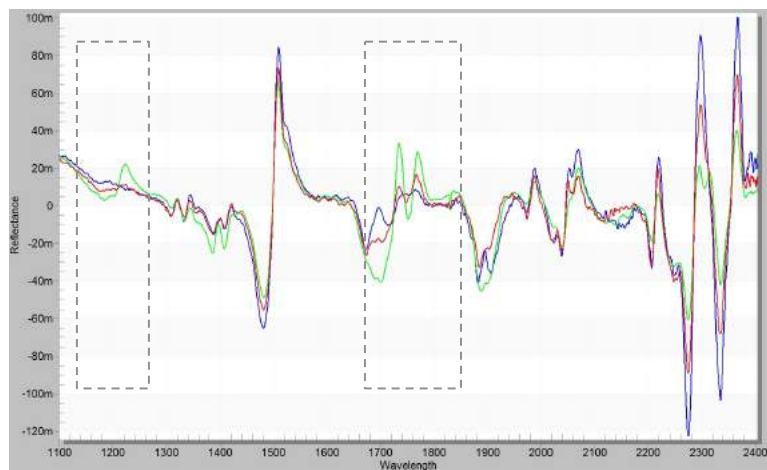


Figure 4.28 1st derivative of reflectance spectra of azurite separately mixed with binding media. Blue = yellow ochre with animal glue; Green = yellow ochre with egg yolk; Red = yellow ochre with linseed oil.

The peaks in the spectral range assigned to C-H bond vibrations should be essential for the discrimination of these three organic materials (Figure 4), as identified in pure materials. However, in the last dash region (2300-2400 nm), there are many absorption peaks due to several combination and overtones belongs to different functional groups in an object to be analyzed. Always, peaks that are very closed to each other cannot be separated in the spectra, and they combine each other to form a new broader peak in the moderated position. The overlapping and shifts of these peaks make the identification work much more difficult and complicated. Instances such as, Prussian blue has two very strong absorption peaks 2404 and 2379 nm due to the combination bands of C-N stretching [41], the difference between the spectra of its mixture with four binders becomes very hard to distinguish in this region. As well

as, the similar situation happens in carbonate pigments which have two strong absorptions at 2275 and 2350 nm due to vibration process of C-O bond.

➤ *Organic pigments*

Figure 4.28 shows the spectra of an organic pigment (red lake) mixed with three binders. The differences among the spectra of these mixtures can be observed, mainly in the region of the C-H combination (the shadow regions in Fig 4.29) and overtone bands mentioned above, but are less evident than in the case of some inorganic pigments. Therefore, the identification of different binders is more difficult. The small differences in the reflection spectra are, in this case, due to the overlap of the peaks of the organic pigment with those of the organic binders. Some other analytical methods should be done on these data.

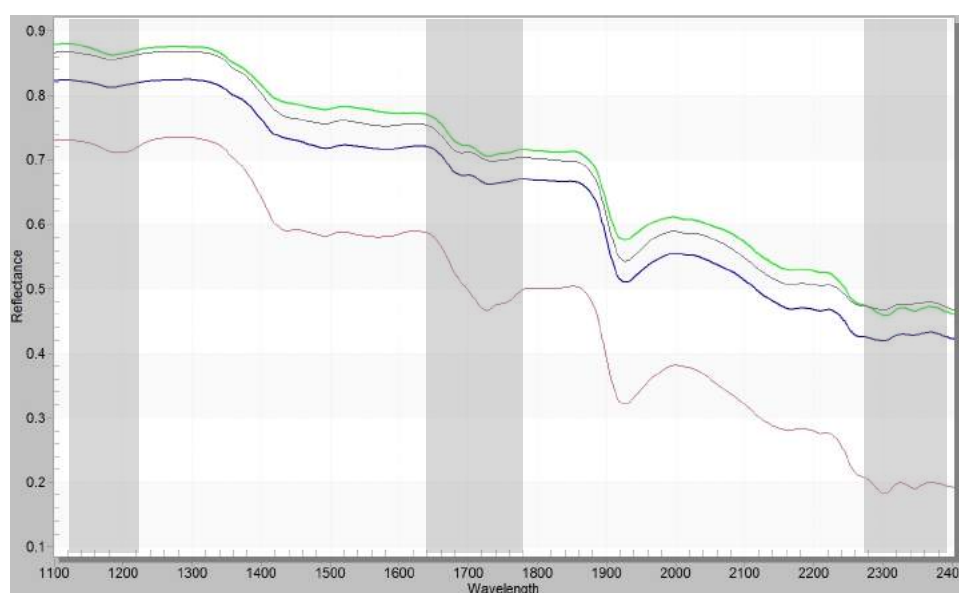


Figure 4.29 Reflectance spectra of three binding media mixed with red lake. Blue = red lake mixed with animal glue; red = red lake mixed with linseed oil; green = red lake mixed with egg yolk; black = red lake with gum Arabic.

To conclude, even though the identification of a binder in a pictorial layers can be done from several characteristic absorption features, the interaction between pigments and binders should be taken in consideration. Here, it is supposed that the characterization of painting surfaces should start from the pigment identification in the visible region, because the peaks mainly due to the electronic process are relatively diagnostic. When the pigment type is generally determined, the observation can be extended to longer wavelengths. The regions where a colorant may affect the absorption features of a binder should be less considered. The difference in the shape, the position and peak intensity of the bands emerged between ca. 1700 and 1800 nm, which general affected by the presence of organic material, should be highlighted. Other two regions also have comparative significance in the identification, but only when the suspected pigment does not have peaks in these two areas.

4.2.2.3 PCA analysis for binder identification in mixtures

Although the characterization of binders can be carried out by diffuse reflectance analysis with both their raw and first derivative spectra, a more straightforward dataset is still necessary to detect and identify different binding media in the mixtures. Considering that each reflectance spectrum is described by 2151 points (350-2500nm), principle component analysis (PCA) should be helpful in this study of identification of four kinds of binders when mixed with different pigments. However, two points must be taken into consideration: first, a reflectance spectrum always has broader

bands than a NMR and FT-IR spectrum; second, the identification of binding media from pigments mixtures is one of the main purposes of the thesis rather than its color. Therefore, an appropriate selection of a set of points from the reflectance spectrum is mandatory. At first, a spectrum of 1301 points was selected between 1100 nm and 2400 nm, with the elimination of the effect caused both by color and the possible noise happened in the short wave ranges. This set of points has been identified according the principal component analysis (PCA) of value in the same range between 1100 and 2500 nm of their raw spectra carried out by using as reference data set about these 84 standard samples (9 points in each sample) containing the four kinds binders: egg, animal glue, gum Arabic and linseed oil. Figure 4.30-4.47 show score plots of each colorant with each binder. The first two principal components account for more than 89% of the variance of the data.

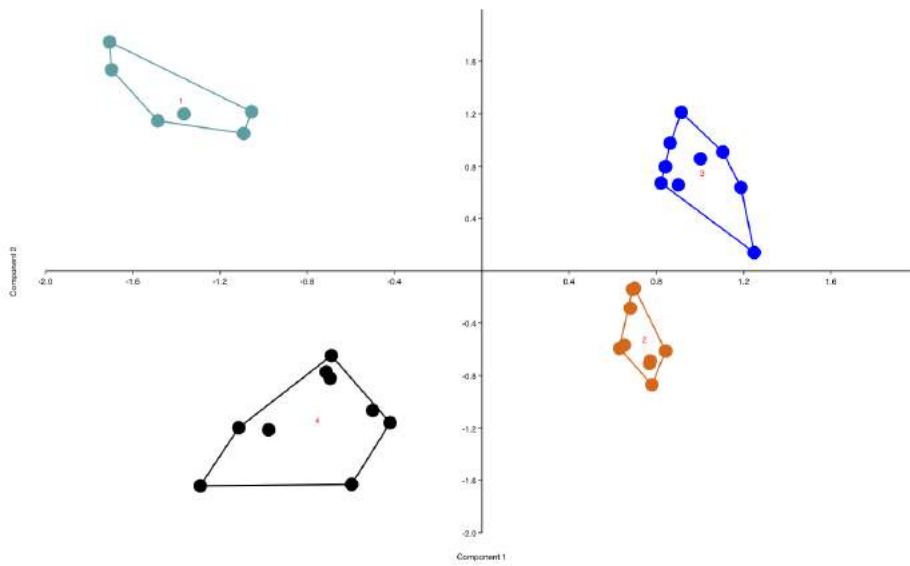


Figure 4.30 Score plot of PCA of azurite with four binders by (Group 1 in green color: with egg yolk; Group 2 in red color: with animal glue; Group 3 in blue color: with gum Arabic; Group 4 in black color with linseed oil)

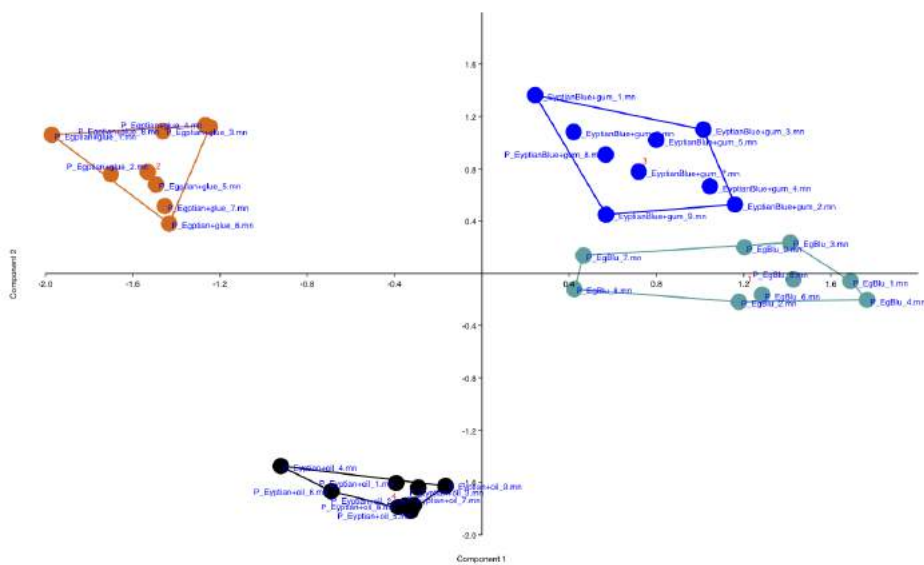


Figure 4.31 Score plot of PCA of Egyptian blue with four binders by (Group 1 in green color: with egg yolk; Group 2 in red color: with animal glue; Group 3 in blue color: with gum Arabic; Group 4 in black color with linseed oil)

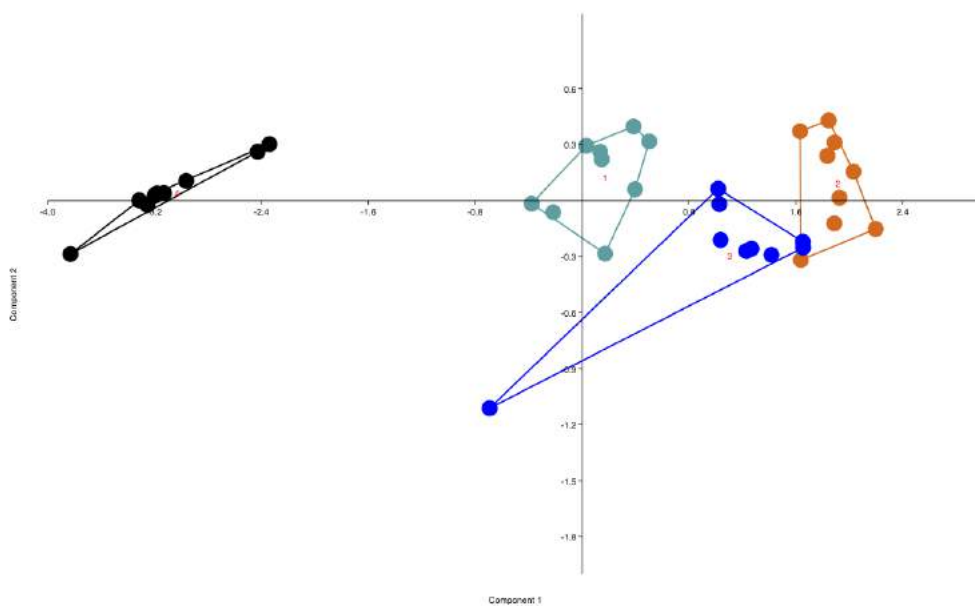


Figure 4.32 Score plot of PCA of indigo with four binders by (Group 1 in green color: with egg yolk; Group 2 in red color: with animal glue; Group 3 in blue color: with gum Arabic; Group 4 in black color with linseed oil)

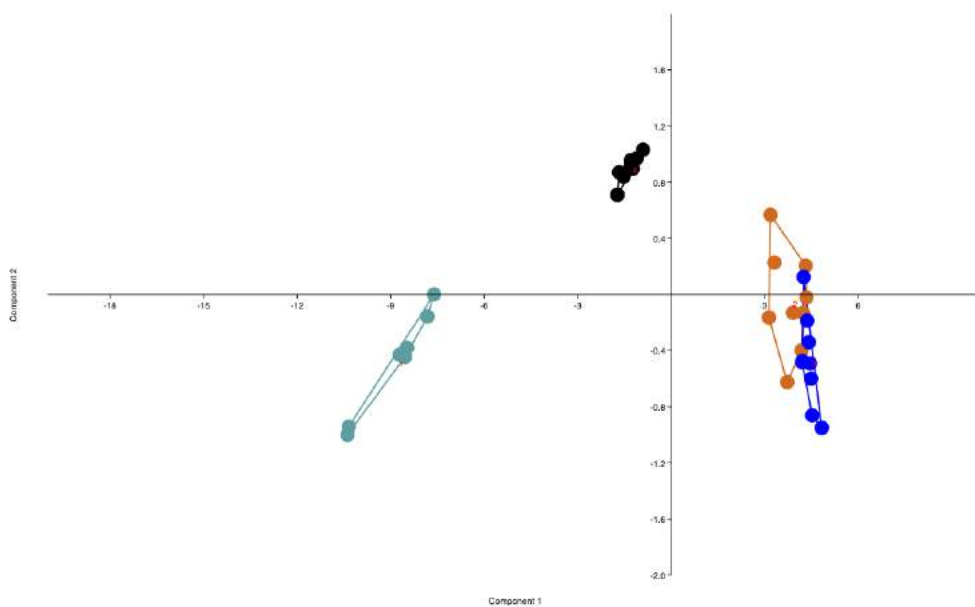


Figure 4.33 Score plot of PCA of lapislazuli with four binders by (Group 1 in green color: with egg yolk; Group 2 in red color: with animal glue; Group 3 in blue color: with gum Arabic; Group 4 in black color with linseed oil)

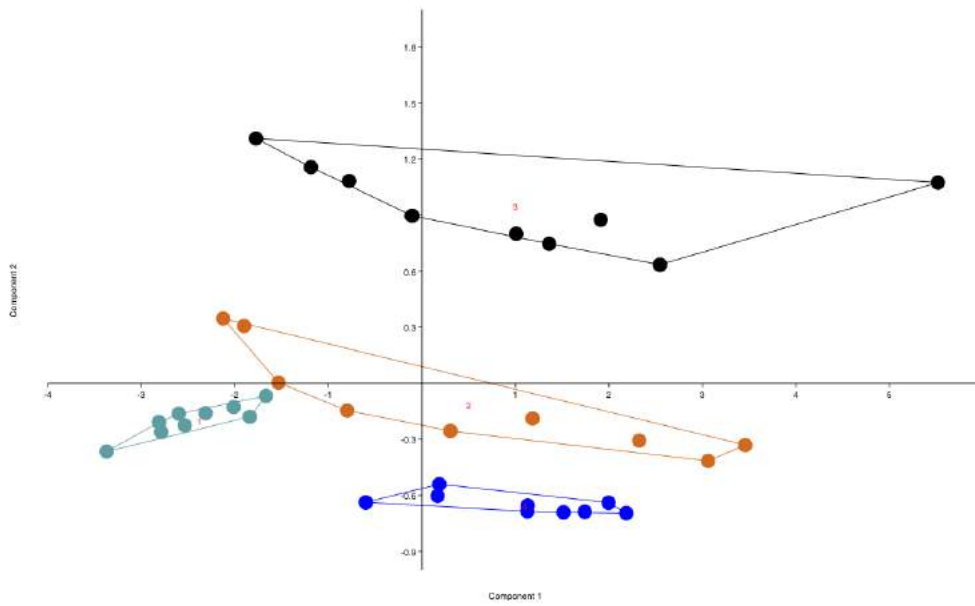


Figure 4.34 Score plot of PCA of smalt with four binders by (Group 1 in green color: with egg yolk; Group 2 in red color: with animal glue; Group 3 in blue color: with gum Arabic; Group 4 in black color with linseed oil)

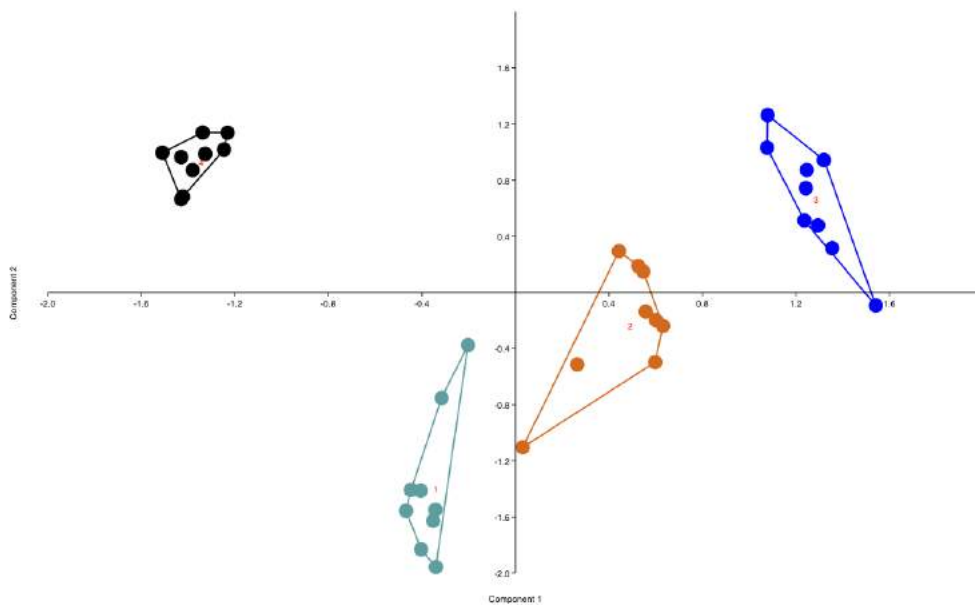


Figure 4.35 Score plot of PCA of synthetic ultramarine blue with four binders by (Group 1 in green color: with egg yolk; Group 2 in red color: with animal glue; Group 3 in blue color: with gum Arabic; Group 4 in black color with linseed oil)

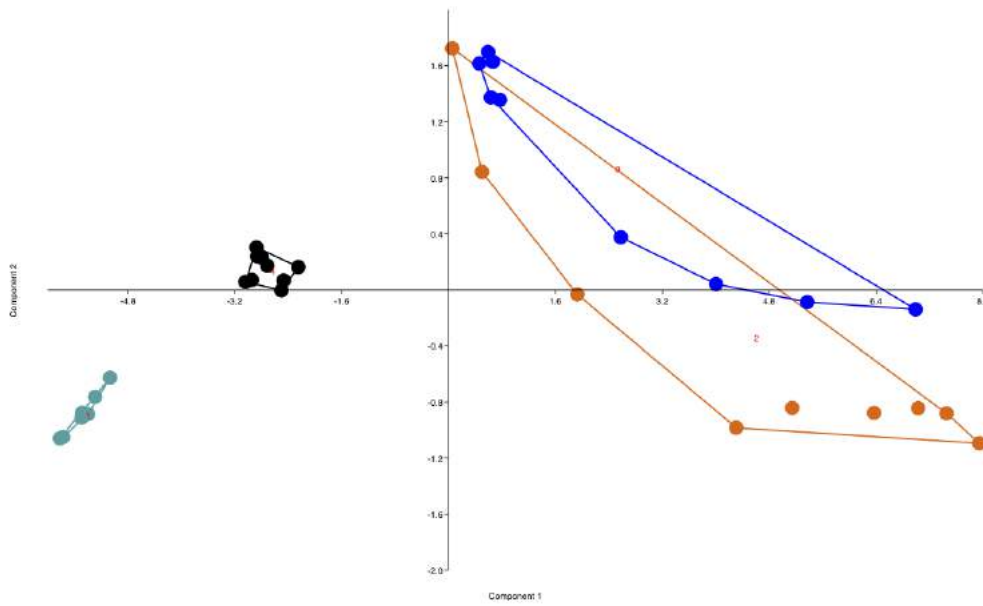


Figure 4.36 Score plot of PCA of malachite with four binders by (Group1 in green color: with egg yolk; Group 2 in red color: with animal glue; Group 3 in blue color: with gum Arabic; Group 4 in black color with linseed oil)

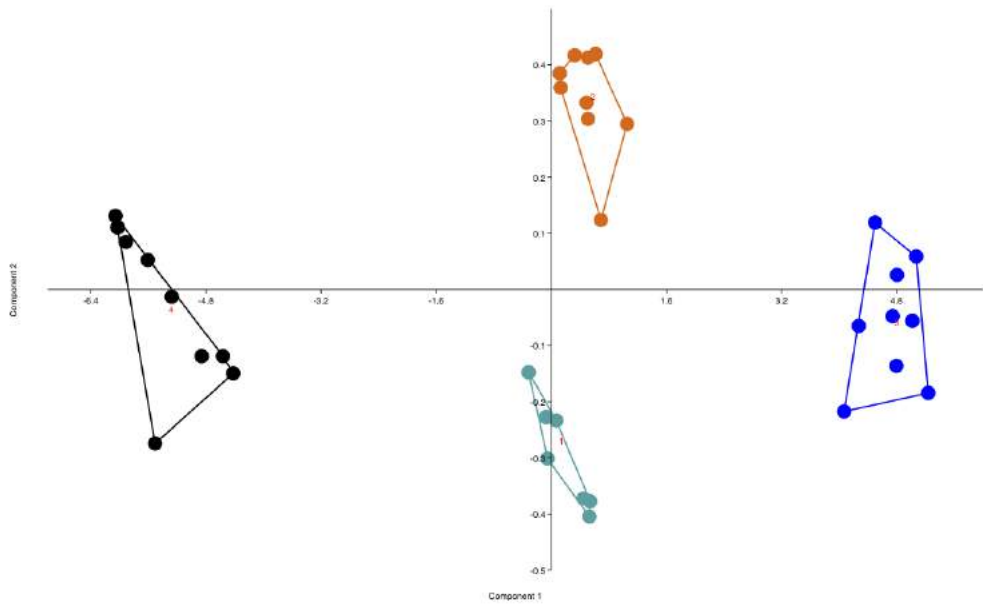


Figure 4.37 Score plot of PCA of green earth with four binders by (Group1 in green color: with egg yolk; Group 2 in red color: with animal glue; Group 3 in blue color: with gum Arabic; Group 4 in black color with linseed oil)

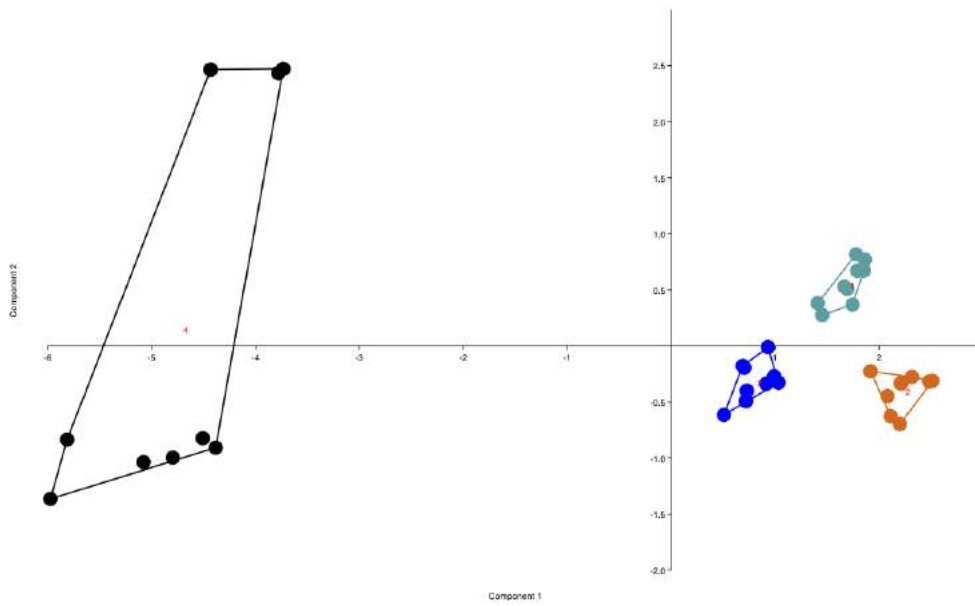


Figure 4.38 Score plot of PCA of Armenian bolo with four binders by (Group1 in green color: with egg yolk; Group 2 in red color: with animal glue; Group 3 in blue color: with gum Arabic; Group 4 in black color with linseed oil)

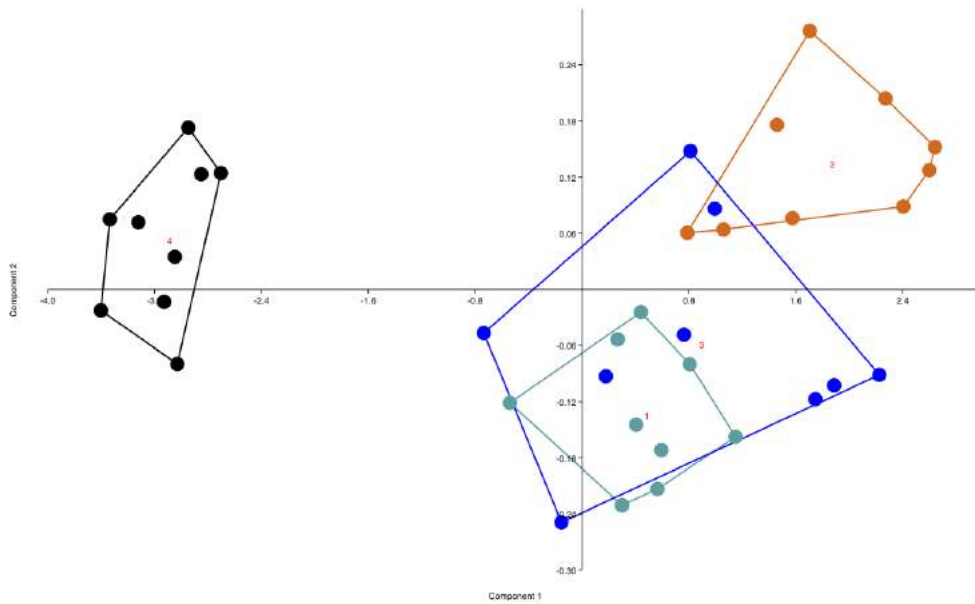


Figure 4.39 Score plot of PCA of Cadmium red with four binders by (Group1 in green color: with egg yolk; Group 2 in red color: with animal glue; Group 3 in blue color: with gum Arabic; Group 4 in black color with linseed oil)

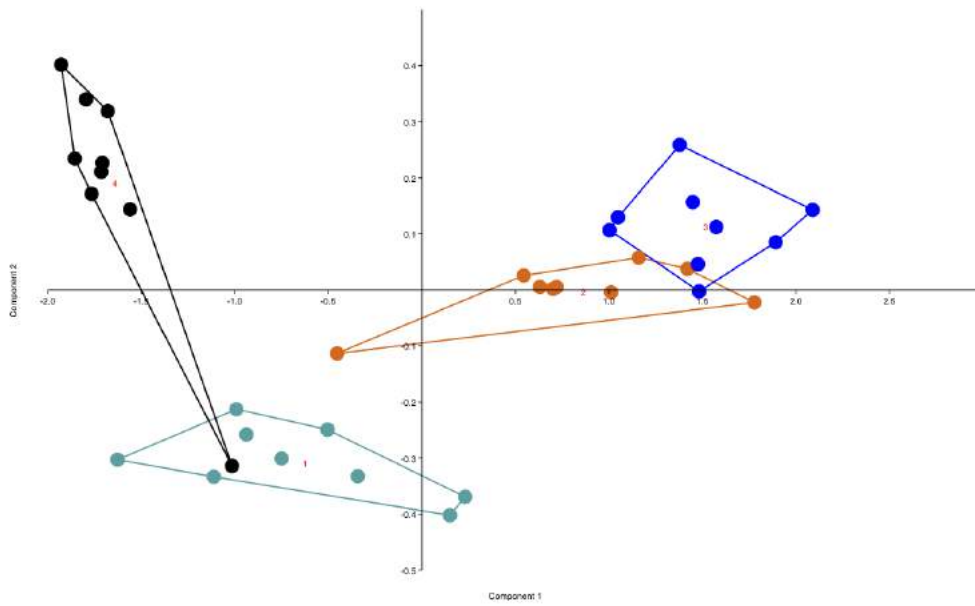


Figure 4.40 Score plot of PCA of English red with four binders by (Group1 in green color: with egg yolk; Group 2 in red color: with animal glue; Group 3 in blue color: with gum Arabic; Group 4 in black color with linseed oil)

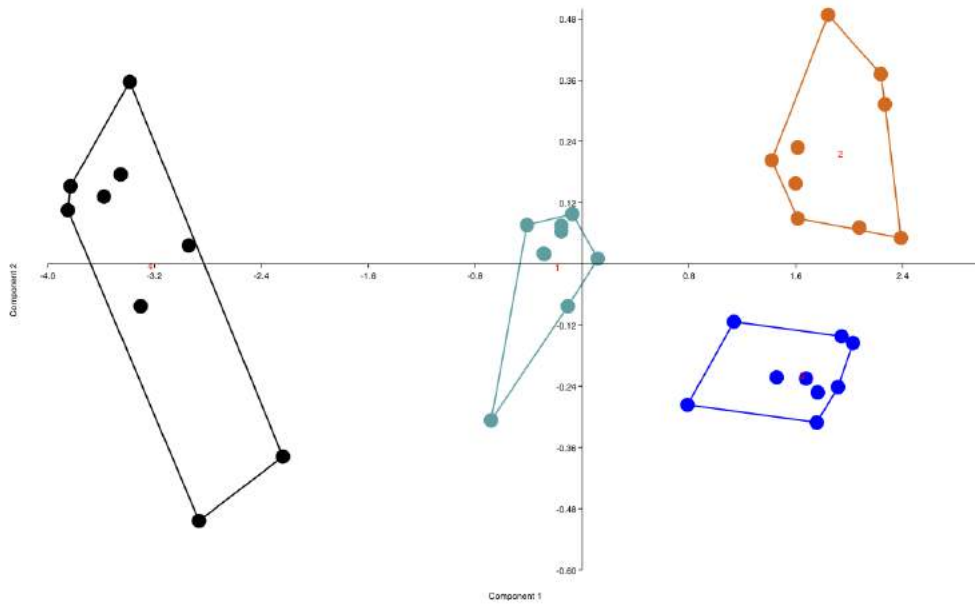


Figure 4.41 Score plot of PCA of Cinnabar from Amiata Mountain (MA) with four binders by (Group1 in green color: with egg yolk; Group 2 in red color: with animal glue; Group 3 in blue color: with gum Arabic; Group 4 in black color with linseed oil)

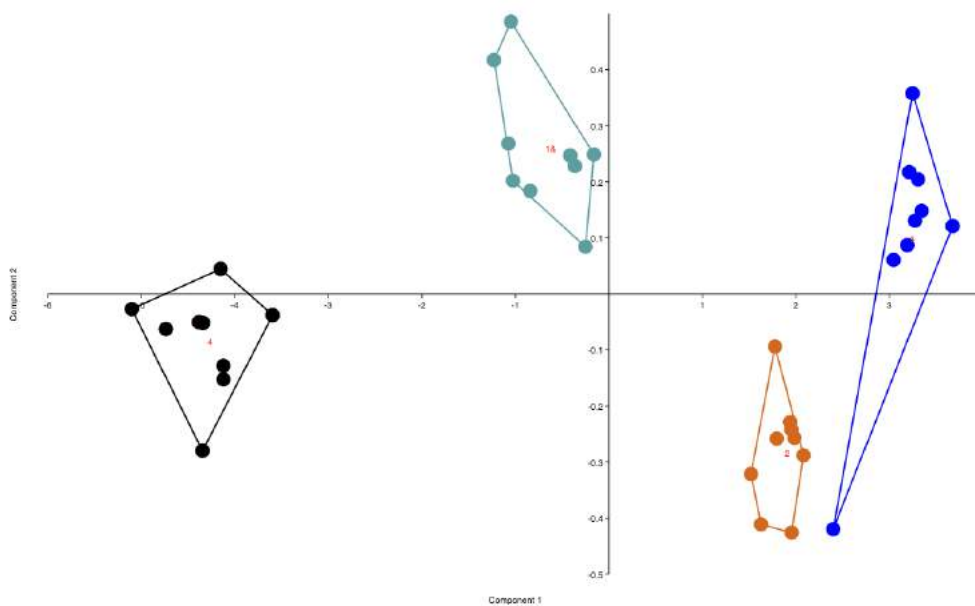


Figure 4.42 Score plot of PCA of red lake with four binders by (Group1 in green color: with egg yolk; Group 2 in red color: with animal glue; Group 3 in blue color: with gum Arabic; Group 4 in black color with linseed oil)

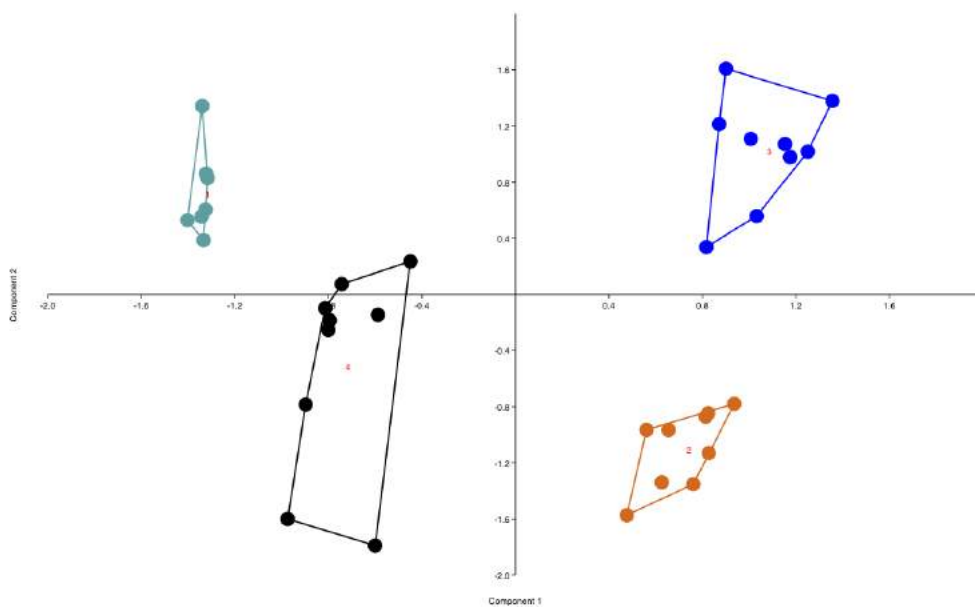


Figure 4.43 Score plot of PCA of lead white with four binders by (Group1 in green color: with egg yolk; Group 2 in red color: with animal glue; Group 3 in blue color: with gum Arabic; Group 4 in black color with linseed oil)

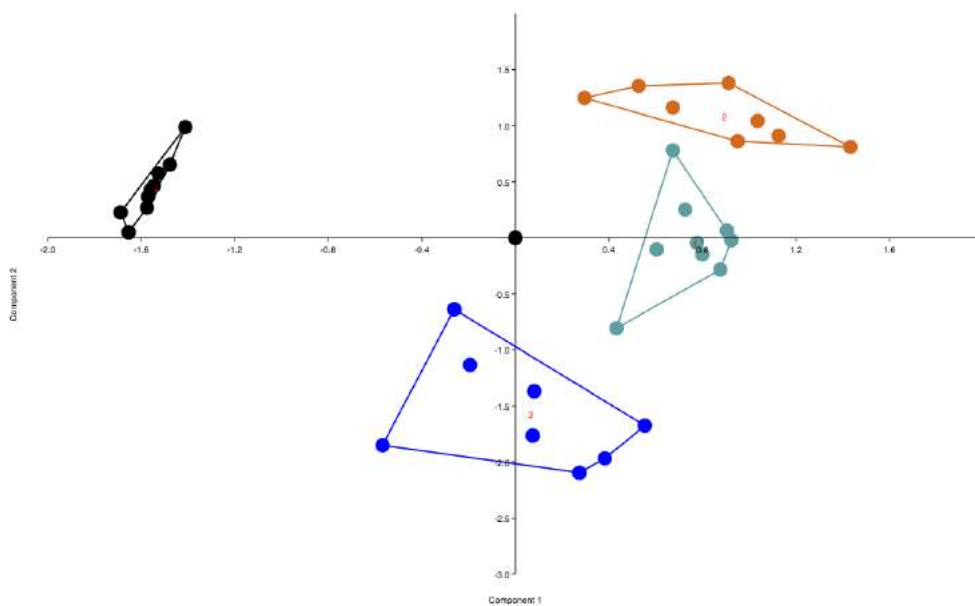


Figure 4.44 Score plot of PCA of lead white with four binders by (Group1 in green color: with egg yolk; Group 2 in red color: with animal glue; Group 3 in blue color: with gum Arabic; Group 4 in black color with linseed oil)

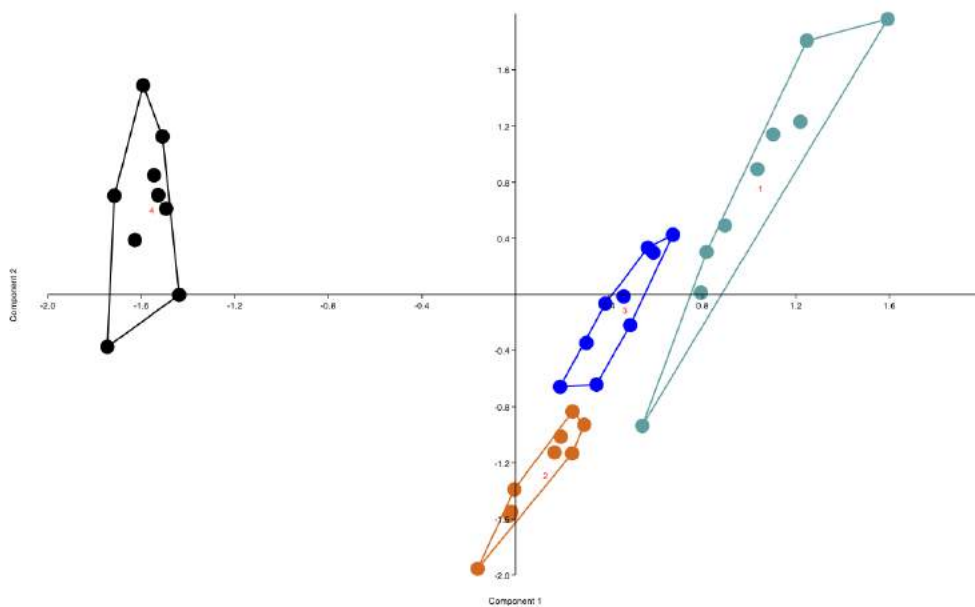


Figure 4.45 Score plot of PCA of Saint John white with four binders by (Group1 in green color: with egg yolk; Group 2 in red color: with animal glue; Group 3 in blue color: with gum Arabic; Group 4 in black color with linseed oil)

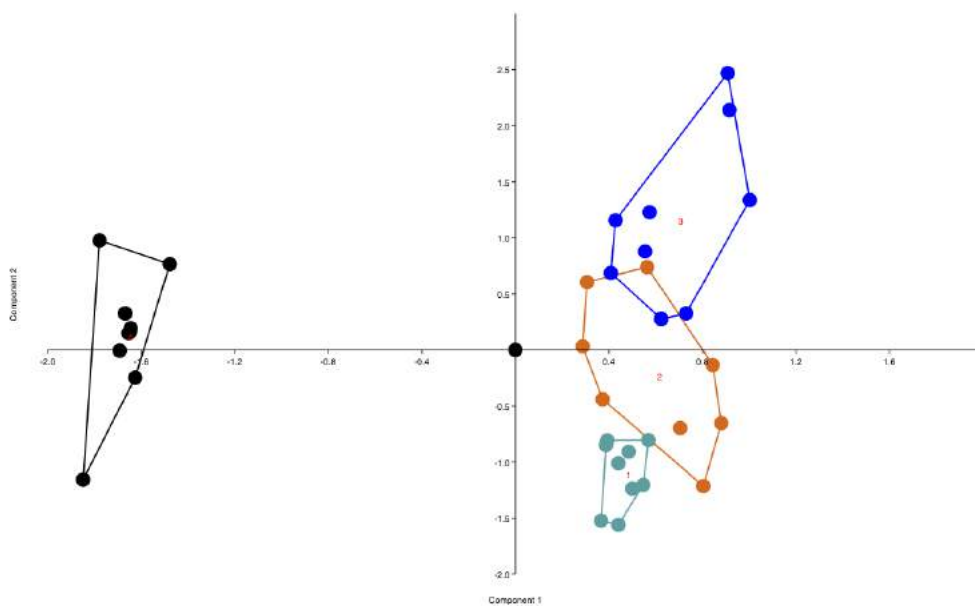


Figure 4.46 Score plot of PCA of zinc white with four binders by (Group1 in green color: with egg yolk; Group 2 in red color: with animal glue; Group 3 in blue color: with gum Arabic; Group 4 in black color with linseed oil)

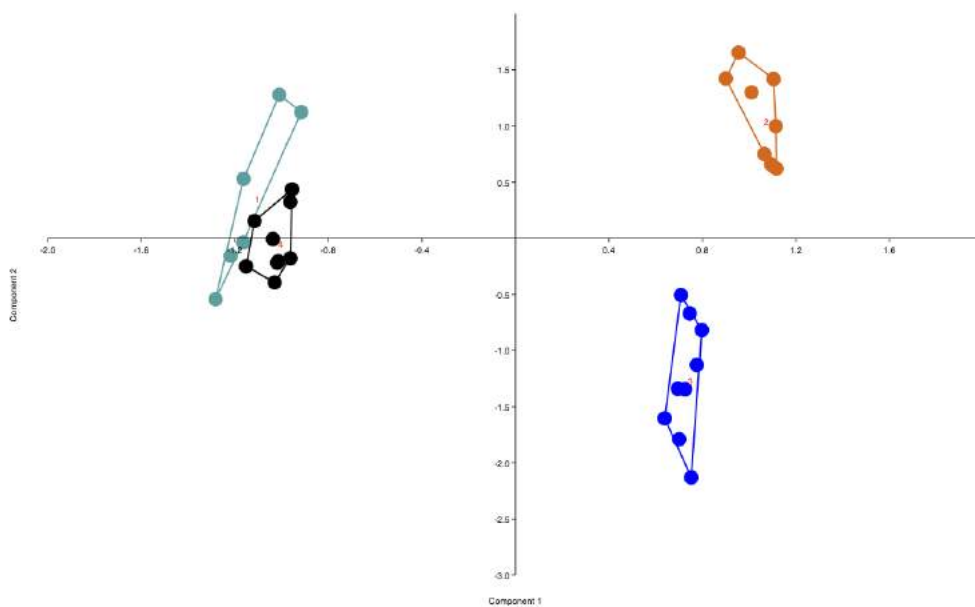


Figure 4.47 Score plot of PCA of Naples yellow with four binders by (Group1 in green color: with egg yolk; Group 2 in red color: with animal glue; Group 3 in blue color: with gum Arabic; Group 4 in black color with linseed oil)

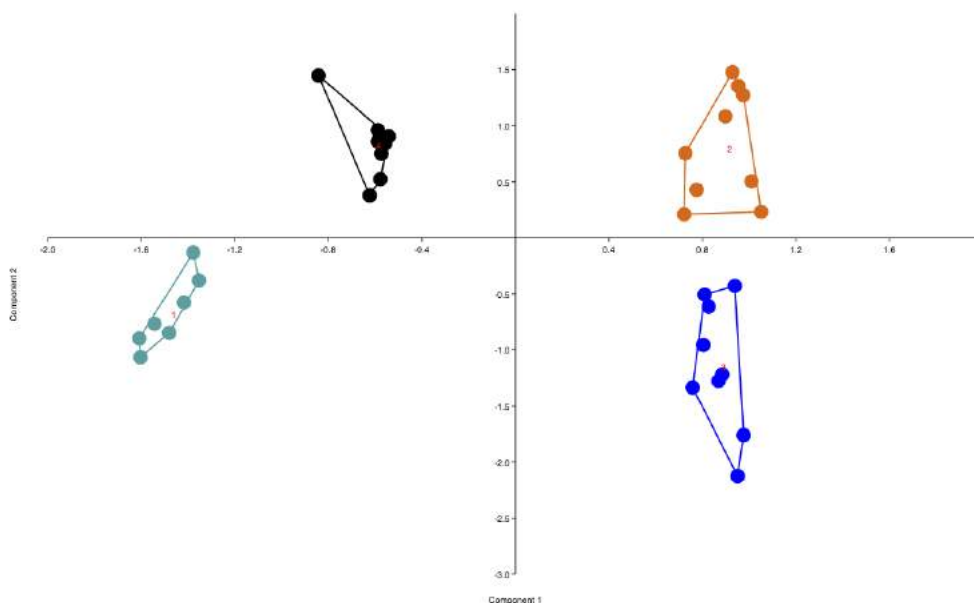


Figure 4.46 Score plot of PCA of yellow ochre with four binders by (Group1 in green color: with egg yolk; Group 2 in red color: with animal glue; Group 3 in blue color: with gum Arabic; Group 4 in black color with linseed oil)

The results of PCA show a relatively clear classification of these four paints in most of the pigment mixtures tested. The identification work, which cannot be fulfilled through the simply observation from the raw spectra, is achieved in many cases by the PCA score plot. One example is the mixture of red lake with four binders seen in Figure 4.41. Contrary to the results found by the analysis of raw spectra and the corresponding 1st derivative, the PCA score plot clearly separates the mixture samples in 4 Groups, in accordance with the binder used. From the score plot of all pigments mixtures, it can be observed that the identification of different binders is possible when a single pigment is considered. In fact, the groups representing the four binders in mixture with different pigments are not in the same position in the PCA plots (or

only sporadically). The plots of the group of linseed oil and egg yolk are always well separated from the other two, while the plots of animal glue and gum Arabic locate very close to each other. This may be due to the fact that these last binders were applied in less amount (as well as the pigments) on the canvas mock-ups. Some more experiments need to be carried out to reach a thicker painting layer.

Chapter V

Case studies

In this chapter, the hyperspectral sensor, ASD FieldSpec FR Pro was employed as a non-invasive analytical tool for real artwork characterization. Based on the analytical protocol proposed and results already obtained in previous chapters, the in-situ identification works of two case studies were carried out. The first one is the characterization of binding medium and pigments used in an easel painting by an unknown author. Another case study is the identification of the restoration and degradation components in the fresco located in the Santo Stefano Church in Lamporecchio. The measurements by FieldSpec were taken directly on the tested surface. The results were validated by other analytical techniques such as Optical microscopy (OM), Fourier Transform Infrared spectroscopy (FT-IR), scanning electron microscopy energy dispersion spectroscopy (SEM-EDS), and Raman spectroscopy.

5.1 Easel painting surface characterization

5.1.1 Basic information on an old painting by an unknown author

The old easel painting under investigation was said to be painted at the end of XIX century. The reflectance spectra were collected on the painted surface after the varnish removal by an Er:YAG laser cleaning. Unfortunately, there is no information about the origin, author, provenance, storage, conservation history etc.

Two areas, indicated by the red rectangular on Figure 5.1 (1:white; 2:black), were selected for characterization of pigments and binding medium just after varnish removal (Er:YAG laser cleaning, using water as wetting agent). The white region was used for reflectance spectra, while the black one for the FT-IR analysis.



Figure 5.1 The old painting used for the validation of the hyperspectral sensor ASD FieldSpec FR Pro as non-invasive and non-destructive method of pigments and binding medium characterization.

5.1.2 Identification of pigments and its binding medium

The region tested by ASD FieldSpec FR Pro was a white area after Er-YAG laser cleaning. The raw spectra collected on the painted surface through the contact probe are shown in Figure 5.2. For the identification procedure the same regions of interest selected before were used, as well as the methodology of data processing. In the visible range (Figure 5.3a), a strong absorption appears in visible range at ca. 375 nm. This absorption matches the characteristic absorption peak of zinc white. This proves that the painting was painted after 1800, since zinc white was widely used after this period.

Yet, zinc white has no absorptions in the regions of organic compounds. As the varnish was firstly removed by the laser cleaning, the peaks in the region 1200-2400 nm are mainly due to the presence of the binding medium. From Figure 5.3b, it can be observed that the absorption features match that of linseed oil. More specially, the peak present at the wavelength of about 2132 nm is due to the combination band of C-O stretching and C-H stretching. The peak present at 1450 nm is assigned to the stretching modes of O-H (2ν) and O-H bonds, as well as the peaks in the three regions showed in Figure 4.14 (shadow areas), assigned to the first and second overtone and combination bands of CH₂ stretching mode. The only exception is, the peak at ca. 1930 nm which is shifted to longer wavelength (ca.1940 nm) in respect to linseed oil. This shift may be mainly derived from the use of H₂O as wetting agent during laser

cleaning, or to the presence of linseed oil transformed products (e.g. formation of salts from the hydrolysis of esters of linseed oil).

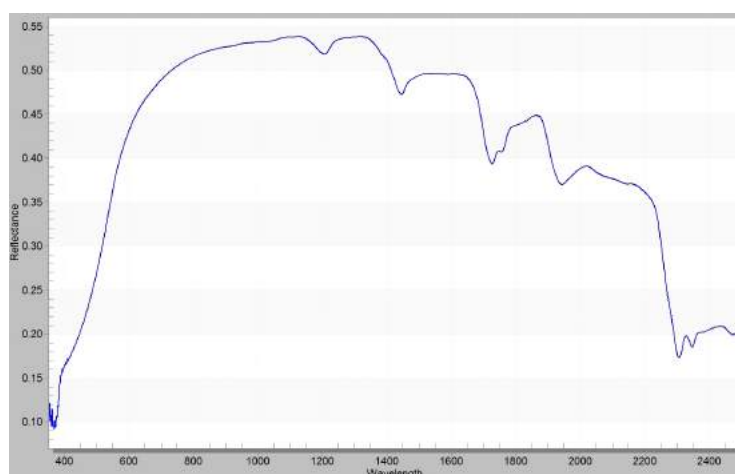


Figure 5.2 Full range reflectance spectrum of the white region in the painting.

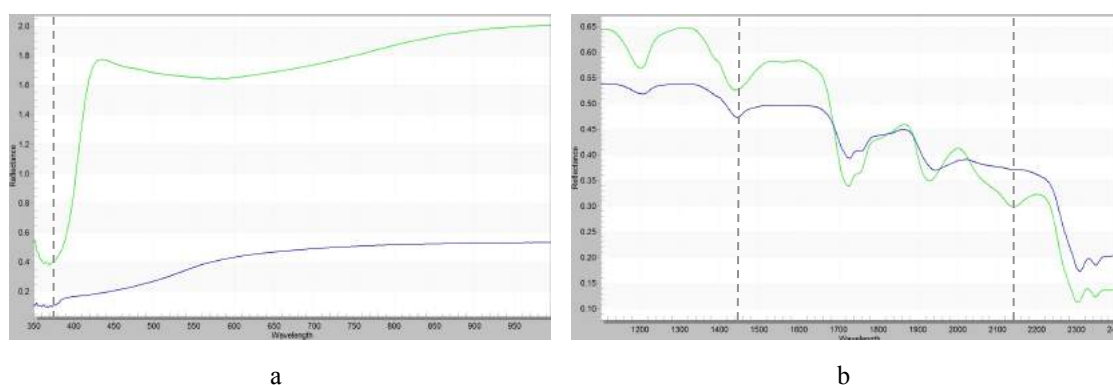


Figure 5.3 Reflectance spectra of the white region in the old painting (blue) in visible and 1100-2400 nm region. Zinc white and linseed oil (green) spectra are also reported for comparison.

To confirm the use of linseed oil as the binder, the 1st derivative spectra were also obtained and shown in Figure 5.4. It can be seen that peaks match the entire characteristic peaks of linseed oil. Although the peak features related to CH₂ bond seem quite similar to those of egg yolk, the peaks shapes differ, especially in two regions, i.e. 1730-1760 nm and 2300-2400 nm (Figure 5.5). Moreover, the 1st derivative spectra collected in 1100 -1250 nm also vary from that of egg yolk. To

support this interpretation, the comparison between egg yolk, linseed oil and the real painting were illustrated in Figure 5.5a, Figure 5.5b and Figure 5.5c for these three regions. It becomes more obvious that the spectra of the real painting match that of linseed oil. Thus, we may confirm that the binder is a kind of oil.

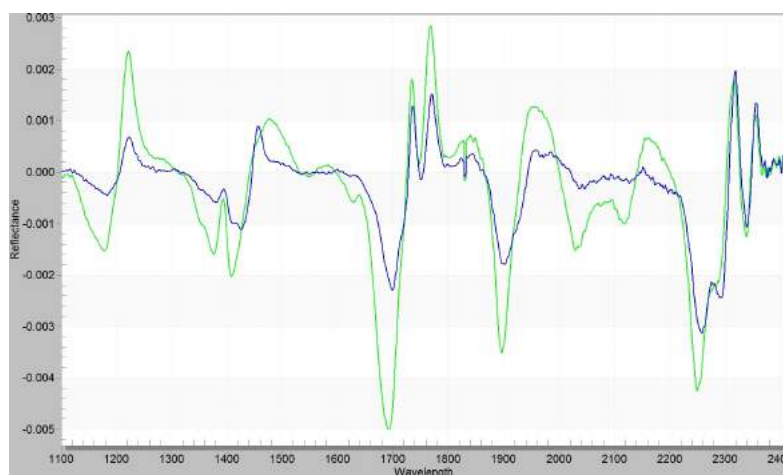


Figure 5.4 1st derivative spectra of the white region in the old painting (green) in 1100-2400 nm region. Linseed oil (blue) is also reported for comparison.

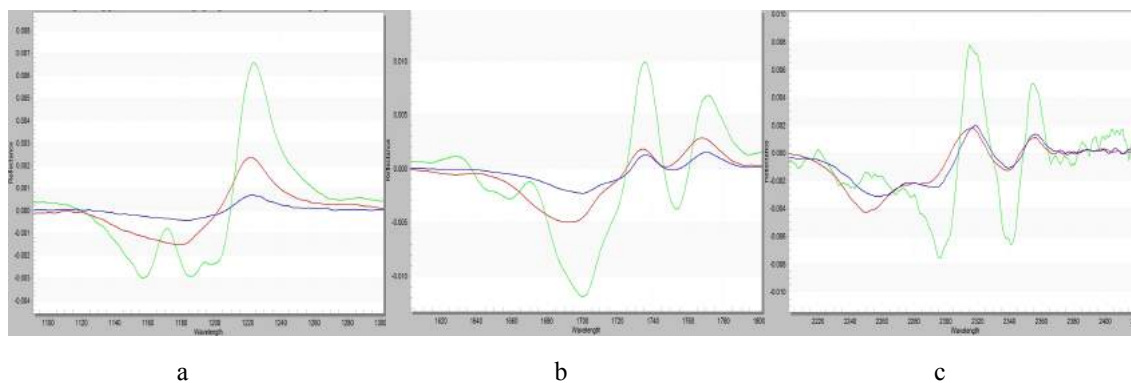


Figure 5.5 Zoomed areas of the 1st derivative spectra of the white region in the old painting (blue): 1100-1300 nm region (a), 1600-1800 nm region (b) and 2200-2400 region (c) nm. Linseed oil (red) and egg yolk (green) are also reported for comparison.

The result was also verified by FT-IR analysis. For this analysis a dark region was selected because it was the best area where the sample was easily taken without damaging the painting.

As it can be seen in Figure 5.6, oil partially transformed in salt was detected after the assignment of the peaks. The presence of salts indicated the aging of the painting.

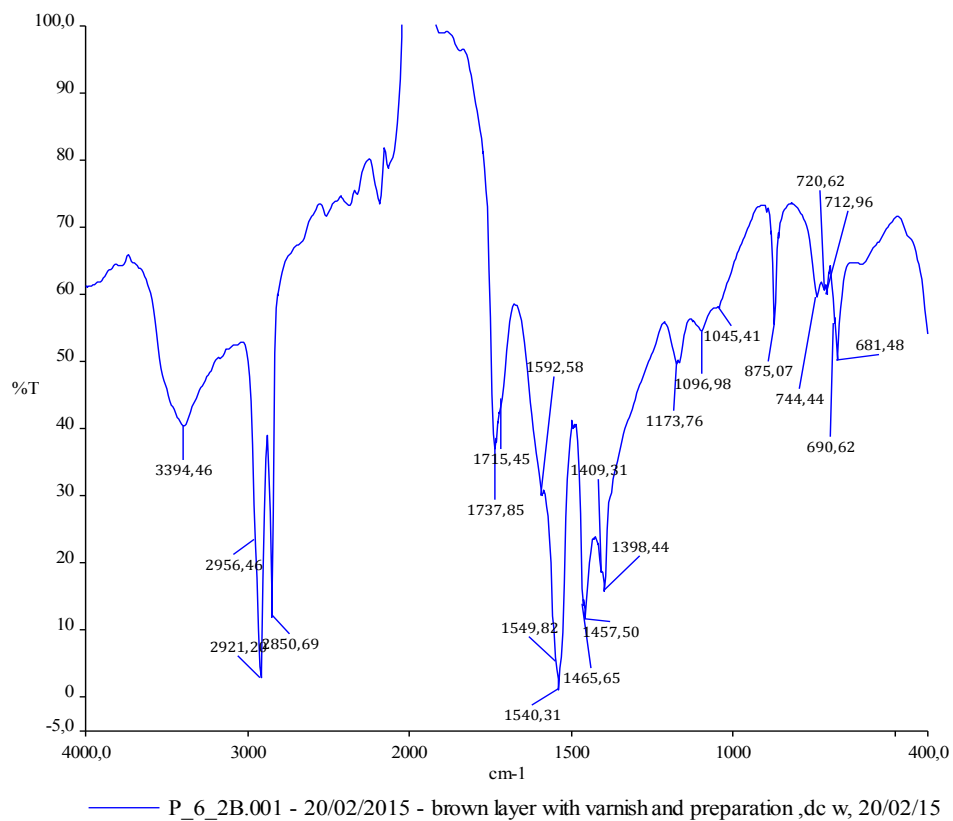


Fig 5.6 FT-IR spectrum of the sample taken from the black area of the real painting

5.2 The characterization of the fresco in the church of Saint Stefano, Lamporecchio, Italy

5.2.1 history and pre-restoration works of the church

The Church of Santo Stefano in Lamporecchio was built between 1900 and 1921 on a pre-existing church which dates back to 13th century. Bernardini was the architect who designed and supervised the construction of church. There are numerous noteworthy works of art inside the church. A remaining treasure is an altarpiece representing the Visitation of the Virgin Mary to Saint Elisabeth which is surrounded by Saint Sebastiano and Saint Rocco. Another famous artwork is the shovel, is attributed to from the XVII century which is made in terracotta and polychrome stained glass, attributed to Giovanni della Robbia (1524-1525). Also, there are several beautiful paintings, such as "Glory of the Angles" (1628-1719), "Virgin with Christ child and Saints" (1750), and so on. A complex restoration of the Church has recently been completed, involving the façade, the altar, the crucifix and other decorative elements of the church of S. Stefano in Lamporecchio. The restoration works began under the direction of the architect Mirta Cappelli, and proceeded with the cleaning, painting and consolidation of the facade, replacing the detached plaster and restoring the fractures of the decorative elements.

The fresco under study is located in a lateral chapel of the church. It was painted in the XVIII century, but many restoration treatments have been realized in the past due to the not well preservation conditions present in the chapel. An image of the church and the chapel where the fresco is located is reported in Figure 5.7.

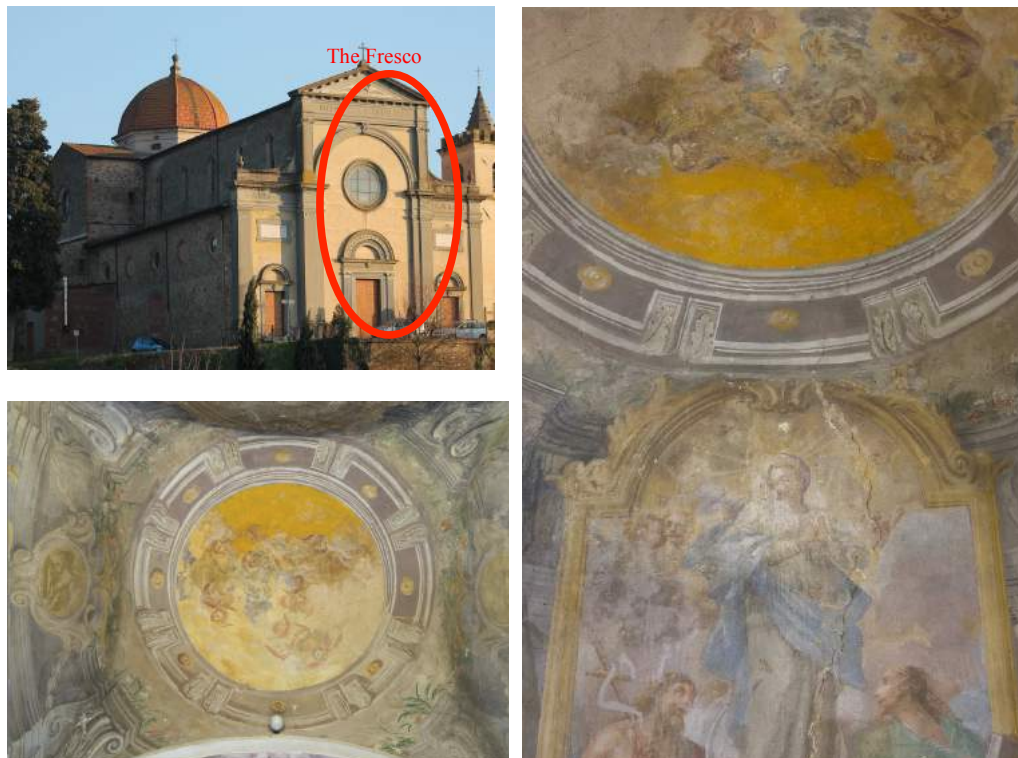


Figure 5.7 The Church of Saint Stefano in Lamprecchio with the location of the fresco. A detail of the fresco is also reported.

5.2.2 Current condition and preliminary scientific investigation of the fresco

This fresco in Saint Stefano Church was frequently restored; the last documented interventions were made in the second half of 1900 (around 1960-1980) . Due to not properly environmental conditions and worship activities, the fresco is now in a

precarious state of conservation. Moreover, it is covered with a layer of black crust, a carbonated layer, heavy re-painted layers and a thick film of a polymeric substance, mainly found on the edges of the round dome. Some colors faded. Moreover, there are some cracks in the fresco because the roof of the dome was leaking. Some preliminary scientific investigations By Ultraviolet observations show that there is a layer of varnish on its surface. The analysis by polarized microscopy on the cross sections of samples revealed the presence of at least two pictorial interventions. The older intervention was a light gray color, consisting of lime layers lightly pigmented with charcoal black. The second intervention, separated from the first one by a thin deposit of dust, consists of lime layer, with or without over-painting.

5.2.3 Characterization work

Our identification work was concentrated on the upper end of the fresco and on the round dome where they are most evidently damaged. In order to search the most accurate method to clean the previous restoration intervention, as well as the materials used in the original painting, we started our work. As described in Chapter I, non-invasive analysis by the hyperspectral sensor was firstly carried out. This measurement was taken on different regions where different colors were present. After a very fast comparison of the reflectance spectra, four areas on the fresco were selected for the collection of micro samples for laboratory analyses. The areas named Area S1-S4, as marked in Figure 5.8. These samples were firstly examined under

optical microscope and then analyzed by FT-IR spectroscopy/Raman spectroscopy as powder, and finally embedded in epoxy resin for SEM-EDS analysis. Our aim was to identify the colorants and varnishes used in this frescoes and to validate the results obtained by the hyperspectral sensor. The results of the non-invasive and invasive analytical methods are shown below.



Figure 5.8 Detail of the fresco and location of the sampling Areas (S1-S4).

5.2.3.1 Area S1 with grey (light blue) & blue colors on the ceiling

- Grey (lighter blue) and blue on the ceiling with yellow analyzed by FieldSpec

Blue colors are widespread on the ceiling of the round dome as the color of sky. As a background color, they are always present with other colors such as yellow and purple. Reflectance spectra were collected at different positions of the sky, in order to figure

out if it was painted with the same blue pigment or not. The two positions: one is at the Area S1; the other is at the area where the blue is mixed with yellow color.

The spectrum taken at area S1 is shown in Figure 5.9b, as well as the photo of detected area (Figure 5.9a). The characteristic features in visible range between 550-650 nm are very clear: three absorption maxima at ca. 535, 593, 650 nm; and reflection maximum at 560 nm. Spectra in Figure 5.10 are all the blue pigments collected by Max or Min S in our database. It is clear, the reflectance and absorption features of this grey (lighter) blue colorant coincide with the characteristic spectral features of smalt (from 550-650 nm). However, the spectrum does not have the absorption features of the black crust in Figure 5.9a. In the rest of the spectral region, the presence of gypsum is well visible by its characteristic features as mentioned in Chapter 4.2.

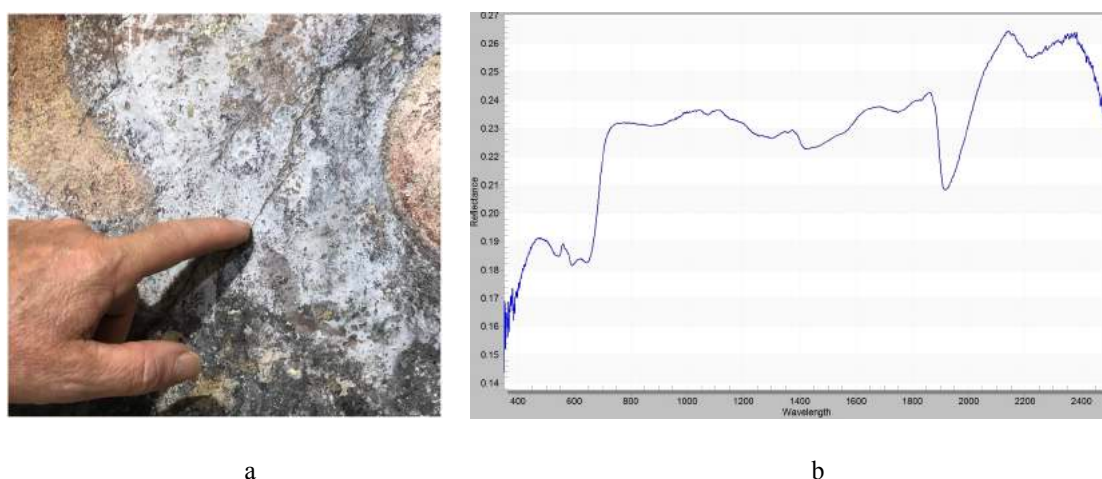


Figure 5.9 Photo of the position of Area S1 and its original reflectance spectra in full range.

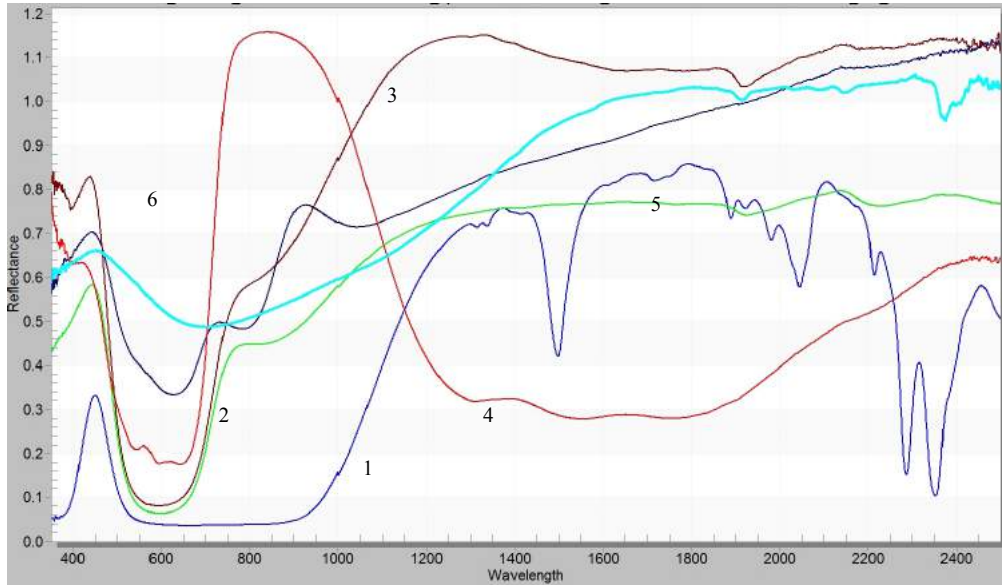


Figure 5.10 Reflectance spectra of all blue colors in full range. Dark blue 1= azurite; green 2 = lapislazuli; brown 3 = synthetic ultramarine; red 4= smalt ; black 5 = Egyptian blue; light blue 6 = Prussian blue.

The blue areas analyzed, were on the ceiling of the round dome. In Figure 5.11 two original spectra collected in the areas at position A and B are reported. Position A: blue color is more abundant than yellow (Position A in Figure 5.11a, spectrum in blue color); Position B: yellow color is more abundant than blue (Position B in Figure 5.11a, spectrum in green color). From the reflectance spectra, it is easy to detect yellow ochre in the two areas, as well as the presence of smalt. As expected, the signal intensity of yellow pigment in Position A is weaker than in Position B, and vice versa the signal intensity of peaks due to smalt. In NIR-SWIR region, gypsum is also found.

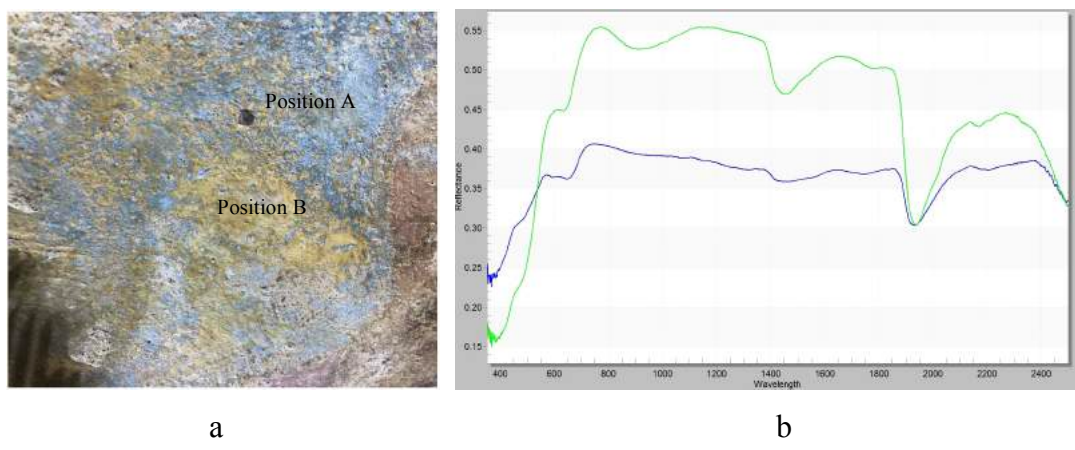


Figure 5.11 Reflectance spectra of Position A (blue) and Position B (green) in full range.

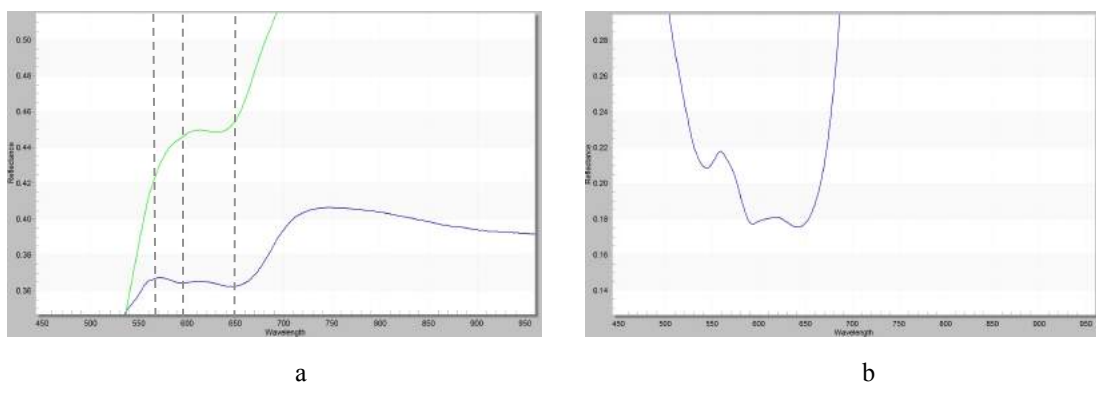


Figure 5.12 Reflectance spectra at Position A (blue) and Position B (green) in 350-1100nm spectral region (a); reflectance spectra of small in the same spectral region (b).

Apparently, the absorption maxima in the spectrum collected at the Position B is more similar to the spectrum of iron yellow, in terms of position and intensity. The spectrum at Position A, however, shows some changes in respect to peak intensity and peak position due to the presence of the blue pigment. More specifically, the reflectance maximum at ca. 450 nm becomes evident as well as another at ca. 567 nm. The absorption maximum at ca. 636 nm is shifted to ca. 650 nm. Besides, there are two more peaks in the spectra: one reflectance maximum at ca. 560 nm and an

absorption maximum at ca. 593 nm, as shown in Figure 5.12a. These characteristic features match the Min S of smalt in this region (Figure 5.12b).

- Samples from Area S1:

Basic description of samples:

The samples were taken from area S1, where the blue painting layer is covered by black crust (Figure 5.13a). Figure 5.13b gives a general view of these sample fragments.

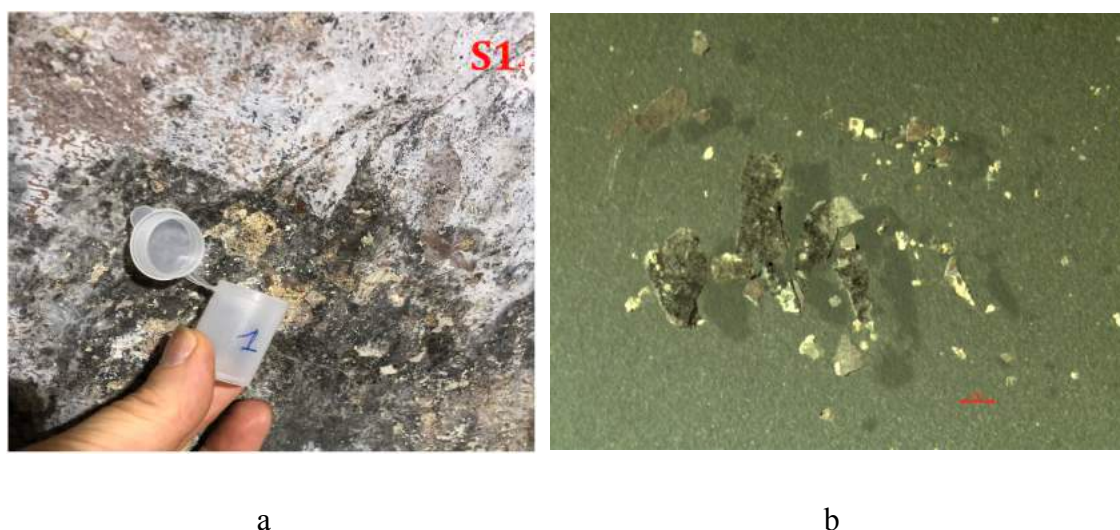


Figure 5.13 Position of sampling (a) and micro photo of sample (b) taken from Area S1.

FT-IR spectroscopic analysis was performed on a fragment where mainly the black crust is present; a detail of the micro-sample investigated by FTIR is shown in Figure 5.14 (named LMP_1wb). The black layer was very fragile and was very hard to separate from the lower white layer. Moreover, from the FTIR analysis (Figure 5.15), it can be seen that a white layer is well visible but black layer seems to have no

absorption features in the mid infrared region (probably it is carbon, not detectable by FTIR spectroscopy). The spectrum of the white layer is mainly composed by calcite, but the black compound cannot be identified.

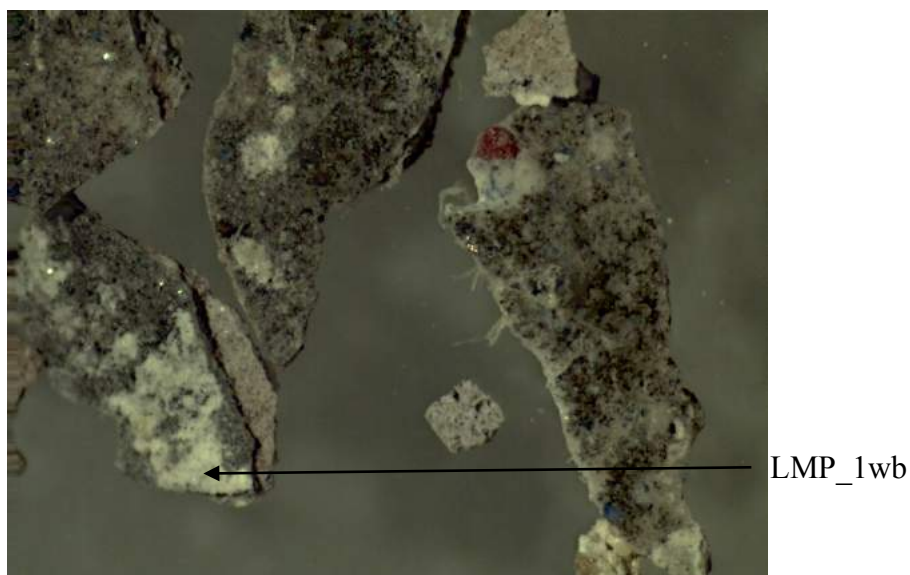


Figure 5.14 The OM imaging of LMP_1wb sample taken for the FTIR analysis from the micro fragment collected on Area S1

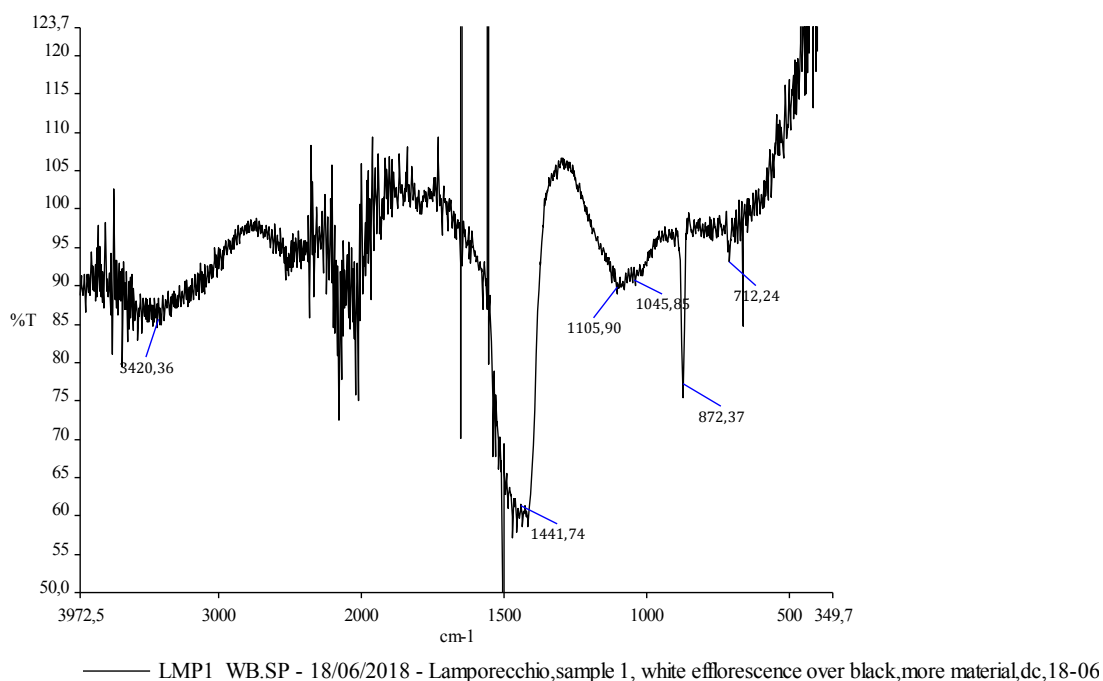
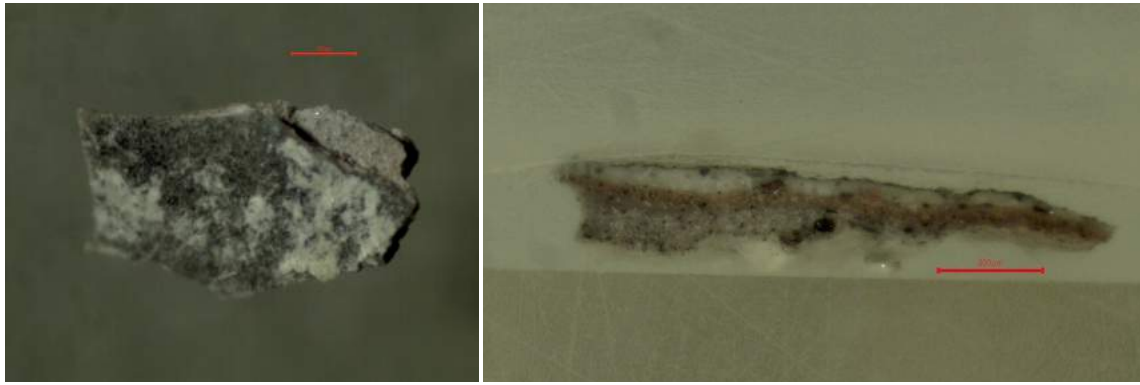


Figure 5.15 The FT-IR spectrum of LMP_1wb

Figure 5.16a is the picture of the front of a fragment named Sample S1 from Area S1. It was later embedded in epoxy resin for SEM-EDS analysis and the photo of the polished cross is reported in Figure 5.16b. It is supposed that there is a blue layer underneath this black crust. Thus this sample was characterized by SEM-EDS. In Figure 5.17, the SEM images in BSE are reported, along with the position of the points where the chemical analysis (by EDS) has been performed.

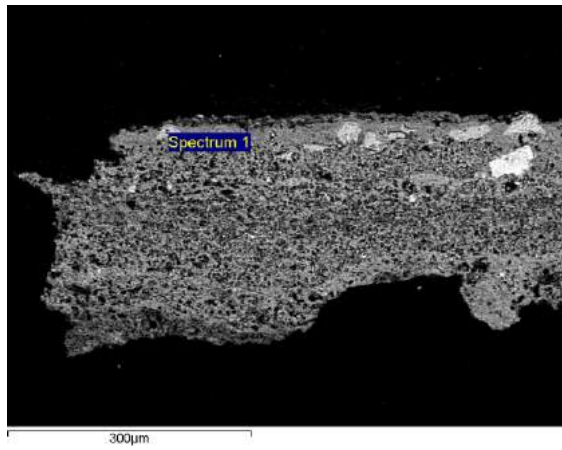
In the cross-section (Figure 5.16b), the blue pigment used for painting the sky on the ceiling is not well visible due to the thin colored layer and to the fact that it is hidden by dark crust (which was proved to be carbon by Raman spectroscopy). However, the EDS analysis of the two points illustrated in Figure 5.17 a and b detected the presence of Co and traces of Ni and As, together with a high amount of Si. This composition is in accordance with the use of smalt to paint the sky. The main component of smalt with a blue color, in fact, is erythrite ($[\text{Co,Ni}]_3[\text{AsO}_4]_2$). The preparation method of smalt blue using quartz and potash mentioned by B. Mühlethaler [94] is also verified by the presence of big amounts of silicon and by the presence of K. The result obtained by SEM-EDS analysis is in agreement with the conclusion of FieldSpec analysis.



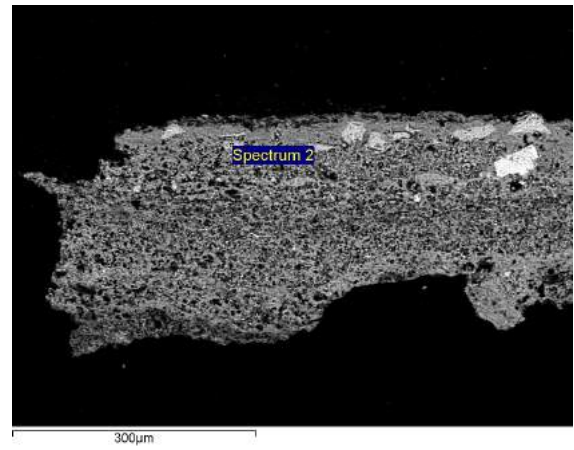
a

b

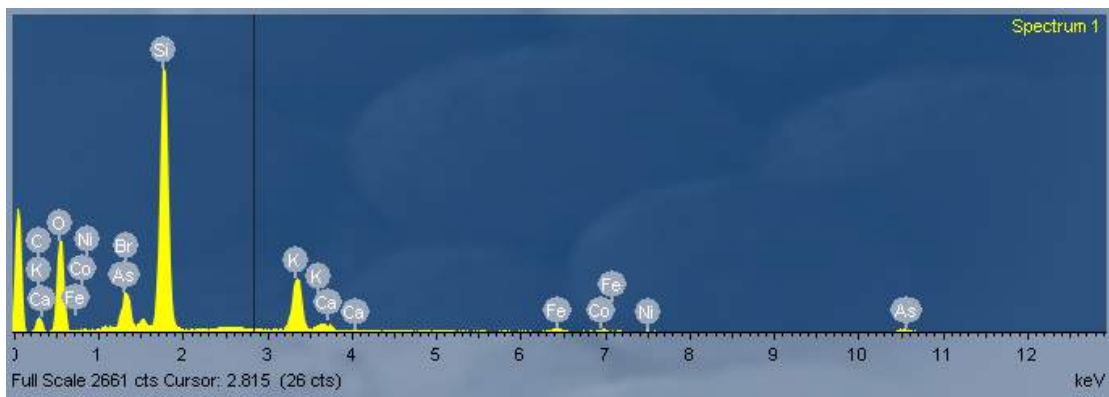
Figure 5.16 OM images of Sample S1 (a) used for SEM-EDS analysis and its polished cross section (b)



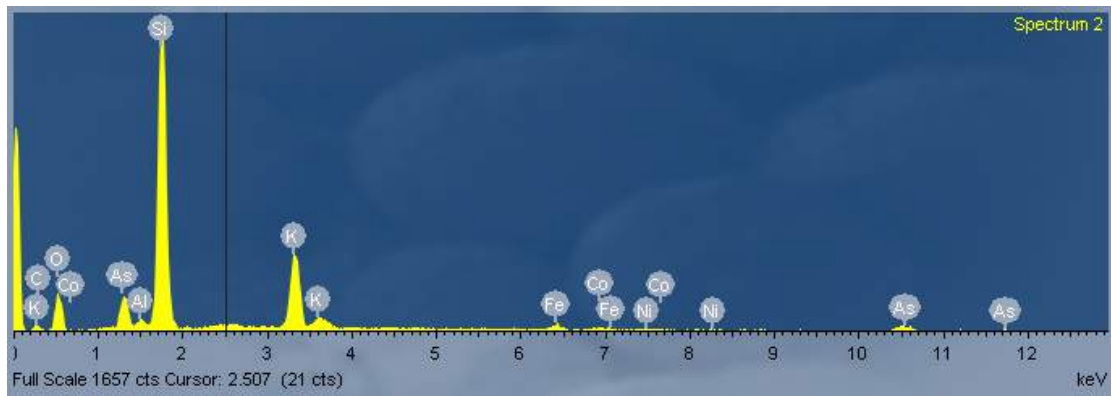
(a)



(b)



(c)



(d)

Figure 5.17 SEM images taken in BSE mode of Sample S1's cross section, the EDS analysis was also done at the points marked as spectrum 1 (a) and spectrum 2 (b). The corresponding spectra with the elemental composition are shown in (c) and (d).

Thus, it can be supposed that smalt was used as the main pigment in painting both grey (lighter blue) and blue in the ceiling. The grey color may be also due to a partial degradation of smalt. In any case, calcite from the lower layer of fresco was not detected by FieldSpec; this is due to the fact that the reflectance spectra are always collected from the surface and not in depth.

5.2.3.2 Area S2 & varnishes on frescoes

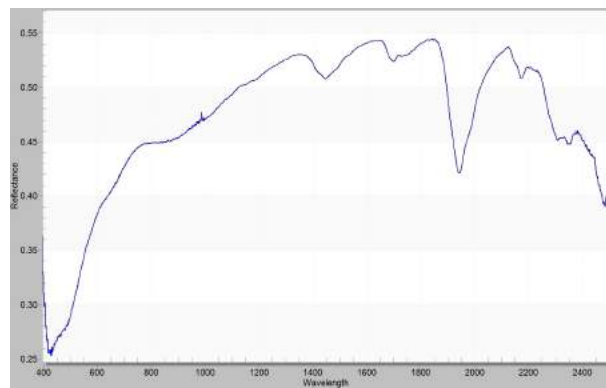
- Varnishes analyzed by FieldSpec

The reflectance spectrum on the Area S2 was collected from a yellow region, where varnish was also visible. In Figure 5.18 the photo of the area S2 (a) and the corresponding spectrum in full range (b) are reported. Yellow ochre and gypsum are easily identified by comparing the reference spectra. For identifying the applied varnishes, several reflectance spectra of natural and synthetic varnishes were collected for comparison. In Figure 5.19 some of these reference spectra are reported. It can be

seen that dammar and mastic, two natural resins commonly used as varnish in paintings, show similar spectra, which differ from other two acrylic resins (Paraloid B 72 and Paraloid B 67) and from the ketone resin, especially in the regions related with the vibration bands of C-H bonds (1150-1200 nm, 1350-1450 nm, 1650-1750 nm and 2250-2350 nm).



a



b

Figure 5.18 Photo of the Area S2 (a) and its original reflectance spectra in full range (b).

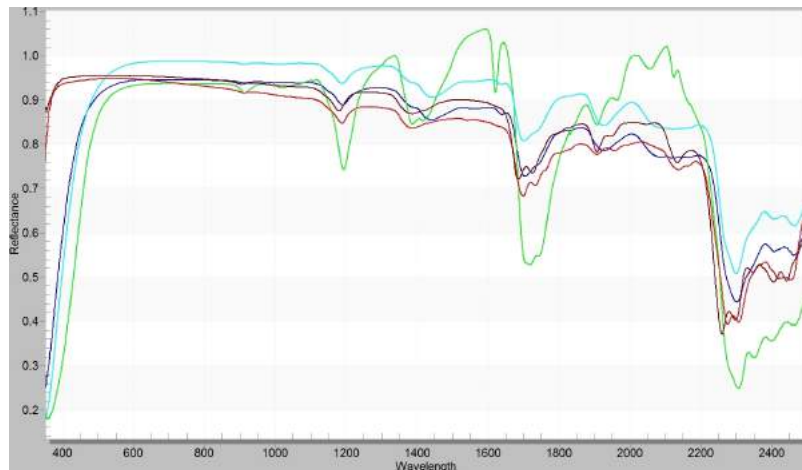


Figure 5.19 Reflectance spectra of some varnishes (database of varnishes). Light blue = mastic; dark blue = dammar; brown = acrylic resin – Paraloid B 67; red = Paraloid B 72; green = ketone resin.

Although gypsum has peaks in the region 1000-2400 nm, the signals of the varnish cannot be influenced by the presence of gypsum because the strongest peak of natural or synthetic resins is located in a region where gypsum does not absorb. Therefore, comparing the reflectance spectra of the varnishes database, the thin layer of varnish can be initially identified as a kind of synthetic varnish rather than a natural one. From Figure 5.20, it can be seen that the peaks located at 1400 nm, 1650-1750 nm and 2300-2400 nm, due to the presence of hydrocarbons, are present. The spectrum shape in the region of 1650-1750 nm is more similar to that found in the spectra of the two acrylic resins, even with some differences. The similarity of the spectrum of the unknown varnish with those of the acrylic resins is an indication that this varnish is a synthetic resin containing ester groups. However, for a correct identification of the varnish, reflectance spectra of more synthetic polymers should be collected.

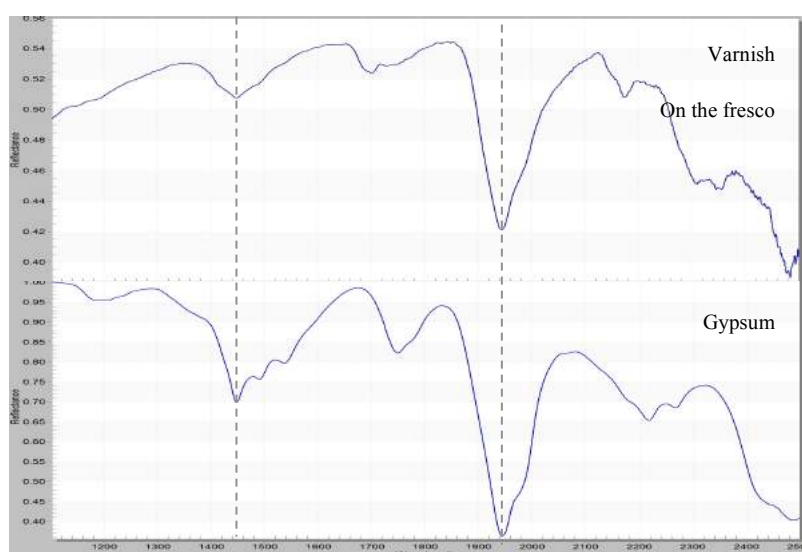


Figure 5.20 Comparison of spectrum of unknown varnish in Area S2 and gypsum in the range of 1100-2500 nm.

- The varnish from Area 2

Basic description:

The varnish layer was taken from the fresco in Area S2 where a glossy layer of varnish is present (Figure 5.21). Since later restoration needs the removal of this layer, it is necessary to identify it and select appropriate solvent for cleaning with minimum damage to other painting materials.



Figure 5.21 Sampling of the varnish was taken from Area S2.

FT-IR analysis was carried out on the sample to characterize this superficial layer. In Figure 5.22 and 5.23 the material sampled for FTIR analysis and the corresponding FTIR spectrum are reported, respectively. The peaks present in the FTIR spectrum are assigned to gypsum, calcite and an acrylic resin (specifically a vinyl toluene-acrylate copolymer - Goodyear PLIOLITE VTAC). (The main IR absorption peaks and corresponding substances identified are assigned and reported in Table 5.1).

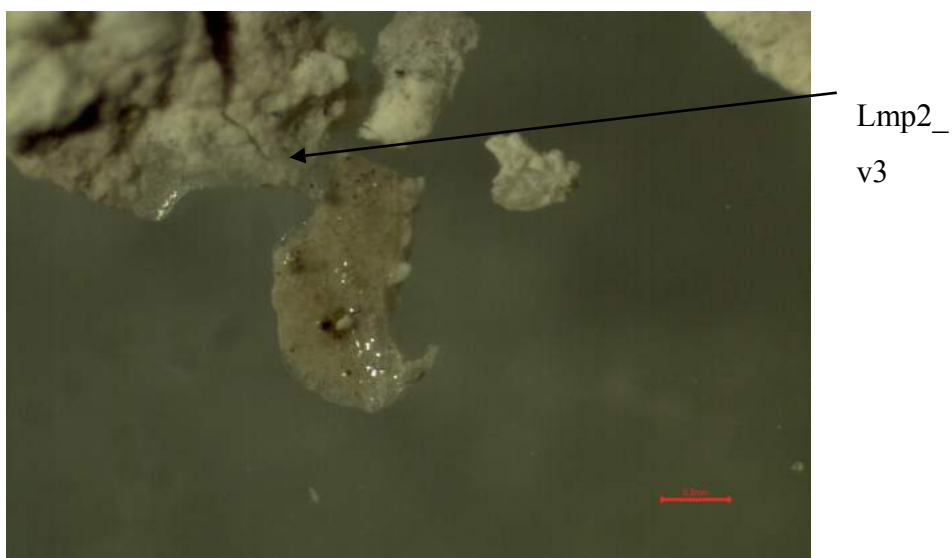


Figure 5.22 OM images of the micro sample (LMP_2v3) selected for the FTIR analysis from the fragments taken on the Area S2

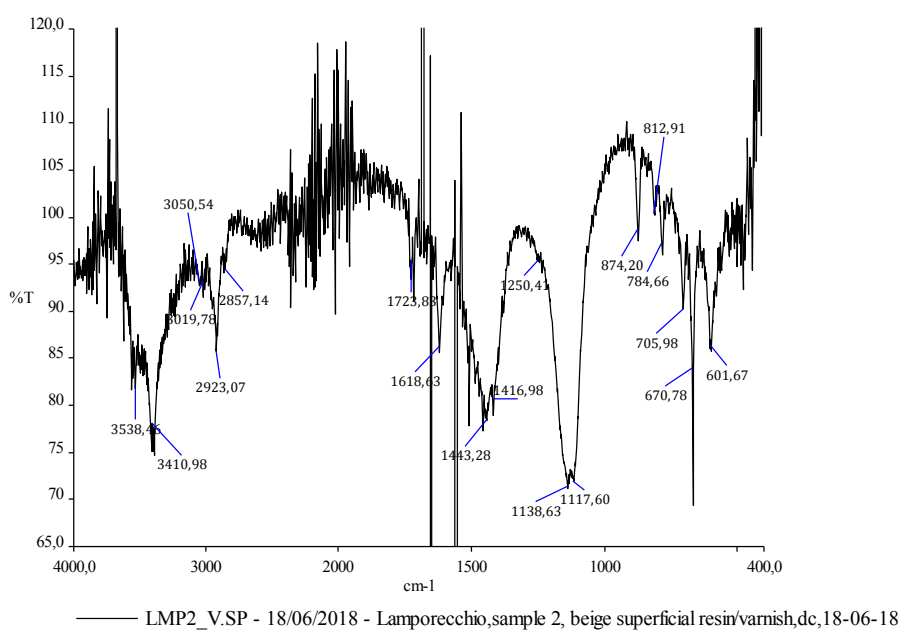


Figure 5.23 The FT-IR spectrum of LMP_2V3

Table 5.1 Assignments of the main IR absorption peaks of Figure 5.22 (cm^{-1})

	$\nu_{\text{O-H}}$	$\nu_{\text{C-H}}$	$\nu_{\text{C=C}}$	$\nu_{\text{C-H}}$	$\nu_{\text{C=O}}$	$\nu_{\text{C=C}}$	$\nu_{\text{C-C}}$	$\delta_{\text{C-H}}$	$\delta_{\text{C-H}}$	ν_{CO_3}	$\nu_{\text{SO}_4}/\delta_{\text{SO}_4}$
		(aromati c)	H				(aromati c)	(aromati c)			
Gypsum	3538	/		/	/	/	/	/		/	1138;

										1117;
										602;67
										0
Calcite	/	/		/	/	/	/	/		1417
										;
										874;
										706;
Vinyl	/	3050;	3020	2928	172	161	1509	1443	813;	/
toluene-acryla				;	3	8		;		/
te copolymer				2857				785;		

5.2.3.3 Area S3 and green overpaints:

- Green overpaintings analyzed by Field Spec

As previously mentioned in Chapter 3, overpaintings in green color at five different positions were characterized to figure out if the same pigment was used (Figure 5.24). The raw spectra collected by FieldSpec on the five areas are shown in Figure 5.25. In the visible region, all the spectra have a reflection maximum in the green region which indicates their colors. However, the differences in the position of their absorption peaks are evidence of the existence of two different kinds of green color: one probably used in previous restorations, while another in the last restoration intervention. At the 1st and the 5th position (see disposition of Figure 5.24), the same green pigment was used; at the 2nd and 3rd positions another green was used; while, at the 4th position, the spectra behave like the mixture of them. The spectra from the former green were similar to that of green earth, as suggested by the overall shape of

the spectrum (Figure 5.26) and two strong absorptions at ca. 440 nm and ca. 650 nm due to the ligand field effect of Fe^{2+} and Fe^{3+} (Figure 5.27a). Even though, peaks of the 4th green match with those of green earth also in the NIR-SWIR region, these features are well identified in all these five spectra, due to the presence of gypsum. The other green used in the other three positions has absorption peaks in the region 450 nm and 600 nm; the cikrant was supposed to be sap green [25] (A dull light green pigment prepared from the juice of the ripe berries of the *Rhamnus cathartica*, or buckthorn and used especially by water-color artists). However, this result needs further confirmation exploiting an implemented database of reflectance spectra and using other analytical methodologies.



Figure 5.24 Five different areas with green overpaintings.

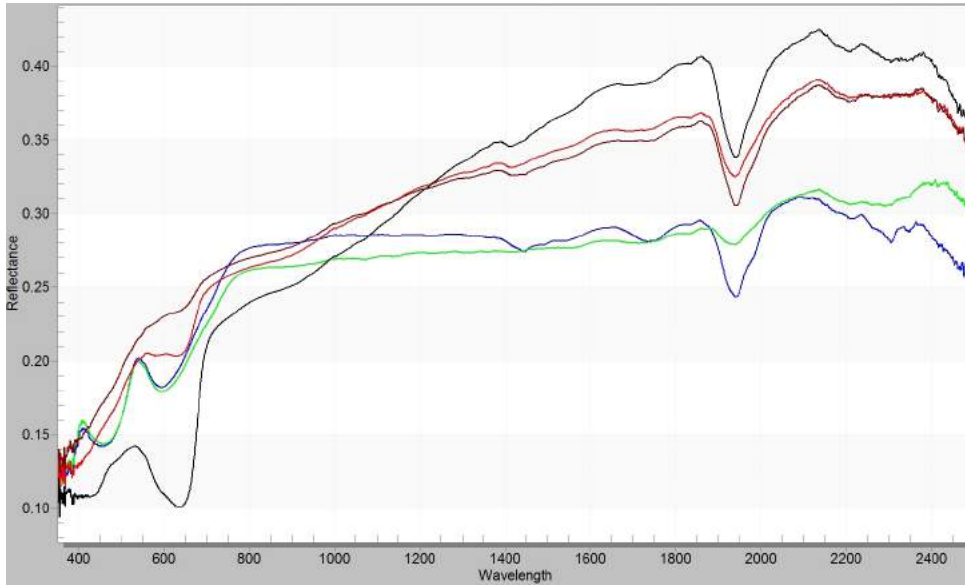


Figure 5.25 Reflectance spectra of five green overpaintings in full range region. Blue = 1st green overpainting; green = 2nd overpainting; red = 3rd overpainting; black = 4th overpainting; brown = 5th overpainting.

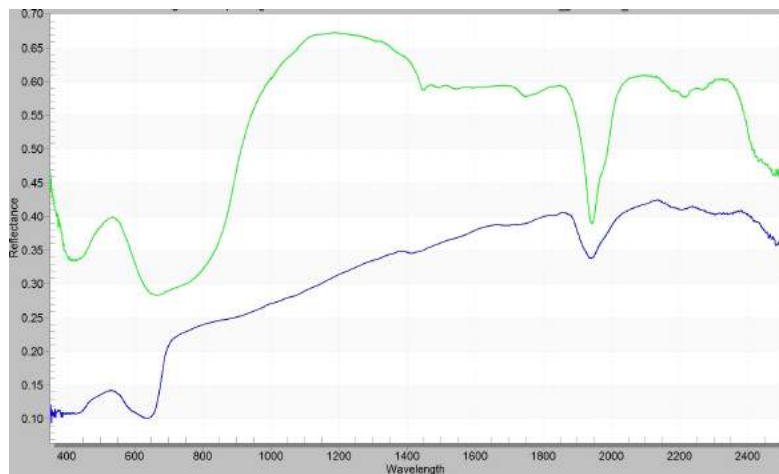


Figure 5.26 Reflectance spectra of the 4th green overpainting (blue) full range region. Green earth (green) is also reported for comparison.

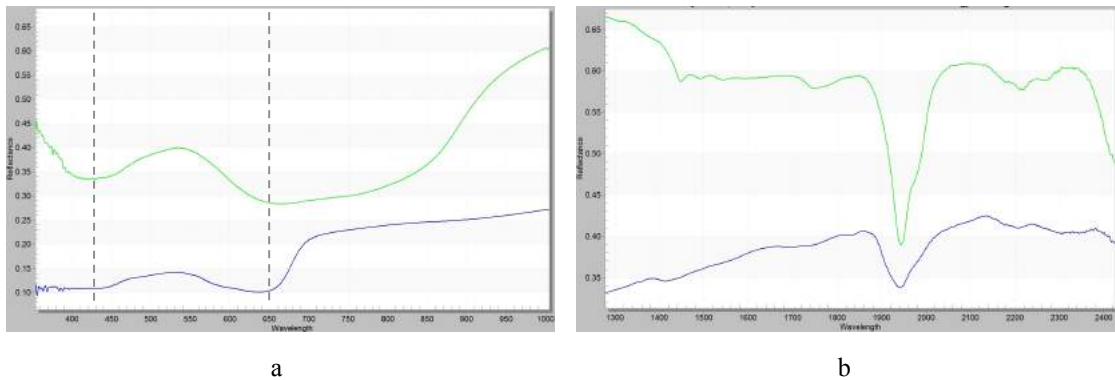


Figure 5.27 Reflectance spectra of the 4th green overpainting (blue) full range region. Green earth (green) is also reported for comparison. a = spectrum in VIS range; b = spectrum in NIR-SWIR range.

- Area S3 (the 4th overpainting region)

Basic sample description:

The decoration color of the fresco is green color, and the main parts painted in green are the plants. The 4th overpainting in Area S3 contains not only the main color painted on the leaves, but also a layer of varnish on the top of it, as seen in Figure 5.28.

FTIR and SEM-EDS analysis was also carried out on the 4th green overpainting sample (Figure 5.29). In Figure 5.30 the FTIR spectrum of the dark green color is reported.



Figure 5.28 Samples taken from the 4th overpainting Area S3.

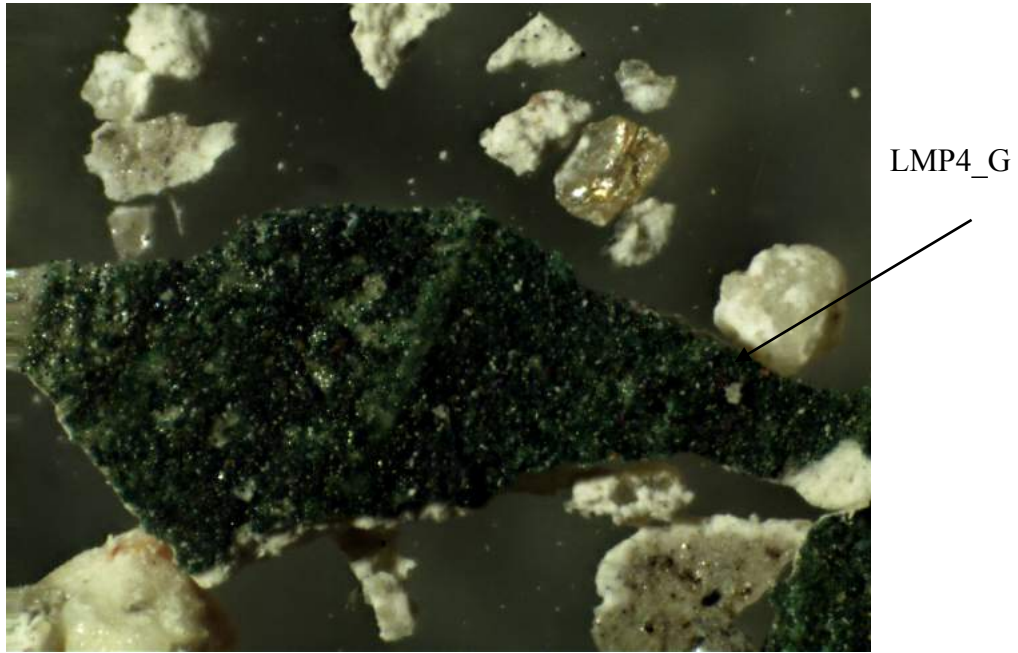


Figure 5.29 OM image of the micro-sample (LMP3_G) used for FTIR analysis and taken from the fragments sampled on Area S3.

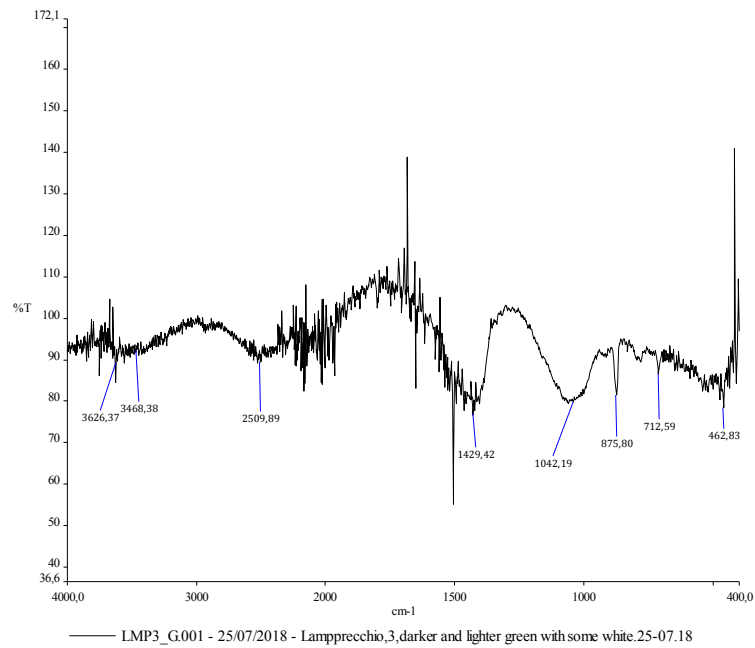
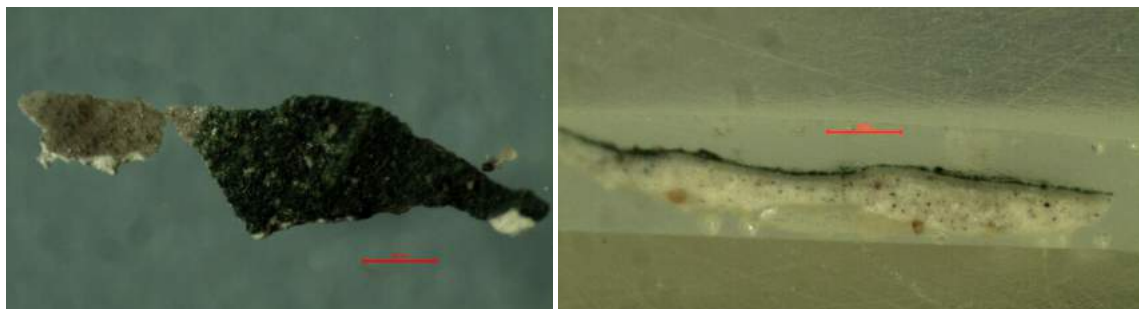


Figure 5.30 FT-IR spectrum of the 4th green overpainting (green) full range region.

The stratigraphic structure of the sample is well observed in Figure 5.31 b, where the polished cross section of the fragment in Figure 5.31a is reported. Since the green

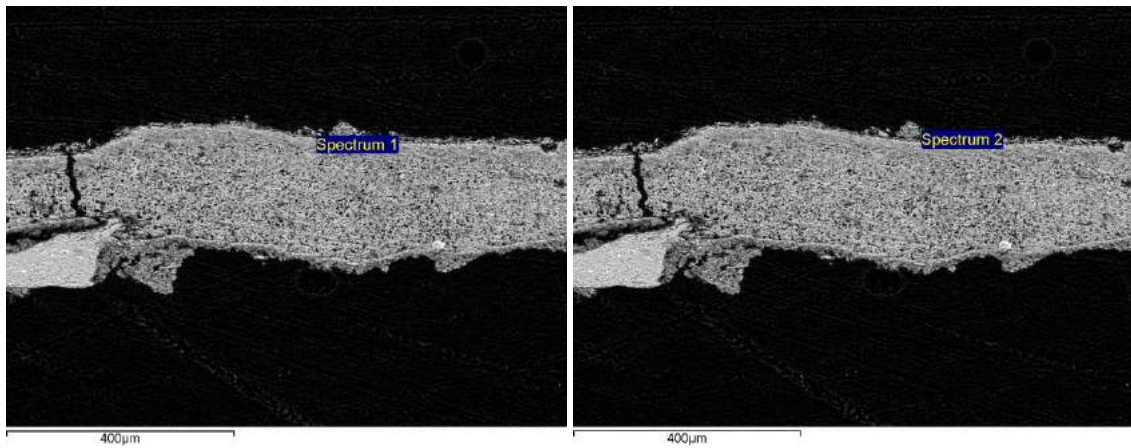
color is mainly present on the 1st layer, EDS spectra on different points were collected from this area (Figure 5.32a and b). The corresponding spectra (Figure 5.32c and Figure 5.32d) obtained from two points show that the K, Al, Mg, Si and Fe are present in this layer, which are in agreement with the composition of green earth, celadonite and glauconite [94].



(a)

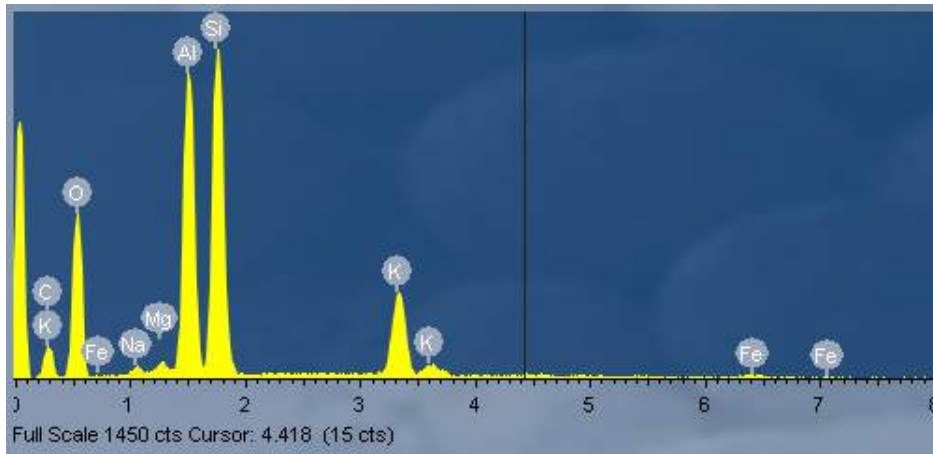
(b)

Figure 5.31 OM images of a fragment sampled in 4th overpainting in Area S3 for SEM-EDS analyses: a) fragment as sampled; b) the same fragment in polished cross section

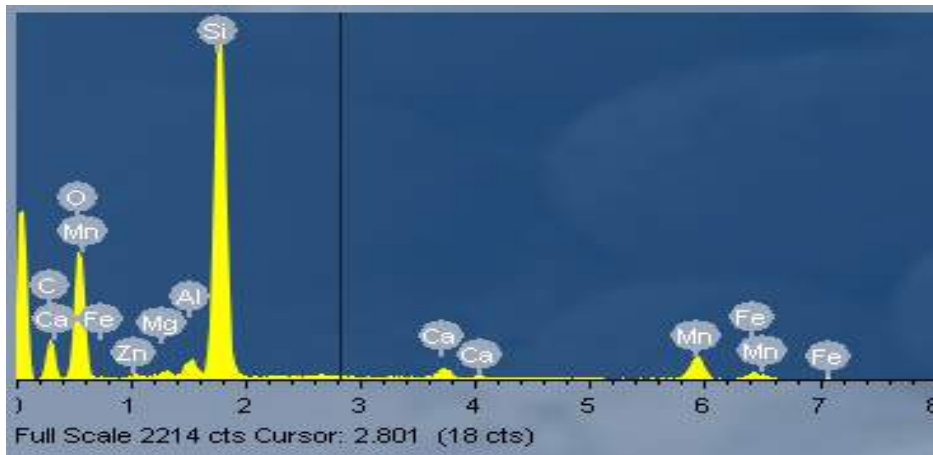


(a)

(b)



(c)



(d)

Figure 5.32 SEM images taken in BSE mode of the 4th green overpainting. The EDS analysis was also done at the points marked as spectrum 1 (a) and spectrum 2 (b). The corresponding spectra are shown in (c) and (d).

From the results obtained by these techniques, it can be concluded that green earth was used as the green pigment in overpainting.

5.2.3.4 Area 4 and red/ violet colors:

- Pink, red and violet analyzed by FieldSpec

Red, pink and violet are other major colors painted on the ceiling. Area 4 was selected for characterizing these three colors, which was on an arm of an angel. FieldSpec

analysis was conducted at Positions A, B and C which are in pink, red and violet colors respectively. Their specific position and corresponding spectra are shown in Figure 5.33. From their reflectance spectra, it can be found that the main coloring component is hematite for all the colors. Gypsum is present in all these reddish colors. The degree of red is related to the amount of gypsum added. The pink color has the highest gypsum content, red has lower and violet has the lowest amount. This may indicate that calcium sulfate was used as additive for getting different color. However, the little shift of the peak at 1440 to 1400 nm and a peak at 2160 nm may indicate presence of kaolinite, like in the spectrum of Armenian bole.

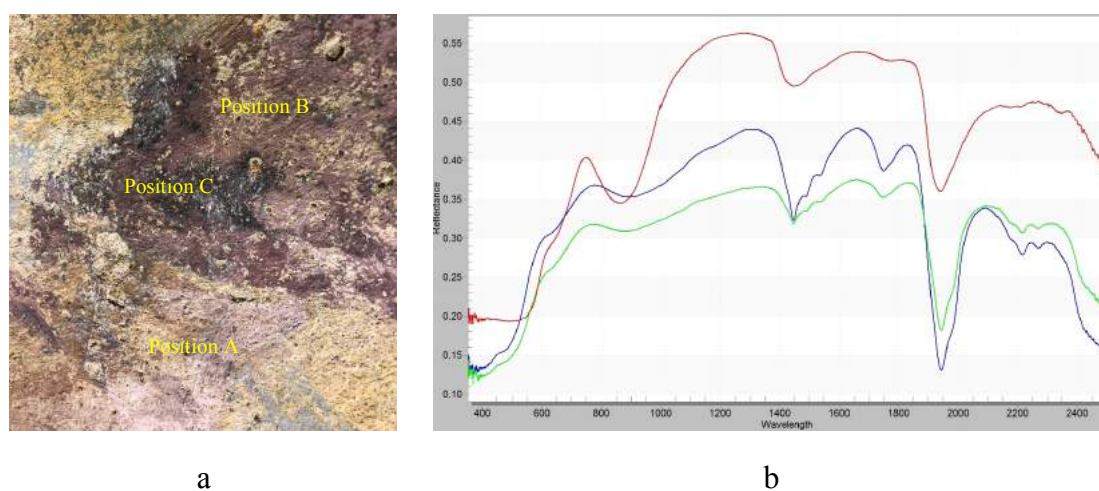


Figure 5.32 Reflectance spectra collected at Position A (green), Position B (blue) and Position C (red) in full range.

- Area 4

Sample description

Samples were collected in an area where a yellow patina covers the violet painting layer (Figure 5.34). The FT-IR spectrum was taken on the violet part of the sample, as shown in Figure 5.35.

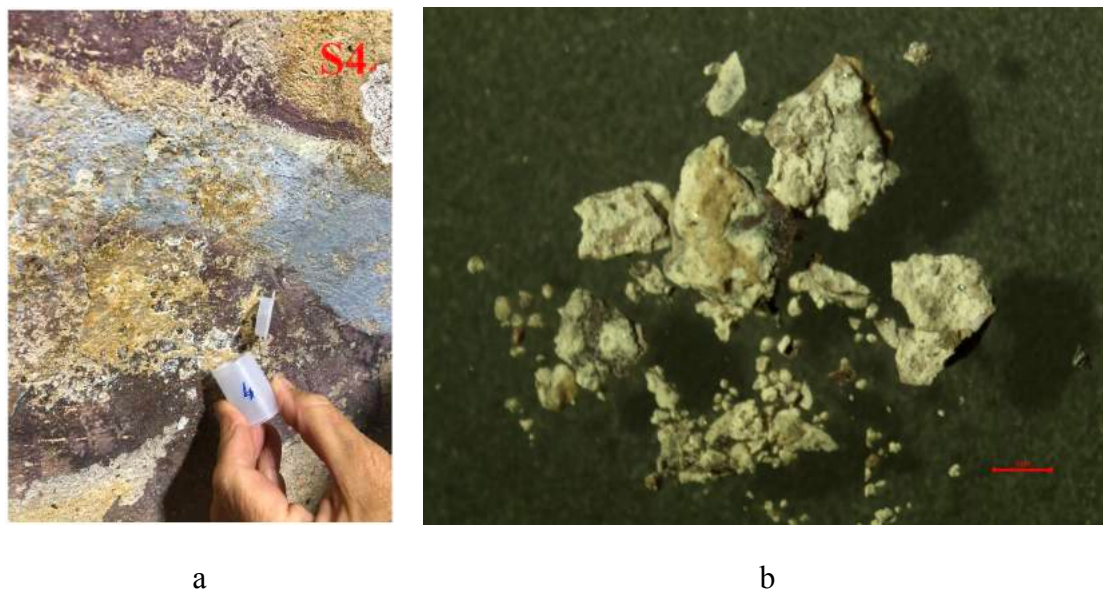


Figure 5.34 Samples taken from Area S4: a) photo of sampling position; b) .OM image of the sampled fragments.

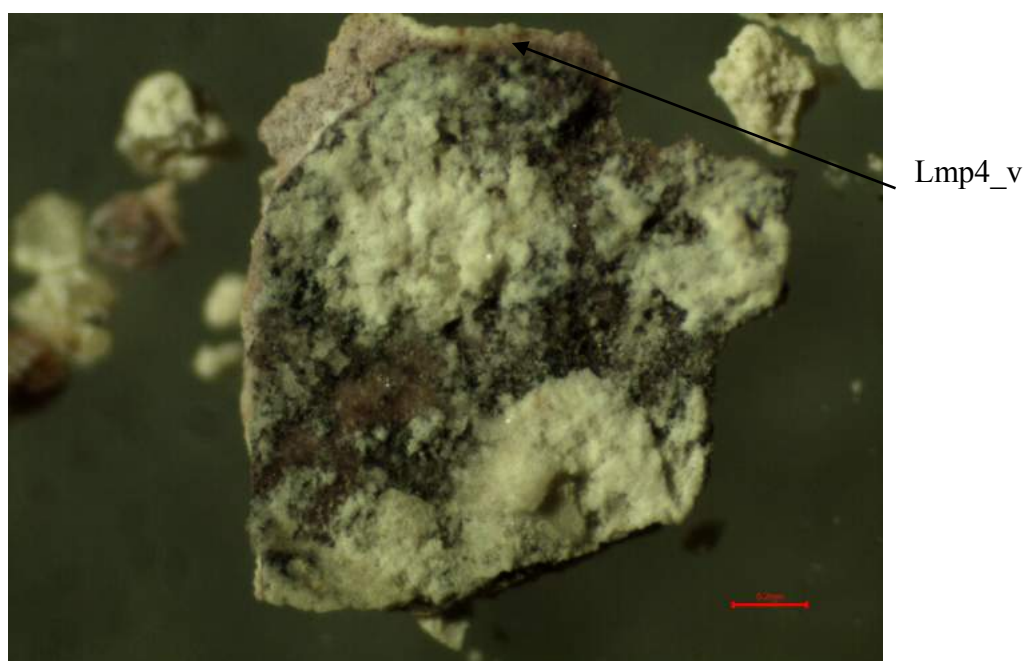


Figure 5.35 OM image of the micro-sample (LMP4_v) used for FTIR analysis and taken from the fragment sampled on Area S4

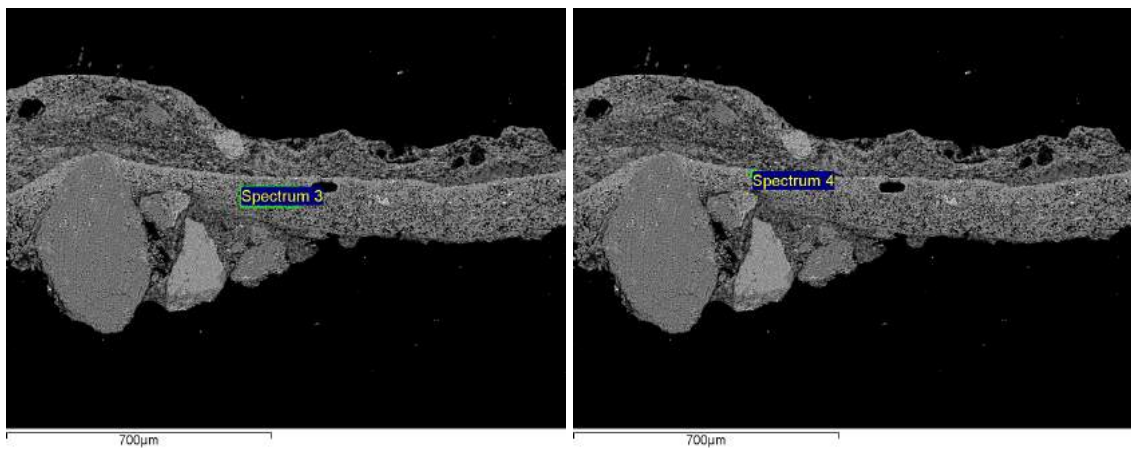
The SEM-EDS analyses of the violet layer were carried out on the polished cross section of the sample shown in Figure 5.36a (fragment before embedding in resin) and Figure 5.36b (polished cross section). The SEM images in BSE with the point of EDS analyses are reported in Figure 5.37 a) and b), while the EDS spectra corresponding to the points marked as Spectrum 3 and Spectrum 4 are reported in Figure 5.37 (c) and (d). The presence of Fe verifies the result obtained by FieldSpec (iron oxides or red ochre). Also Si is present.



(a)

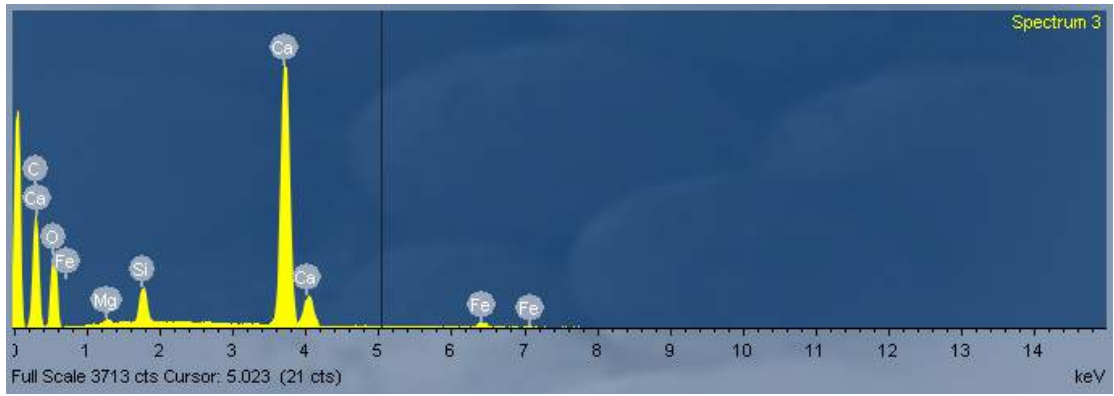
(b)

Figure 5.36 OM image of the fragment taken from Area S4 and used for SEM-EDS analysis (a: before embedding in resin; b:polished cross-section of the same fragment)

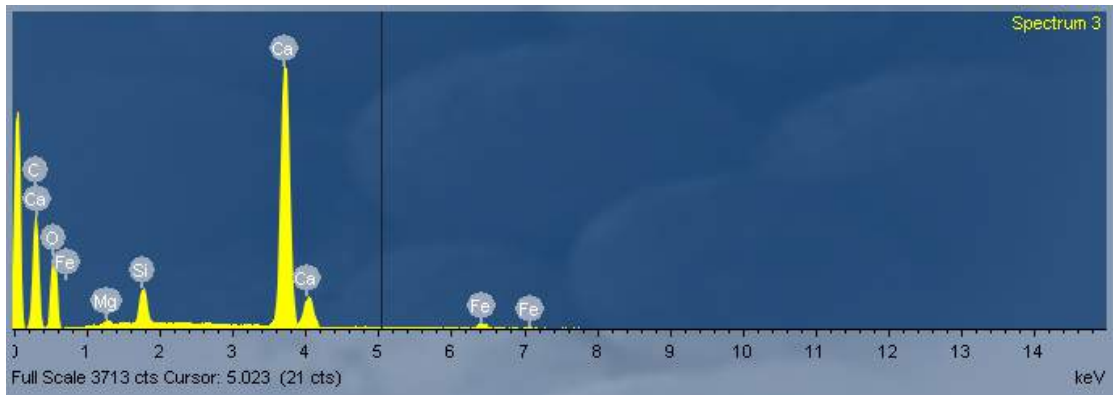


(a)

(b)



(c)



(d)

Figure 5.37 SEM images taken in BSE mode of the red/violet fragment from Area S4; the EDS analysis was also done at the points denoted as spectrum 1 (a) and spectrum 2 (b). The corresponding spectra are shown in (c) and (d).

Chapter VI

Conclusion

In the study, reflectance spectroscopy, as a non-invasive analytical method for the characterization of painting surfaces is improved by a hyperspectral sensor, ASD Field Spec FR Pro. This spectroradiometer is able to acquire punctual reflectance spectra in the full range (350-2500 nm), from which both elemental and molecular information of a material can be obtained.

The validation of this hyperspectral sensor for the identification of a painted surface started from database construction (pure painting materials, i.e. colorants and binding media). For colorants, materials in the form of powder, the amount (particle concentration) in the detected areas has a large impact on quality of reflectance spectra when other factors (incident light intensity, particle size and size distribution) remain constant.

The results showed that the best “Min” spectrum of a colorant was obtained by the 1st way (i.e. simply brushing colorant powder on a glass support) which gives more information on a colorant, especially in the NIR-SWIR region. Through other two methods (i.e. using water or other organic solvents to disperse colorant powder on a glass support; brushing colorant powder on cling film by electromagnetic effects.), it

is also possible to reach a smaller amount, however there are several drawbacks. As regard to the second method, the use of a dispersing solvent induces interferences. It is almost impossible to find an appropriate solvent that fulfills all the requirements suitable for dispersing all the colorants, and the reasons are: 1) with low boiling point but easy to apply; 2) no dissolving or reacting with additive components in commercial pigments; 3) no harmful for human beings and environment. When referring to the third method, two problems may cause losing of information in the NIR region of spectra. One is that the “wave” shape caused by the gas bubble between cling film and glass is unpredictable. Besides, the cling film (polyvinyl chloride) is not uniformly thick, which was observed in reflectance spectrum. Its absorption features cannot be completely removed by white reference correction. Thus, considering the spectral quality and the feasibility of sampling methods, the method of collecting the “Min” spectra of colorants should be: simply brushing powder on a glass support. The white reference spectrum is ought to be taken on the surface of the corresponding glass and the Teflon plate every time.

Comparative studies conducted on “Min” and “Max” spectra of one substance show that reflectance spectroscopy is more influenced by the amount of detected substances compared to other analytical spectroscopic techniques. Max spectra collected with a larger amount of material show stronger peak intensity in the full region, and well detailed features in the NIR-SWIR range (1000-2500 nm) are seen. This is of paramount importance in the identification of colorants which have characteristic

features in this region, especially the commercial products which generally contain additive compounds. However, the large amount of substances also induces too much absorption in the VIS-NIR range (350-1100 nm), resulting in the loss of some significant spectra features (i.e. peaks, shoulders) due to electronic processes. Min spectra, which are relatively weaker in peak intensity, manifest the exactly opposite results. Though a better understanding will be obtained through Min spectrum of a substance at lower wavelength, the recognition is harder when it has less absorption (the peak positions are difficult to identify). More importantly, in their corresponding 1st derivative spectra the noise is greatly increased, which is not suitable for identification.

Therefore, the selection of Max and Min spectrum depends on whether a colorant has absorption peaks in near infrared and short wave infrared regions. For example, a colorant like cinnabar, which only has characteristic features in shorter wavelength, Min spectrum is selected as the standard spectrum. While, for a colorant, especially organic dyes, VIS-NIR (350-1000 nm) of Min spectrum and NIR-SWIR (1000-2500 nm) of Max spectrum should both be exploited for better understanding in terms of color and chemical composition. For the commercial products which may contain different additive components, Max spectrum is also suggested in order to maximize the peculiarity. The 1st derivative spectrum of colorants will be obtained by transforming their corresponding raw spectrum (either Min or Max spectrum).

For organic binders, the preparation of a material for characterization was proved to be important. Spectrum of a binder film collected on a Teflon support has clearer absorption features than on a glass support. The identification work was fulfilled by the recognition of the characteristic features in their original spectra. The most characteristic peaks and regions for characterizing these four binders (i.e. egg yolk, animal glue, linseed oil and gum Arabic) are located in the following regions: 1150-1250 nm, 1650-1800 nm and 2250-2400 nm. These regions are assigned to the combination and overtone bands of C-H bonds. Other variances can be found in the wavelength locate at ca. 1507, 1945, 2050 and 2150 nm thanks to the difference between their chemical essences. Although the original reflectance spectra of pigment/binding medium mixtures can give us useful information for identification, a more accurate differentiation can be seen from the 1st derivative spectra. More obvious variance can be observed using their corresponding derivatives in the region(s) above mentioned.

The Identification work becomes more complicated when a mixture composed of colorants and binders must be analyzed. Even though the identification of a binder from pictorial layers can be done exploiting its characteristic absorption features based on the created database, the interferences caused by interactions between pigments and binders should be taken in careful consideration. Possible shifts in wavelength in respect to pure materials are expected when a matrix with pigments is realized. It is found that, most of the “fingerprints” in the raw spectra recognized in

pure materials can be observed at the same wavelength, except two changes. They can be found in all the colorant mixtures regardless of the type and color of pigments, and regardless of whether the pigment has absorption peaks in NIR region. One occurs in proteinaceous materials, i.e. animal glue and egg yolk. The first overtone band of N-H stretching mode observed as shoulder at 1507 nm cannot be found once it is mixed with colorants. The second change is the strong peak between 1930-1943 nm which shifts to lower wavelength along with the broadening of the peak. The spectrum of the mixture in which linseed oil was used as binder has the smallest shifts about 5 nm, rather than 15-20 nm in other painting mixtures. The possible reason for this bigger shift in binders except linseed oil is that the position of the combination of the O-H stretching and bending mode is very easy to be interfered. Consequently, these two wavelengths are not recommended for characterization.

Considering the amounts of binders used by artists vary from one to another, the spectra of different amount of binders were also compared. The results indicate that the spectra of larger amount of a binder exhibit stronger peak intensity compared to the smaller, especially in the regions where the overtone and combination bands of C-H, but the wavelengths did not change. However, even with bigger amount, the absorption maxima at ca.1507 nm which is assigned to the first overtone band of N-H stretching mode for egg yolk cannot be found.

In the final part of mixture characterization, the identification of four binders from mixtures with the same colorant (both organic and inorganic pigment) was discussed. The results show that the identification work can be done with the characteristic regions seen in the spectra of pure materials. Besides, the 1st derivative transformation demonstrates better contrast in the case when peaks of a colorant and a binder overlap, or their spectra intensity are relatively low. But it is found that in the region between 2300 and 2400 nm, which is essential for identification of binders, may be not suitable for all the colorants mixtures. One example is when a colorant has C-N bond. In this situation, peaks that are very close to each other will combine with each other to form a new broader peak in the moderated position, hence they cannot be separated even with their 1st derivative transformation. The overlapping and shifts of these peaks make the identification work much more difficult.

Thus, it is supposed that the characterization of painting surfaces should start from pigment identification using visible regions, because the peaks, mainly due to the electronic process, are relatively diagnostic. When the colorant is identified, the observation can extend to the longer wavelength over 1000 nm. The regions where a colorant may affect the absorption features of a binder should be less considered as diagnostic regions. The difference in the shape, position and peak intensity of the bands emerged between ca. 1700 and 1800 nm, which is general affected by the presence of organic material, should be always highlighted. Other two regions, due to the vibration process of C-H bonds are also significant in the identification only when

the suspected pigment does not have peaks in these two areas. Moreover, PCA was also proved to be an efficient method for the classification of different binders, especially when the identification is performed on mixtures with the same pigment. However, the selection of different sets of points from raw spectra, or their 1st derivative, than those used in this work are expected to produce a good classification of different binders regardless the pigment used in the mixture.

In the case studies, the majority of pigments and the binder used for the easel painting and on the fresco were successfully identified based on the database created and the identified characteristic regions. Linseed oil was found to be the binding medium of easel painting, while zinc white is the white pigment. These results are in accordance with the materials expected to be used in the period of the painting manufacturing, i.e. XIX century. On the other hand, smalt, caput mortum (iron oxide rich), yellow ochre, and green earth are identified as the main pigments of blue, red, yellow, and green color of the fresco, respectively. A synthetic acrylic copolymer (i.e. vinyl-styrene methacrylate) was employed as the varnish. These results were also confirmed by other micro invasive analytical techniques, e.g. FI-IR, Raman spectroscopy and SEM-EDS.

To conclude, it has been proved that the portable hyperspectral sensor is a powerful tool in identifying both inorganic and organic components in the full range (350-2500 nm), in a rapid and non-invasive way. All results obtained indicate this portable

reflectance spectroscopy is very valuable for practical conservation and restoration work.

Bibliography

- [1] E. R. De la Rie, 1987, The influence of varnished on the appearance of paintings, *Studies in conservation*, 32 (1987) 1-13.
- [2] N. Khandekar, A survey of the conservation literature relating to the development of aqueous gel cleaning on painted and varnished surfaces, *Reviews in Conservation*, 45 (2000) 10-20.
- [3] R. Wolbers, Notes for the workshop on new Methods in the Cleaning of Paintings, Getty Trust Publications: Marina del Rey, 1988.
- [4] Leavengood P., Twilley J., Asmus F. J., 2002, Lichen removal from Chinese spirit Path figures of marble, *Journal of Cultural Heritage*, pp. S71–S74.
- [5] G. Wheeler, Alkoxysilanes and the consolidation of stone, Getty Publications, Los Angeles-USA, Printed in Canada by FRIESENS, 2015 ISBS: 9780892368150.
- [6] M. Bacci, V. Cappellini and R. Carlà, Diffuse reflectance spectroscopy: An application to the analysis of artworks, *Journal of Photochemistry and Photobiology B-Biology* 1, 1987, pp. 132-133.
- [7] I. J. Berezhanoy, Digital analysis of paintings, TICC Dissertation Series No. 10, 2008 ISBN: 9789085595984.
- [8] E. W. Fitzhugh, Artists' pigments: a handbook of their history and characteristics, National Gallery of Art, London, Archetype Publication, 1997 ISBN: 9781904982760.
- [9] G. B. Armenini, On the true precepts of the art of painting, Burt Franklin & Co. Inc. 1977 ISBN 978-0891021001.
- [10] A. Phenix, K. Sutherland, The cleaning of paintings: effects of organic solvents on oil paint films, *Studies in Conservation*, 2 (2001) 47-60.
- [11] E. Rene de la Rie and Alexander M, (1989) The chemistry of ketone resins and the synthesis of a derivative with increased stability and flexibility, *Studies in Conservation*, **34**, 9-19.
- [12] D. Erhardt, J. S. Tsang, The extraction components of oil paint films, *Studies in Conservation*, (1990) 93-97.

- [13] R. Feller, N. Strolow, H. E. Jones, *On Picture Varnish and Their Solvents*, National Gallery of Art, London 1985 ISBN: 9780894680847.
- [14] C. Wang, Hyperspectral sensor: a new approach for evaluating the efficacy of laser cleaning in the removal of varnishes and overpaintings. Master's degree thesis, University of Bologna, 2015.
- [15] S. Siano, F. Margheri, P. Mazzinghi, R. Pini, R. Salimbeni, M. Vannini, Laser ablation in the artworks restoration: benefits and problems in *Proceedings of International Conference LASERS*, December 1995, pp. 441–444.
- [16] P. Bracco, G. Lanterna, M. Matteini, K. Nakahara, O. Sartiani, A. de Cruz, M. L. Wolbarsht, E. Adamkiewicz, M. P. Colombini, Er:YAG laser: an innovative tool for controlled cleaning of old paintings: testing and evaluation, *Journal of Cultural Heritage*, 4 (2002) 202–208.
- [17] C. Daffara, R. Fontana, Multispectral infrared reflectography to differentiate features in paintings, *Microscopy and Microanalysis*, 17 (2011) 691–695.
- [18] H. Liang, R. Lange, H. Howard, J. Spoone, Non-invasive investigations of wall painting using optical coherence tomography and hyperspectral imaging, in *Optics for Arts, Architecture, and Archaeology III*, edited by L. Pezzati, R. Salimbeni, *Proceedings of SPIE*, 2011, 80840F.
- [19] S. Hwang, H. Song, S. Cho, C. Kim, C. Kim, K. Kim (2017), Optical measurements of paintings and the creation of an artwork database for authenticity, *PLOS ONE*, 12 (2017) e0171354.
- [20] F. Presciutti, J. Perlo, F. Casanova, S. Glöggler, C. Miliani, B. Blümich, B. Giovanni Brunetti, A. Sgamellotti, Noninvasive nuclear magnetic resonance profiling of painting layers, *Applied Physics Letters*, 93 (2008), 033505.
- [21] M. Ortega-Aviles, P. Vandenabeele, D. Tenorio, G. Murillo, M. Jimenez-Reyes, N. Gutierrez, Spectroscopic investigation of a 'Virgin of Sorrows' canvas painting: A multi-method approach, *Analytica Chimica Acta*, 550 (2005) 164–172.
- [22] M. Bacci, S. Baronti, A. Casini, F. Lotti, Non-Destructive Spectroscopic Investigations on Paintings Using Optical Fibers, *Symposium J-Materials Issues in Art and Archaeology*, 267 (1992) 265-283.
- [23] M. Bacci, Fibre optics applications to works of art, *Sensors and Actuators B*, 29 (1995)190-196.

- [24] M. Aceto, A. Agostino, G. Fenoglio, A. Idone, M. Gulmini, M. Picollo, P. Ricciardie, J. K. Delaney, Characterisation of colourants on illuminated manuscripts by portable fibre optic UV-visible-NIR reflectance spectrophotometry, *Analytical Methods*, 6 (2014) 1488-1500.
- [25] P. Ricciardi, A. Pallipurath, K. Rose, 'It's not easy being green': a spectroscopic study of green pigments used in illuminated manuscripts, *Analytical Methods*, 5 (2013) 3819–3824.
- [26] C. Cucci, J. K. Delaney, M. Picollo, Reflectance hyperspectral imaging for investigation of works of art: old master paintings and illuminated manuscripts, *Accounts of Chemical Research*, 49 (2016) 2070–2079.
- [27] C. Pelosi, G. Agresti, U. Santamaria, E. Mattei, Artificial yellow pigments: production and characterization through spectroscopic methods of analysis, *e-Preservation Science*, 7 (2010) 108-115.
- [28] M. P. Colombini, F. Modugno, R. Fuoco, A. Tognazzi, A GC-MS study on the deterioration of lipidic paint binders, *Microchemical Journal*, 73 (2002) 175–185.
- [29] A. Casoli, P. C. Musini, G. Palla, Gas chromatographic-mass spectrometric approach to the problem of characterizing binding media in paintings, *Journal of Chromatography A*, 731 (1996) 237-246.
- [30] K. B. Kalinina, I. Bonaduce, M. Perla Colombini, I. S. Artemieva, An analytical investigation of the painting technique of Italian Renaissance master Lorenzo Lotto, *Journal of Cultural Heritage*, 13 (2012) 259–274.
- [31] A. Andreotti, W. P. Brown, M. Camaiti, M. P. Colombini, A. DeCruz, Diagnosis of materials and effectiveness of Er:YAG Laser cleaning in a Borrassa's Panel Painting (15th Cent.), *Applied Physics A*, 122 (2016) 572-584.
- [32] D. G. Smith, H. J. R. Clark, Raman microscopy in art history and conservation science, *Studies in Conservation*, 46 (2001) 92-106.
- [33] M. Leona, J. Stenger, E. Ferloni, Application of surface-enhanced Raman scattering techniques to the ultrasensitive identification of natural dyes in works of art, *Journal of Raman Spectroscopy*, 37 (2016) 981-992.
- [34] S. Prati, E. J. Joseph, G. Sciutto, R. Mazzeo, New advances in the application of FTIR microscopy and spectroscopy for the characterization of artistic materials, *Accounts of Chemical Research*, 43 (2010) 792-801.

- [35] G. Kortüm, *Reflectance Spectroscopy, Principles, Methods, Applications*, Springer-Verlag Berlin Heidelberg, 1969 ISBN: 978-3-642-88073-5.
- [36] R. K. Vincent, G. R. Hunt, Infrared Reflectance from Mat Surfaces, *Applied Optics*, 7 (1968) 53-59.
- [37] B. van Ginneken, M. Stavridi, J. J. Koenderink, Diffuse and specular reflectance from rough surfaces, *Applied Optics*, 37 (1989) 130-139.
- [38] M. Fabbri, M. Picollo, S. Porcinai, M. Bacci, Mid-infrared fiber-optics reflectance spectroscopy: a noninvasive technique for remote analysis of painted layers. Part I: Technical Setup, *Applied Spectroscopy*, 55 (2001) 420-427.
- [39] P. J. Brimmer, P. R. Griffiths, N. J. Harrick, Angular dependence of diffuse reflectance infrared spectra. part I: FT-IR spectrogoniophotometer, *Applied spectroscopy*, 40 (1986) 258-265.
- [40] R. N. Clark, *Spectroscopy of rocks and minerals, and principles of spectroscopy*. In Rencz A (ed), *Manual of Remote Sensing*, John Wiley and Sons, Inc, New York, 1999 pp. 1-63.
- [41] J. Workman, L. Weyer, *Practical guide and spectral atlas for interpretive near-infrared spectroscopy*, 2nd edition, CRC Press Taylor & Francis Group, Boca Raton, 2012 ISBN 978-1-4398-7526-1.
- [42] International museums office. *Manual on the conservation of paintings*. Paris: International Institute of Intellectual Cooperation, 1940.
- [43] Jr W. A. Hovis, Infrared spectral reflectance of some common minerals, *Applied Optics*, 5 (1966) 245-248.
- [44] K. Nassau, *The physics and chemistry of color* 2nd edition, Wiley-Interscience, 2001 ISBN 978-0471391067.
- [45] R. H. Graham, Spectral signature of particulate minerals in the visible and near infrared, *Geophysics*, 42 (1977) 501-513.
- [46] R. N. Clark, T. V. V. King, M. Klejwa, G. A. Swayze, High spectral resolution reflectance spectroscopy of minerals. *Journal of Geophysical Research*, 95 (1990) 12653-12680.
- [47] R. N. Clark, G. A. Swayze1, R. Wise, K. E. Livo, T. M. Hoefen, R. F. Kokaly, S. J. Sutley, 2003 <http://pubs.usgs.gov/of/2003/ofr-03-395/ofr-03-395.html>.
- [48] M. Bacci, V. Cappellini, R. Carlà, Diffuse reflectance spectroscopy: An application to the analysis of artworks, *Journal of Photochemistry and*

- Photobiology B-Biology*, 1 (1987) 132-133.
- [49] M. Bacci, F. Baldini, R. Carlà, R. Linari, A color analysis of the Brancacci Chapel Frescoes, *Applied Spectroscopy*, 45 (1991) 26-31.
- [50] M. Bacci, S. Baronti, A. Casini, F. Lotti, M. Picollo, O. Casazza, Non-destructive spectroscopic investigations on paintings using optical fibers. Materials Research Society Symposium Proceedings, 27 April-1 May 1992, San Francisco, USA. pp. 265-283.
- [51] M. Picollo, M. Bacci, A. Casini, F. Lotti, S. Porcinai, B. Radicati, L. Stefani, *Fiber Optics Reflectance Spectroscopy: a non-destructive technique for the analysis of works of art*, in S. Martellucci, A. N. Chester and A. G. Mignani (ed.), *Optical Sensors and Microsystems: New concepts, Materials, Technologies*, Kluwer Academic / Plenum Publishers, New York, 2000, pp. 259-265
- [52] G. Dupuis, M. Elias, L. Simonot, Pigment Identification by Fiber-Optics Diffuse Reflectance Spectroscopy, *Applied Spectroscopy*, 56 (2002) 1329-1336.
- [53] N. Knighton, B. Bugbee, A mixture of barium sulfate and white paint is a low-cost substitute reflectance standard for Spectralon, *Techniques and Instruments*, 2004, paper 11.
- [54] A. Cosentino, Identification of pigments by multispectral imaging; a flowchart method, *Heritage Science*, 2 (2014) 8.
- [55] K. A. Dooley, S. Lomax, J. G. Zeibel, C. Miliani, P. Ricciardi, A. Hoenigswald, M. Loew, J. K. Delaney, Mapping of egg yolk and animal skin glue paint binders in Early Renaissance paintings using near infrared reflectance imaging spectroscopy, *Analyst*, 138 (2013) 4838-4848.
- [56] M. Bacci, M. Picollo, G. Trumpy, M. Tsukada, D. Kunzelman, Non-invasive identification of white pigments on 20th century oil paintings by using fiber optic reflectance spectroscopy, *Journal of the American Institute for Conservation*, 46 (2007) 27-37.
- [57] C. Cucci, L. Bigazzi, M. Picollo, Fibre Optic Reflectance Spectroscopy as a non-invasive tool for investigating plastics degradation in contemporary art collections: A methodological study on an expanded polystyrene artwork, *Journal of Cultural Heritage*, 14 (2013) 290-296.
- [58] K. A. Dooley, J. Coddington, J. Krueger, D. M. Conover, M. Loew, J. K. Delaney, Standoff chemical imaging finds evidence for Jackson Pollock's

- selective use of alkyd and oil binding media in a famous ‘drip’ painting, *Analytical Methods*, 9 (2017) 28-37.
- [59] A. Cosentino, FORS Spectral Database of Historical Pigments in Different Binders, *e-conservation Journal*, 2 (2014) 53-65.
- [60] A. Daveri, S. Paziani, M. Marmion, H. Harju, A. Vidman, M. Azzarelli, M. Vagnini, New perspectives in the non-invasive, in situ identification of painting materials: The advanced MWIR hyperspectral imaging, *Trends in Analytical Chemistry*, 98 (2018) 143-148.
- [61] <https://pubs.usgs.gov/of/2003/ofr-03-395/DESCRIPT.mineral.template.html>
- [62] <http://fors.ifac.cnr.it>
- [63] A. Cosentino, Effects of different binders on technical photography and infrared reflectography of 54 historical pigments, *International Journal of Conservation Science*, 6 (2015) 287-298.
- [64] A guide to UV spectroradiometry: instruments & Applications for the Ultraviolet, Issue 2.01 - January 2014.
- [65] K. L. Castro-Esau, G. A. Sánchez-Azofeifa, B. Rivard, Comparison of spectral indices obtained using multiple spectroradiometers, *Remote Sensing of Environment*, 103 (2006) 276–288.
- [66] L. Giannoni, F. Lange, I. Tachtsidis, Hyperspectral imaging solutions for brain tissue metabolic and hemodynamic monitoring: past, current and future developments, *Journal of Optics*, 20 (2018) 044009.
- [67] R. Johnston-Feller, *Color Science in the Examination of Museum Objects: Nondestructive Procedures*, the Getty Conservation Institute, Los Angeles, 2001 ISBN: 0892365862.
- [68] G. Schaepman-Strub, M. E. Schaepman, T. H. Painter, S. Dangel, J. V. Martonchik, Reflectance quantities in optical remote sensing—definitions and case studies, *Remote Sensing of Environment*, 103 (2006) 27–42.
- [69] R. N. Clark, *Rock physics and phase Relations—Handbook of Physical Constants*, American Geophysical Union, Washington DC, 1995 ISBN: 9780875908533.
- [70] D. Ramakrishnan, R. Bharti, Hyperspectral remote sensing and geological applications, *Current Science*, 108 (2015) 879-891.
- [71] R. N. Clark, *Remote Sensing for the Earth Sciences: Manual of Remote Sensing*. In A. N. Rencz, Ed. *Spectroscopy of Rocks and Minerals, and Principles of*

- Spectroscopy, John Wiley & Sons, Inc. New York, 1999 ISBN: 978-0-471-29405-4.
- [72] M. Kalacska, A. G. Sanchez-Azofeifa, Hyperspectral remote sensing of tropical and subtropical forests, 2008 ISBN-13: 978420053418.
- [73] I. D. Sanches, M. P. Tuohy, M. J. Hedley, M. R. Bretherton, Large, durable and low-cost reflectance standard for field remote sensing applications, *International Journal of Remote Sensing*, 30 (2009) 2309-2319.
- [74] F. H. Goetz, G. Vane, B. N. Solomon, N. Rock, Imaging Spectrometry for Earth Remote Sensing. *Science*, 228 (1985) 1147–1152.
- [75] E. Ben-Dar, Y. Inbar, Y. Chen, The reflectance spectra of organic matter in the Visible Near-Infrared and Short Wave Infrared Region (400-2500 nm) during a controlled decomposition process, *Remote Sensing Environment*, 61 (1997) 1-15.
- [76] M. Camaiti, M. Benvenuti, P. Costagliola, F. Di Benedetto, S. Moretti, (2017). Hyperspectral sensors for the characterization of Cultural Heritage surfaces. In Masini, N. & Soldovieri, F. eds, Sensing the Past - From artifact to historical site, Geotechnologies and the Environment, Cham (Switzerland): Springer International Publishing, 2017, pp. 289-311.
- [77] M. Camaiti, S. Vettori, M. Benvenuti, L. Chiarantini, P. Costagliola, F. Di Benedetto, S. Moretti, F. Paba, E. Pecchioni, Hyperspectral sensor for gypsum detection on monumental buildings, *Journal of Geophysics and Engineering* 8 (2008) 126-131.
- [78] M. Camaiti, S. Vettori, M. Benvenuti, L. Chiarantini, P. Costagliola, F. Di Benedetto, S. Moretti, F. Paba, E. Pecchioni, Hyperspectral sensor for gypsum detection on monumental buildings, *Journal of Geophysics and Engineering*, 8 (2011) 126-131.
- [79] L. Alparone, M. Benvenuti, M. Camaiti, L. Chiarantini, P. Costagliola, F. Garfagnoli, S. Moretti, E. Pecchioni, S. Vettori, Hyperspectral instruments as potential tools for monitoring decay processes of historical building surfaces, in *Proceedings COST*, 2011, pp. 192-194.
- [80] M. A. Maynez-Rojas, E. Casanova-González, J. L. Ruvalcaba-Sil, Identification of natural red and purple dyes on textiles by Fiber-optics Reflectance Spectroscopy, *Spectrochimica Acta Part A: Molecular and Biomolecular Spectroscopy*, 178 (2017) 239-250.

- [81] P. Ricciardi, J. K. Delaney, M. Facini, J. G. Zeibel, M. Picollo, S. Lomax, M. *Angewandte Chemie International Edition*, 124 (2012) 5705.
- [82] K. A. Dooley, D. M. Conover, L. D. Glinsman, John K. Delaney, Complementary Standoff Chemical Imaging to Map and Identify Artist Materials in an Early Italian Renaissance Panel Painting, *Angewandte Chemie International Edition*, 53 (2014) 13775-13779.
- [83] G. Piva, L'arte del restauro, 1988 ISBN 88-203-1413-4.
- [84] C. Cennini, Il libro dell'arte, S.p.A Armando Paoletti, Firenze, 1991 ISBN 88-00-85999-2.
- [85] T. Fuan, W. Philpot, Derivative analysis of hyperspectral data, *Remote Sensing of Environment*, 66 (1998) 41–51.
- [86] M. Elias, C. Chartier, G. Prevot, H. Garay, C. Vignaud, The colour of ochres explained by their composition, *Materials Science and Engineering B*, 127 (2006) 70–80.
- [87] Jr W. A. Hovis, Infrared spectra spectral reflectance of some common minerals, 1966, *Applied Optics*, 5 (1966) 245-248.
- [88] J. Carter, F. Poulet, J. P. Bibring, S. Murchie, Detection of Hydrated Silicates in Crustal Outcrops in the Northern Plains of Mars, *Science*, 25 (2010) 1682-1686.
- [89] M. Bacci, D. Magrini, M. Picollo, M. Vervat. A study of the blue colors used by Telemaco Signorini (1835–1901), *Journal of Cultural Heritage*, 10 (2009) 275-280.
- [90] M. Aceto, A. Agostino, G. Fenoglioc, M. Gulminie, V. Biancoe, E. Pellizzif, Non invasive analysis of miniature paintings: proposal for an analytical protocol, *Spectrochimica Acta Part A: Molecular and Biomolecular Spectroscopy*, 91 (2012) 352-359.
- [91] F. Grandjean, L. Samain, G. J. Long, Characterization and Utilization of Prussian Blue and its Pigments, *Dalton Transactions*, 15 (2016) 18018-18044.
- [92] M. Vagnini, C. Miliani, L. Cartechini, P. Rocchi, B. G. Brunetti, A. Sgamellotti, FT-NIR spectroscopy for non-invasive identification of natural polymers and resins in easel paintings, *Analytical and Bioanalytical Chemistry*, 395 (2009) 2107–2118.
- [93] B. Muhlethaler, J. Thissen, Smalt, *Studies in Conservation*, 14 (1969): 47–61.
- [94] D. Hradil, T. Grygar, M. Hruskova, P. Benzdicka, K. Lang, O. Schneeweiss, M,

Chvatal, Green earth pigment from the kadan region, czech republic: use of rare Fe-rich smectite, *Clays and Clay Mineral*, 52 (2004) 767-778.

Appendix

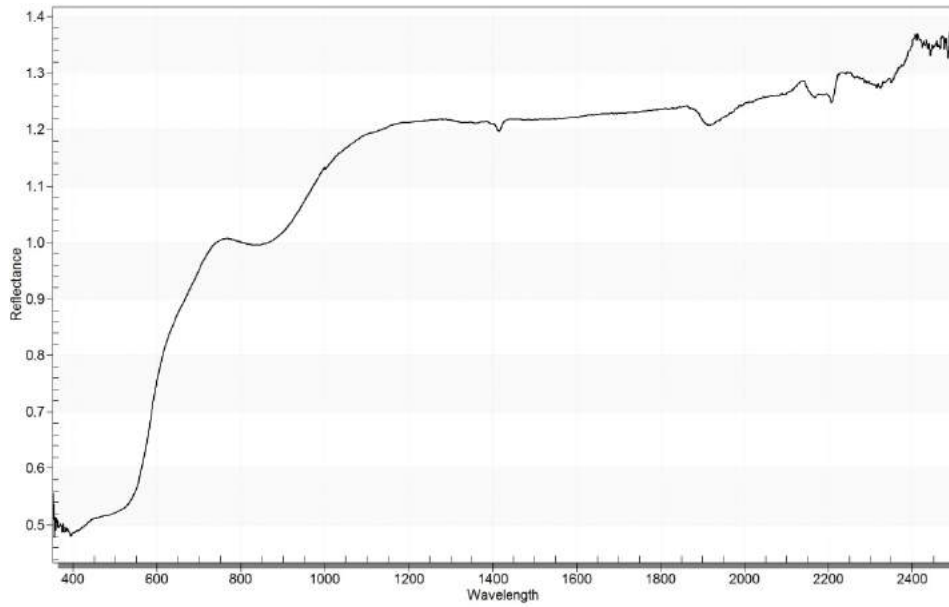


Figure 1 Original spectrum of Armenian Bole.

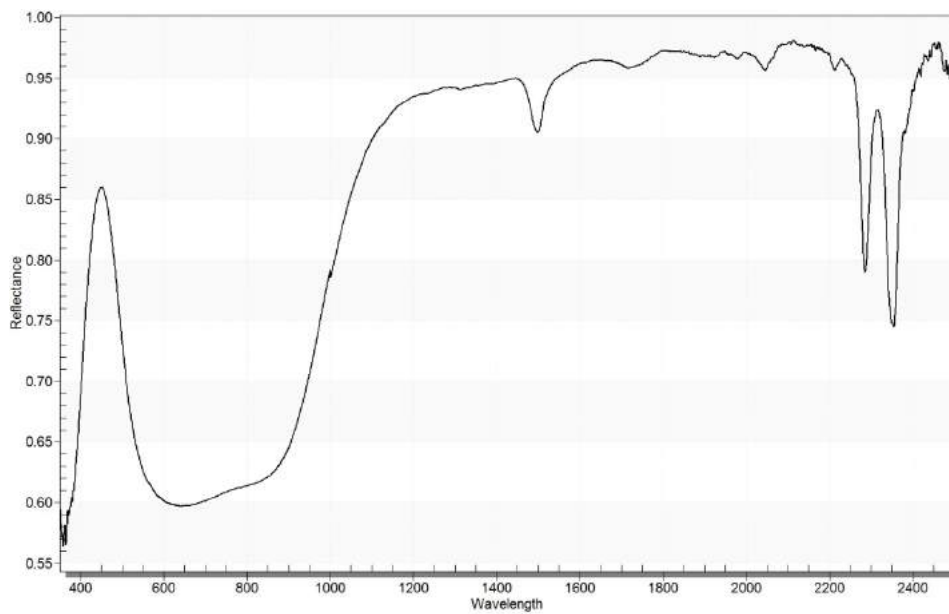


Figure 2 Original spectrum of azurite.

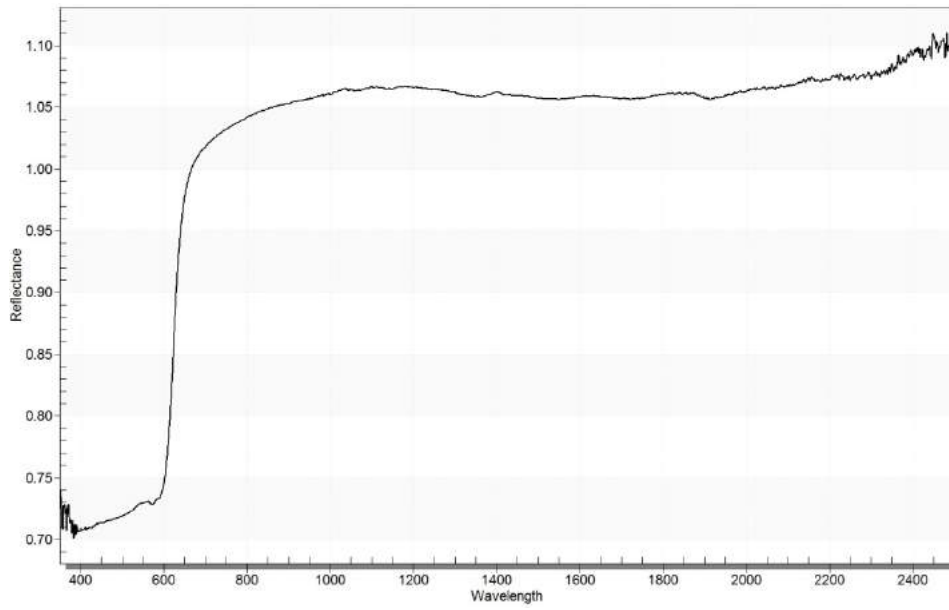


Figure 3 Original spectrum of red cadmium.

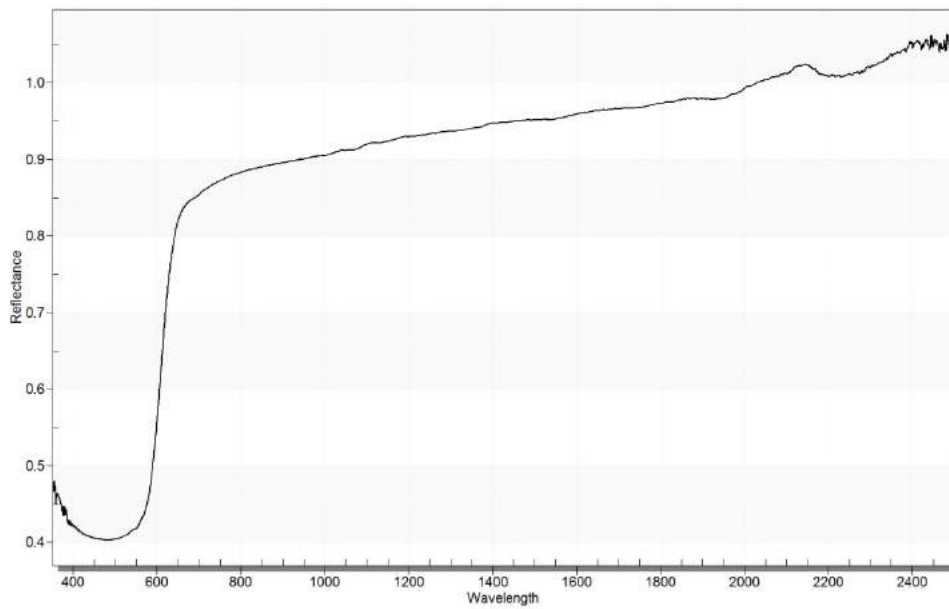


Figure 4 Original spectrum of cinnabar.

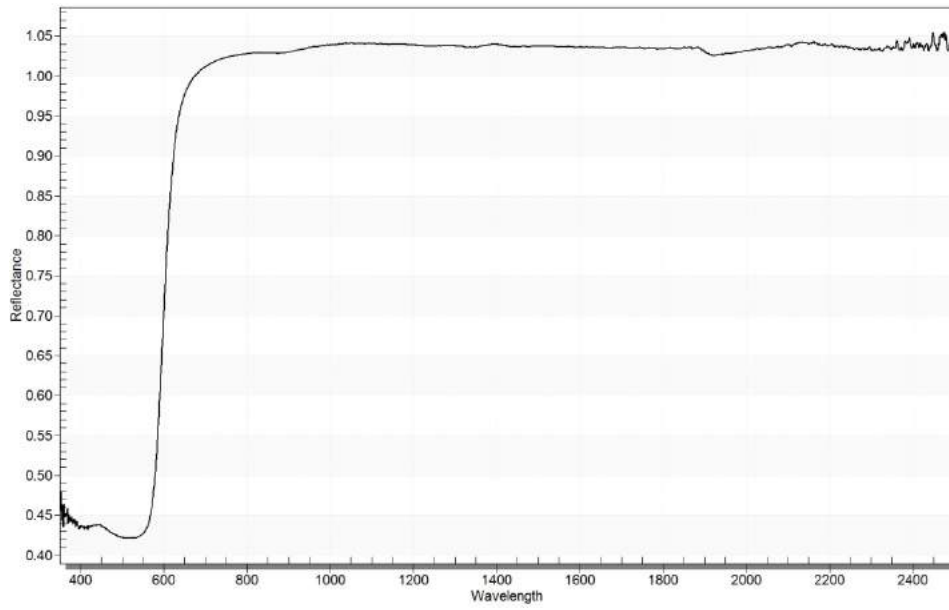


Figure 5 Original spectrum of cinnabar mountain Amiata.

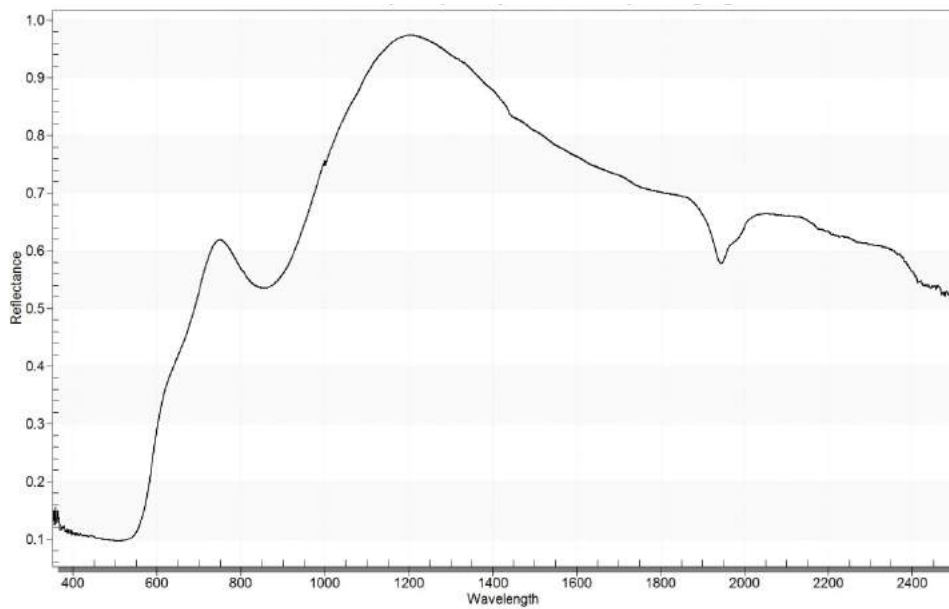


Figure 6 Original spectrum of English red.

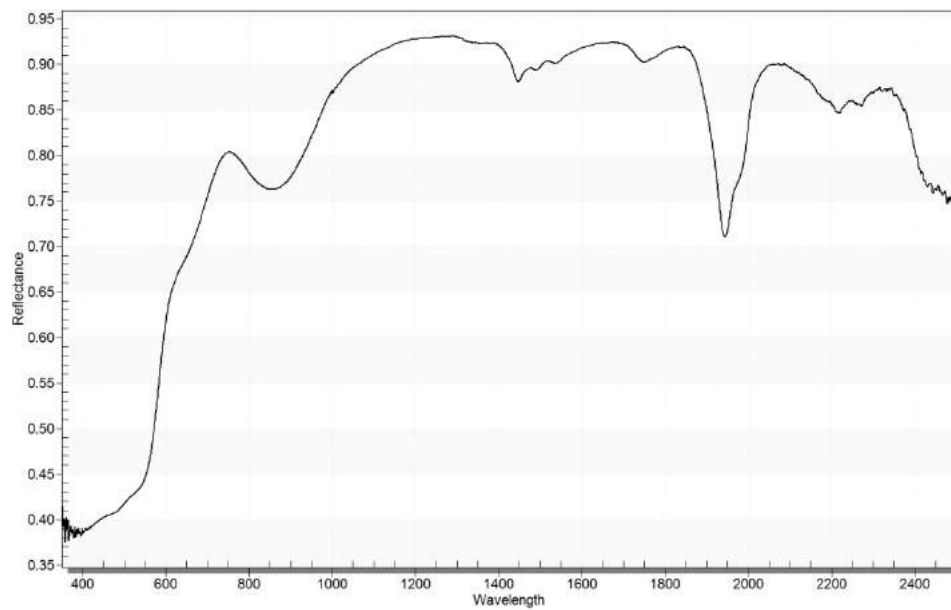


Figure 7 Original spectrum of Ercolano red.

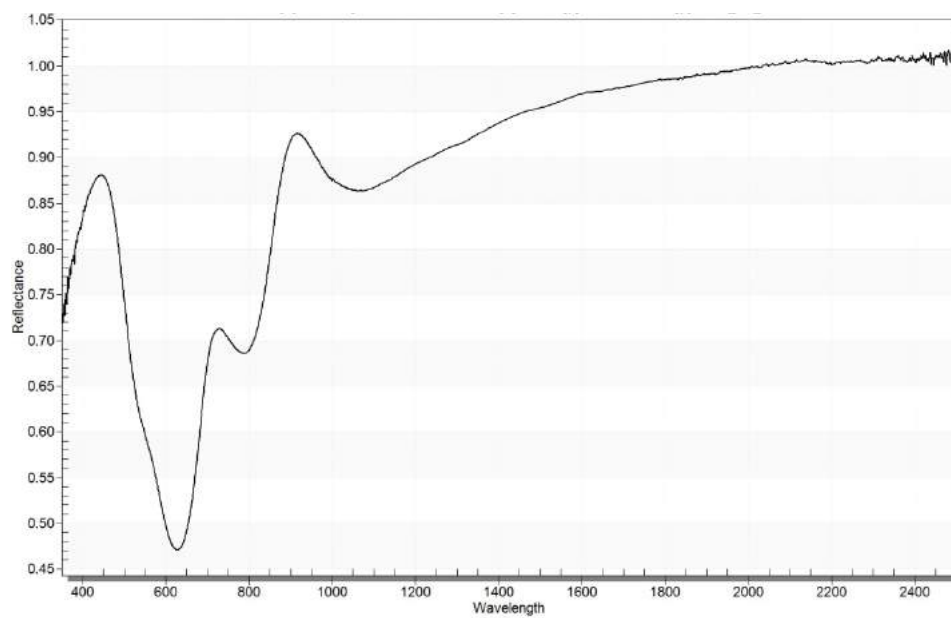


Figure 8 Original spectrum of Egyptian blue.

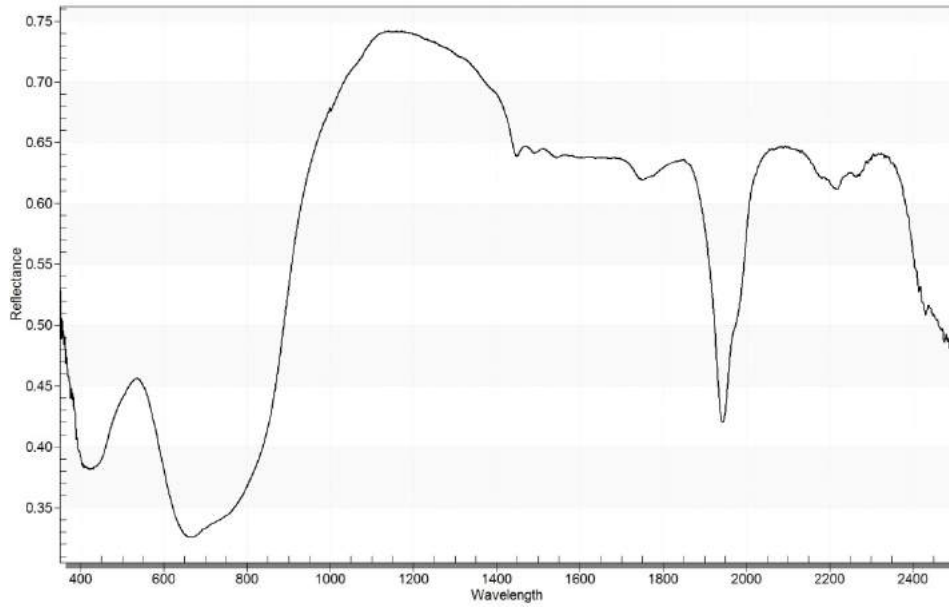


Figure 9 Original spectrum of green earth.

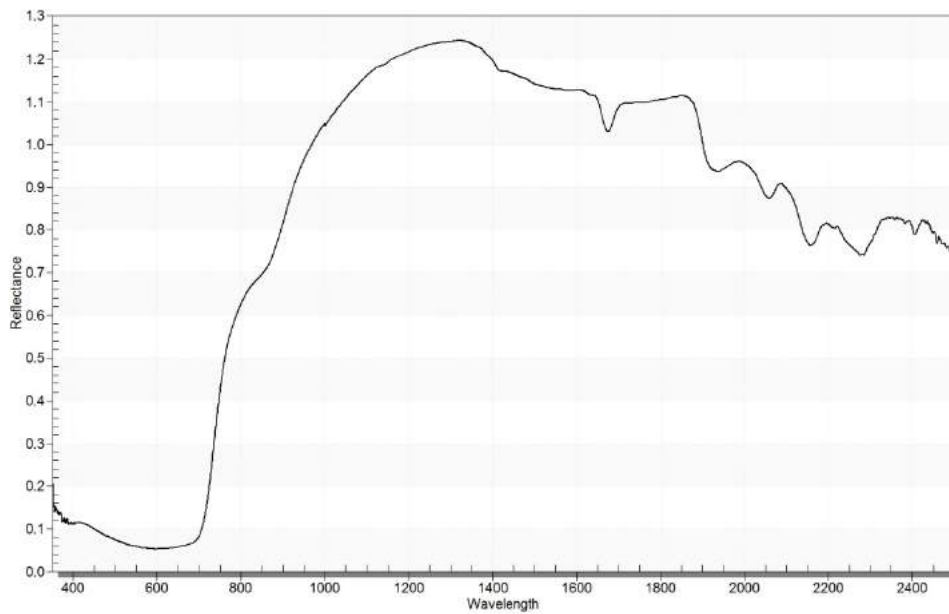


Figure 10 Original spectrum of indigo.

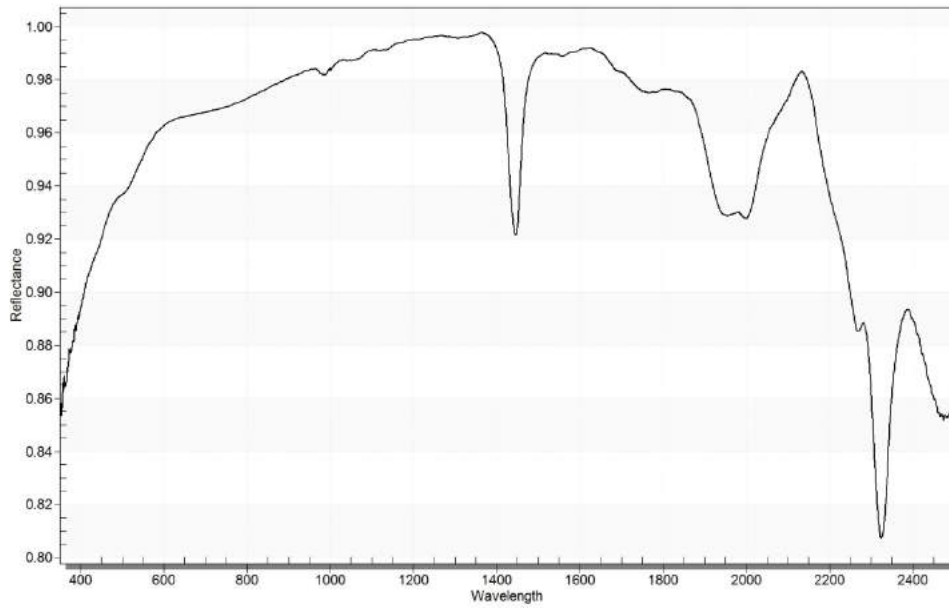


Figure 11 Original spectrum of Lead white.

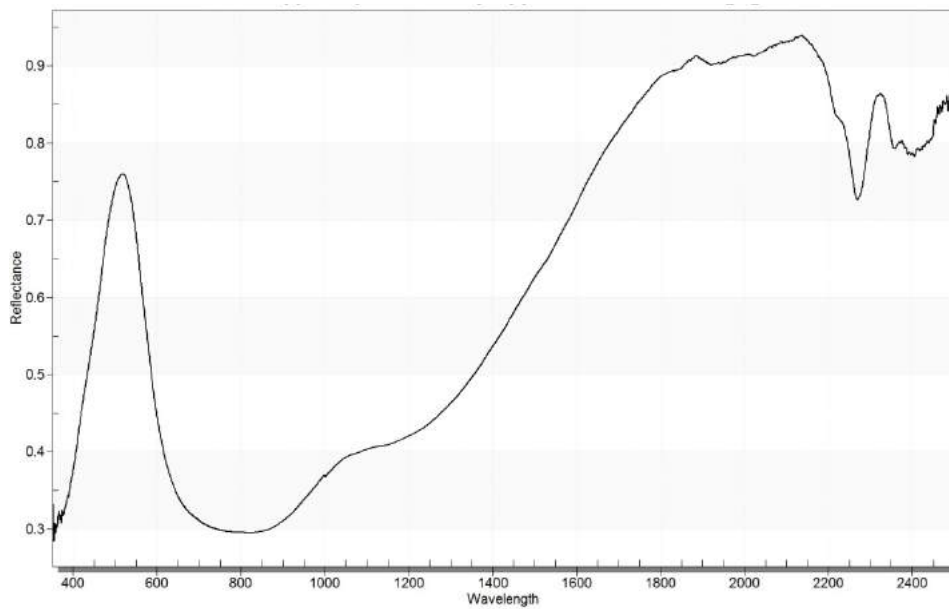


Figure 12 Original spectrum of malachite.

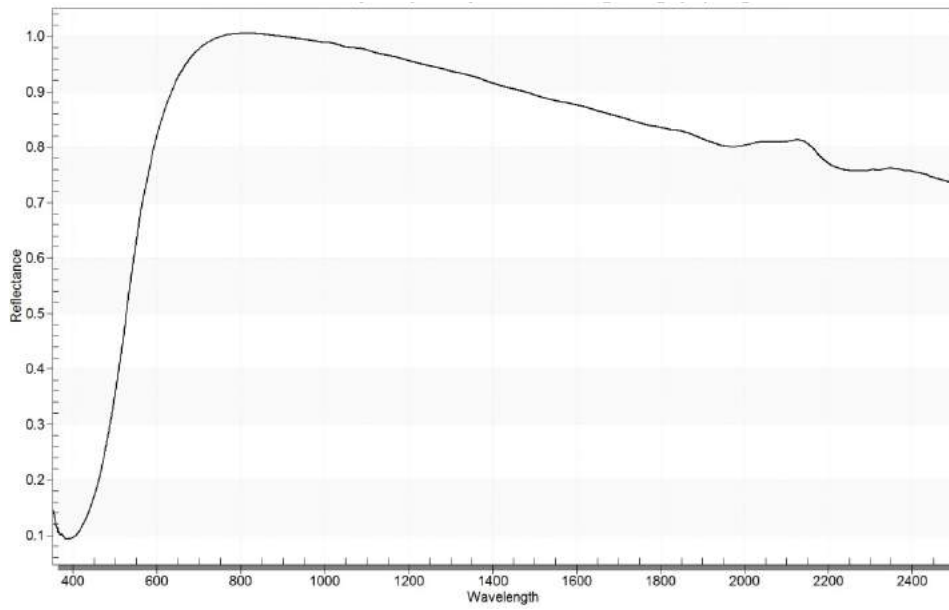


Figure 13 Original spectrum of Naples yellow.

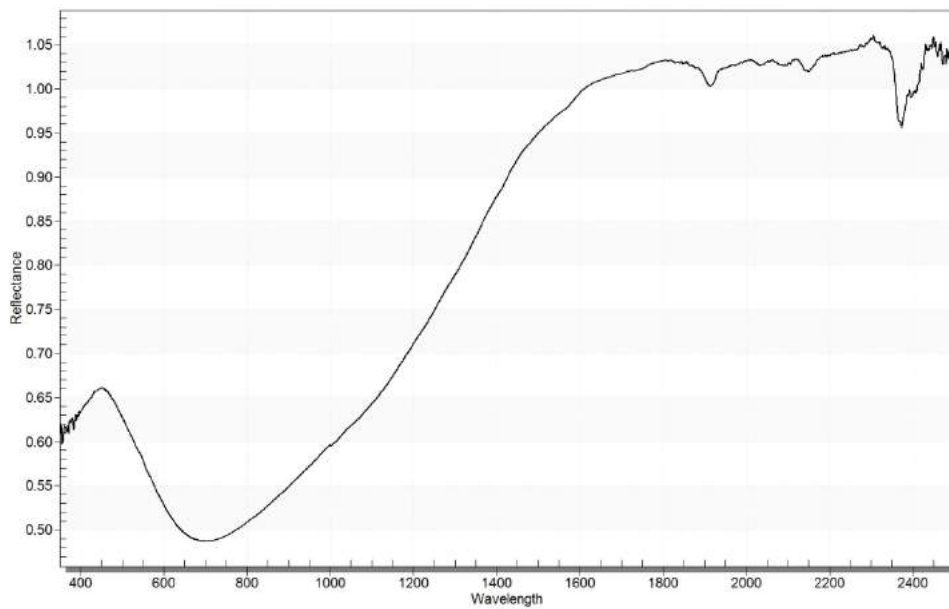


Figure 14 Original spectrum of Prussian blue.

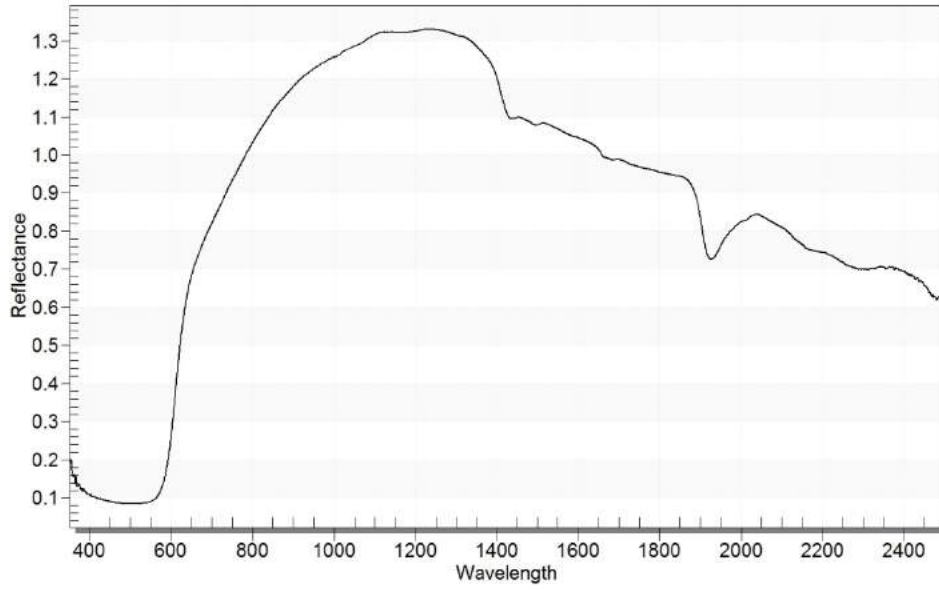


Figure 15 Original spectrum of red lake.

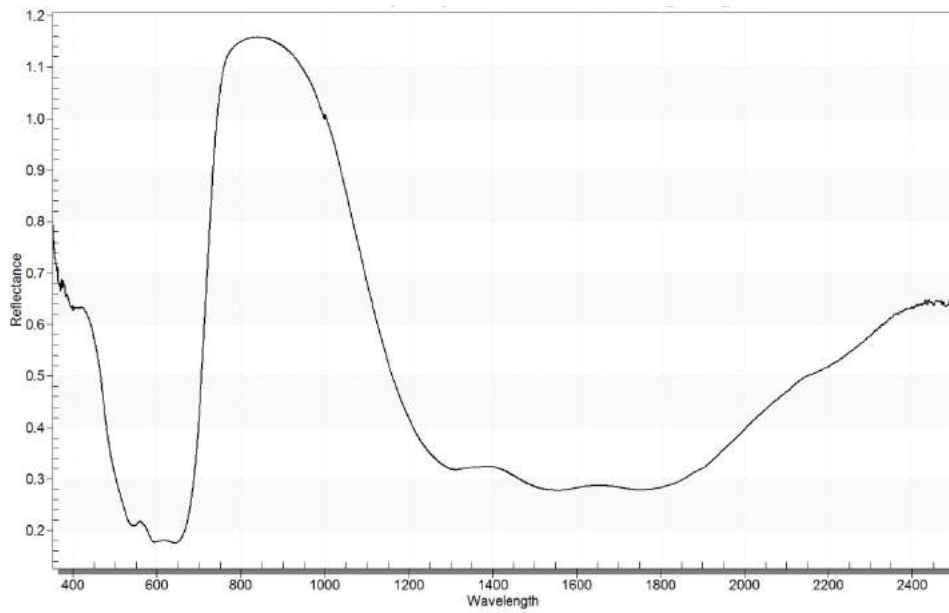


Figure 16 Original spectrum of smalt.

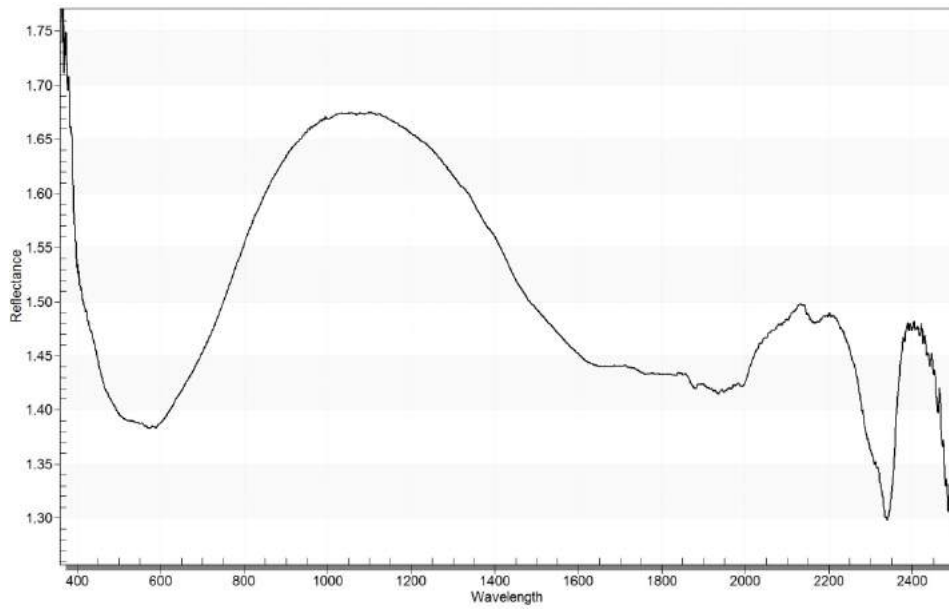


Figure 17 Original spectrum of Saint John's white.

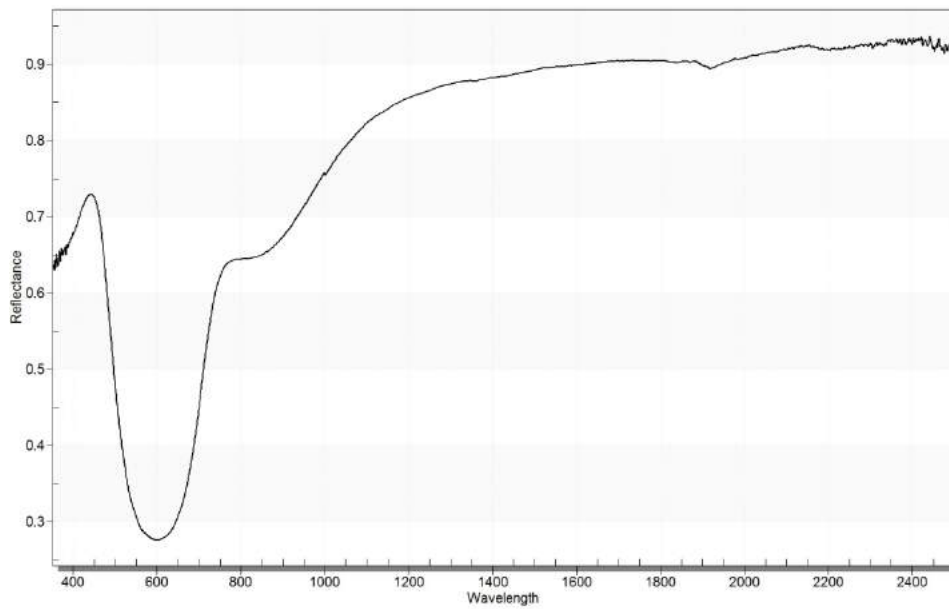


Figure 18 Original spectrum of synthetic ultramarine blue.

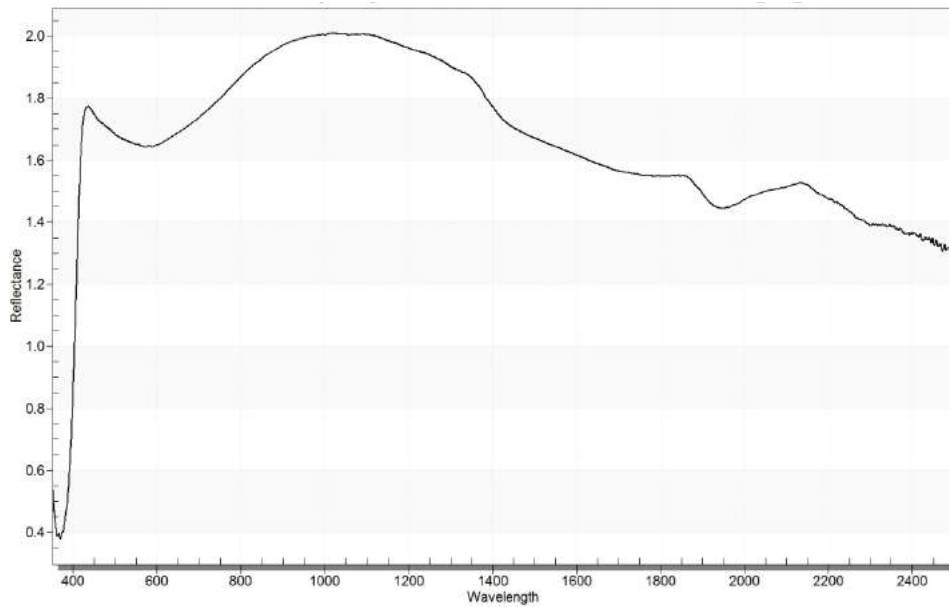


Figure 19 Original spectrum of titanium white.

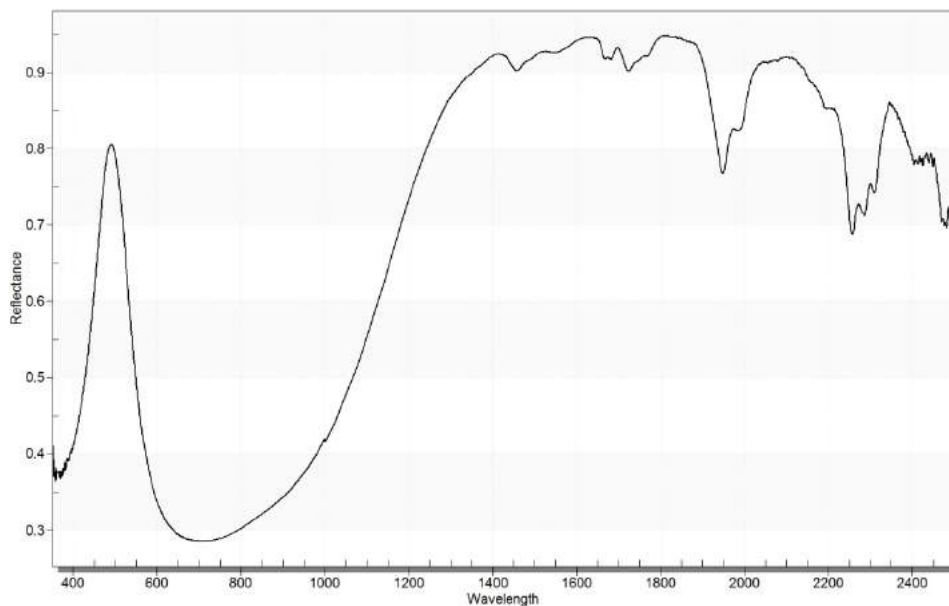


Figure 20 Original spectrum of verdigris.

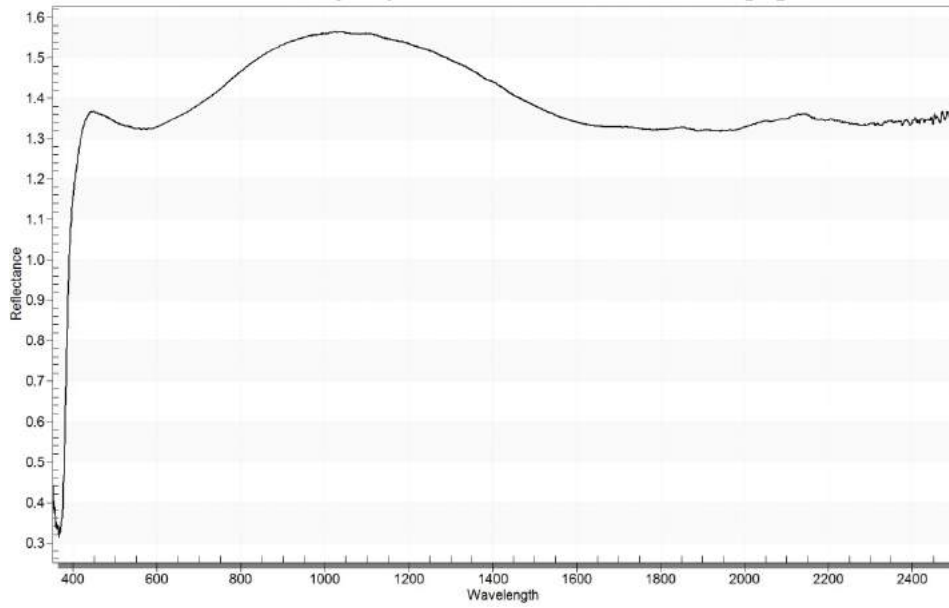


Figure 21 Original spectrum of zinc white.

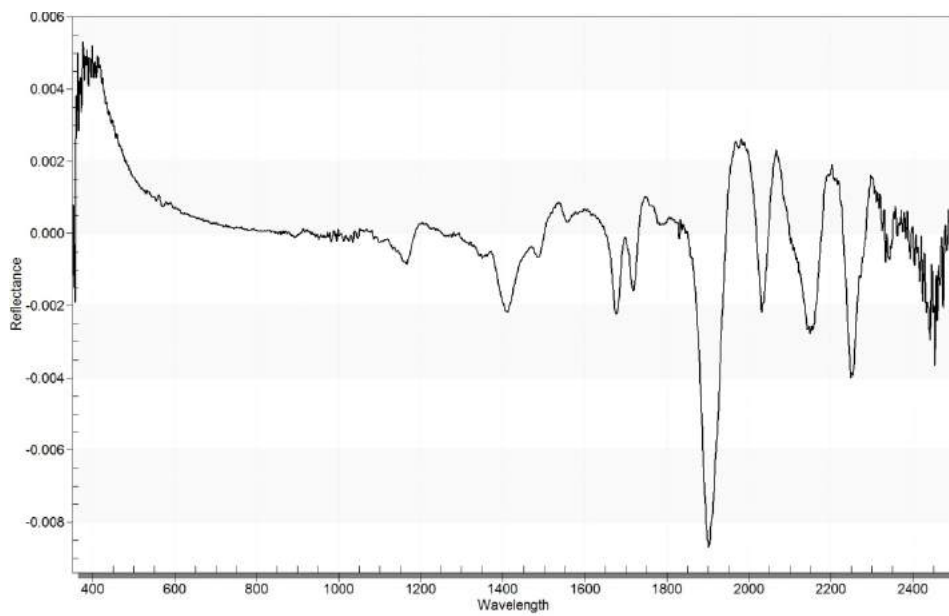


Figure 22 Original spectrum of animal glue.

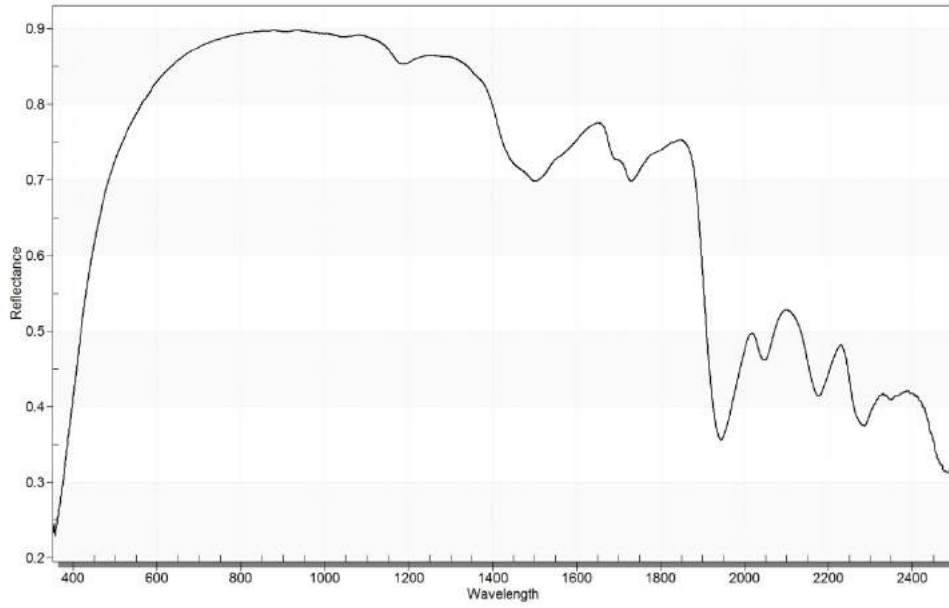


Figure 23 Original spectrum of dry animal glue.

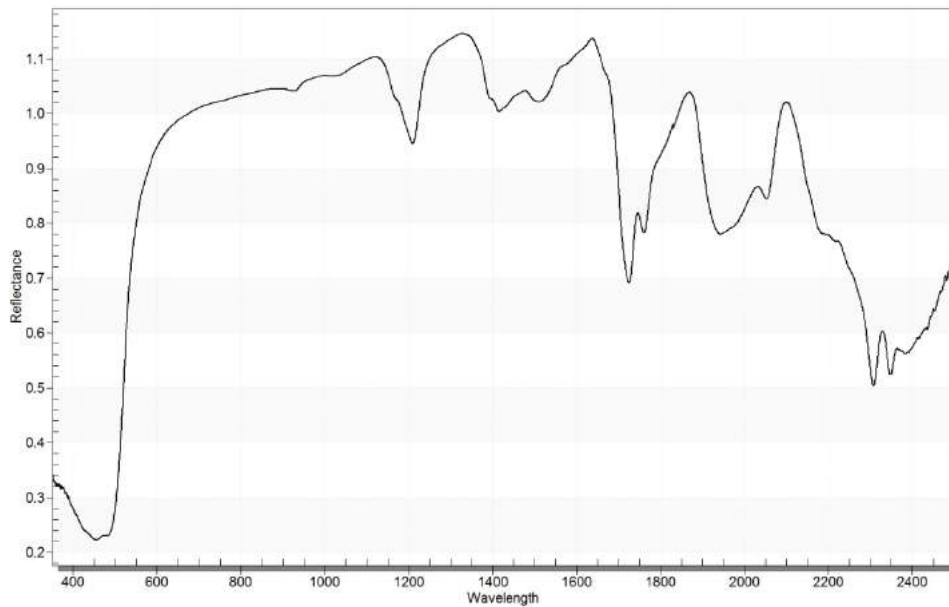


Figure 24 Original spectrum of egg yolk (on teflon).

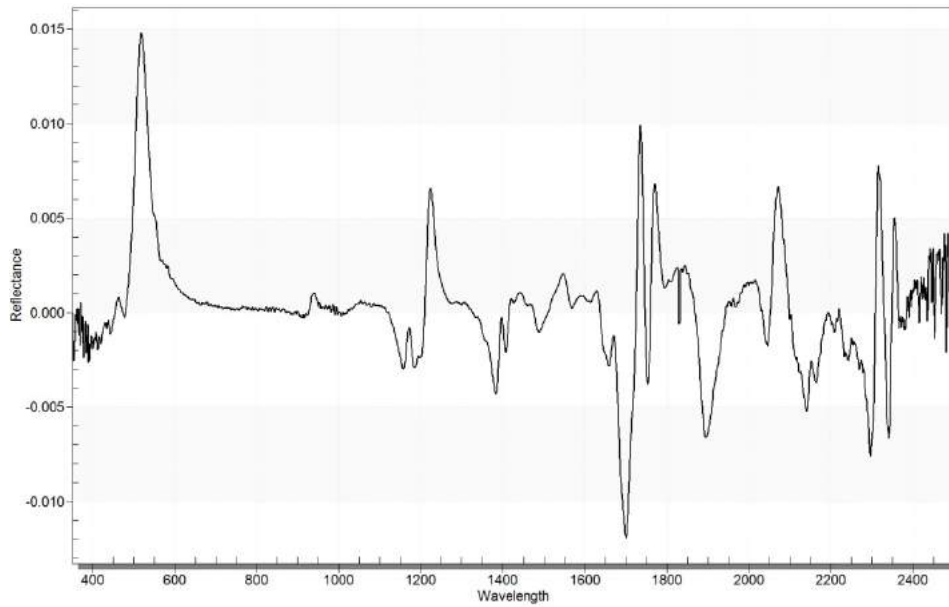


Figure 25 1st derivative spectrum of egg yolk.

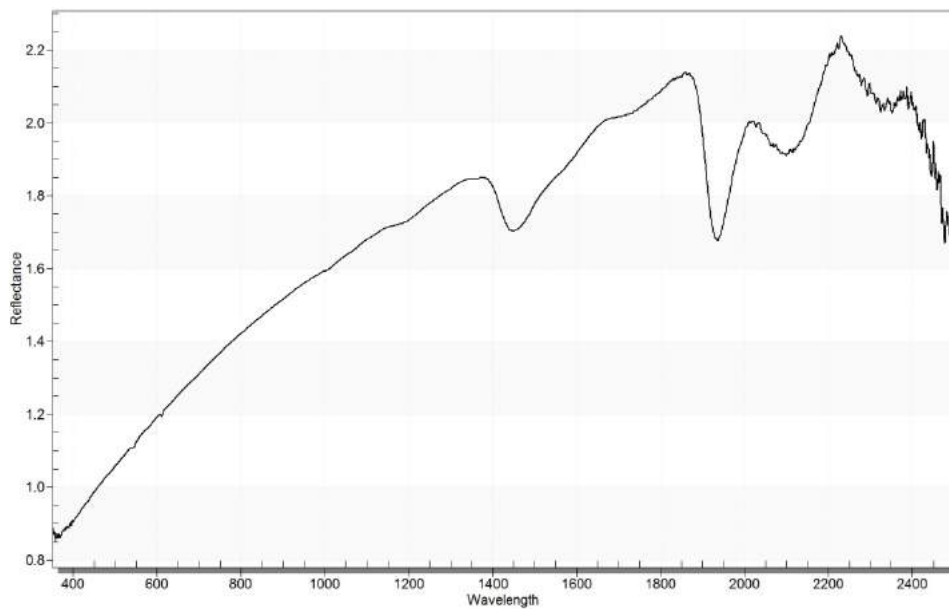


Figure 26 Original spectrum of gum Arabic.

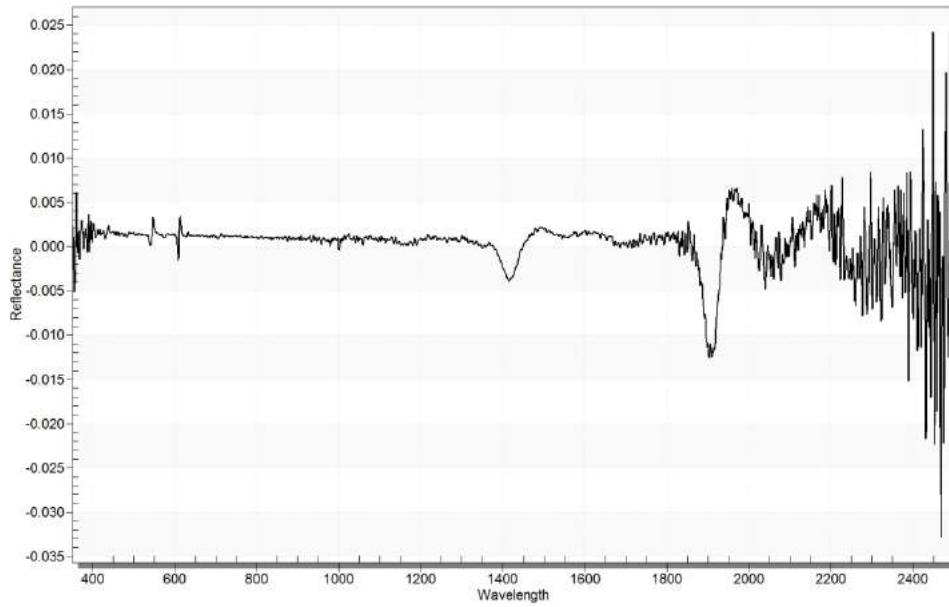


Figure 27 1st derivative spectrum of gum Arabic.

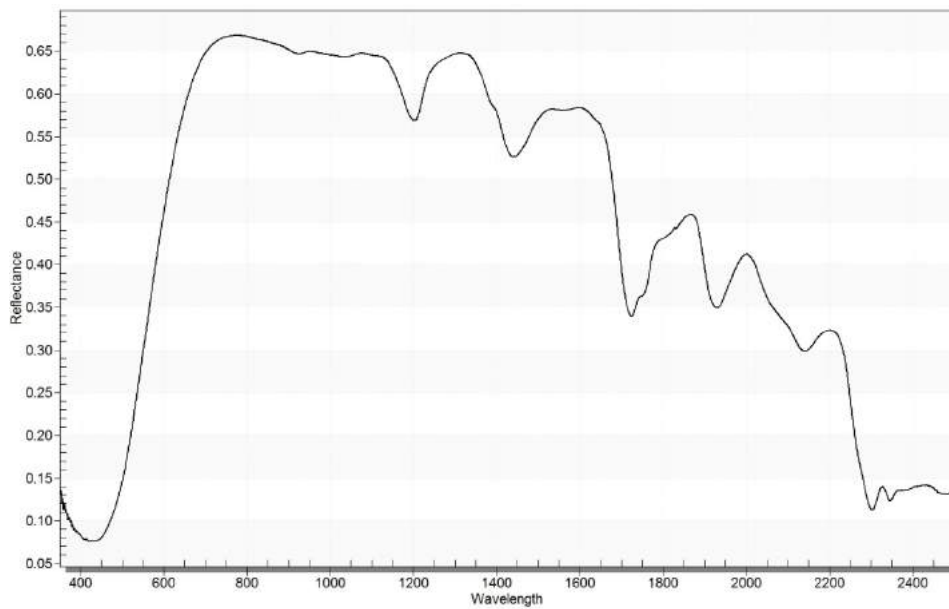


Figure 28 Original spectrum of Linseed oil.

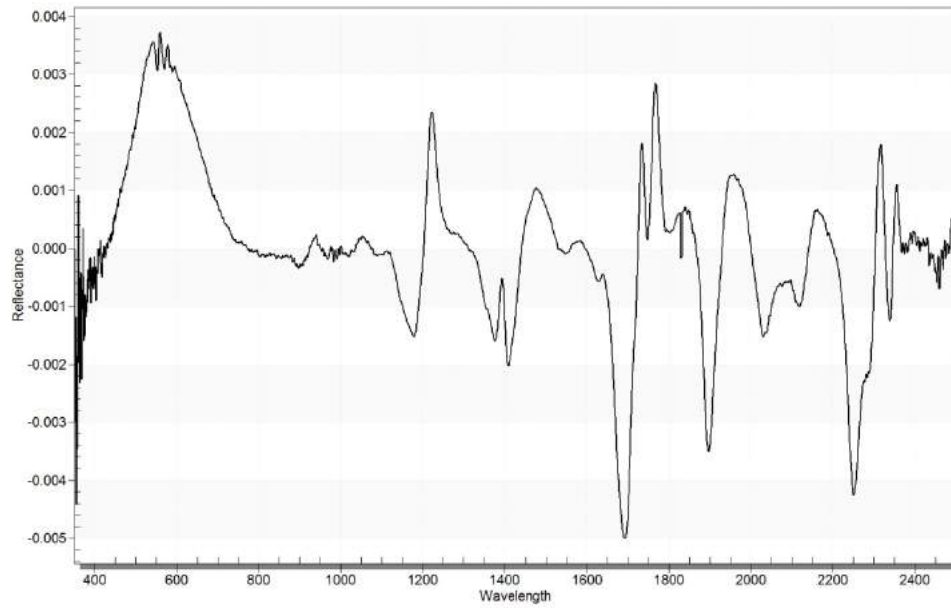


Figure 29 1st derivative spectrum of linseed oil.

Acknowledgement

Firstly, I would like to express my sincere gratitude to my advisors Prof. Sandro Moretti and Dr. Mara Camaiti for the continuous support of my Ph.D study and related research, for their patience, supports, motivations, and immense knowledge. Their guidance helped me in all the time of research and writing of this thesis.

Besides my advisors, I would like to thank Dr. Teresa Salvatici for helping me use the main instrument (ASD Field Spec FR Pro) and its corresponding software for my research. All the discussions with her always inspired me in my field of study from the use of the instrument to data elaboration.

I thank my fellow lab mate—Yijian Cao for discussions of findings and confusions during these years, for the sleepless nights we were working together before deadlines, and for all the fun we have had together.

Last but not the least, I would like to thank my family: my parents for supporting me spiritually and physically throughout the study in abroad from 2012 till now. More than six years studying aboard is a relative long period both for them and me to

separate, since I am the only child of my family. Thanks the university and CNR institute to give me the opportunity to finish my Ph.D here in Florence, Italy.